ETUDE D'HYDROGELS MULTIFONCTIONNELS A BASE DE PVA AVEC DES ADDITIFS NANOPARTICULAIRES ET MOLECULAIRES

par

Nina Ravandi

Mémoire présenté au Département de chimie en vue
de l'obtention du grade de maître ès sciences (M.Sc.)

FACULTE DES SCIENCES

UNIVERSITE DE SHERBROOKE

Sherbrooke, Québec, Canada, novembre 2022

STUDY OF MULTIFUNCTIONAL PVA BASED HYDROGELS WITH NANOPARTICLE AND MOLECULAR ADDITIVES

by

Nina Ravandi

Thesis presented to the Department of Chemistry in view

obtaining the degree of Master of Science (M.Sc.)

FACULTY OF SCIENCES

UNIVERSITY OF SHERBROOKE

Sherbrooke, Québec, Canada, November 2022

Le 04 novembre 2022

le jury a accepté le mémoire de Madame Nina Ravandi
dans sa version finale.

Membres du jury

Professeur Yue Zhao
Directeur de recherche
Département de chimie

Professeur Armand Soldera
Évaluateur interne
Département de chimie

Professeur Pierre Harvey
Évaluateur interne
Département de chimie

Professeur Céline Guéguen
Président-rapporteur
Département de chimie

SOMMAIRE

Dans cette étude, l'effet de différents additifs de renforcement, les nanocristaux de cellulose (CNC) et l'acide tannique (TA), sur l'hydrogel d'alcool polyvinylique (PVA), préparé à l'aide de la méthode de congélation/décongélation, a été examiné. L'influence de la CNC en tant qu'additif de nanoparticules et de l'AT en tant qu'additif moléculaire sur la structure et les propriétés des hydrogels a été étudiée à l'aide de la spectroscopie infrarouge à réflexion totale atténuée (ATR-IR), de la diffraction des rayons X sur poudre (XRD) et du balayage différentiel calorimétrie (DSC). Les propriétés mécaniques, d'auto-guérison et de mémoire de forme des hydrogels ont également été étudiées.

Les résultats expérimentaux ont révélé que les hydrogels PVA-CNC et PVA-TA préparés ont des propriétés différentes bien que des liaisons H soient formées entre la matrice PVA et les deux additifs dans les deux hydrogels. L'ajout de TA améliore plus significativement les propriétés mécaniques (module d'Young, résistance à la traction, allongement à la rupture et ténacité) que le CNC.

Cependant, l'hydrogel PVA-CNC conserve de manière significative la capacité d'auto-guérison, contrairement à l'hydrogel PVA-TA qui perd considérablement la fonction d'auto-guérison. De plus, une étude comparative détaillée a été réalisée en utilisant des hydrogels PVA-CNC et PVA-TA contenant la même quantité de 1% en poids d'additif. L'ensemble de ces travaux indique que les additifs nanoparticulaires et moléculaires des hydrogels de PVA préparés dans les mêmes conditions peuvent donner lieu à des propriétés très différentes, et que les liaisons H (nombre, nature, force) entre l'additif et la matrice ainsi que les leur interfaces peuvent être un facteur déterminant.

Mots-clés : Poly (alcool vinylique) ; hydrogel ; nanocristaux de cellulose; acide tannique; auto-guérison; mémoire de forme, propriétés mécaniques

SUMMARY

In this study, the effect of different reinforcing additives, Cellulose Nanocrystals (CNC) and Tannic acid (TA), on Polyvinyl Alcohol (PVA) hydrogel, prepared using the freeze/thaw method, has been examined. The influence of CNC as a nanoparticle additive, and TA as a molecular additive on the structure and properties of the hydrogels was investigated using attenuated total reflection-infrared spectroscopy (ATR-IR), X-ray powder diffraction (XRD), and differential scanning calorimetry (DSC). The mechanical, self-healing, and shape memory properties of hydrogels were also studied.

The experimental results found that the prepared PVA-CNC and PVA-TA hydrogels have different properties although H-bonds are formed between the PVA matrix and the two additives in both hydrogels. The addition of TA improves more importantly the mechanical properties (Young's modulus, tensile strength, elongation at break and toughness) than CNC.

However, the PVA-CNC hydrogel retains significantly the self-healing capability, in contrast to PVA-TA hydrogel that loses greatly the self-healing function. Furthermore, a detailed comparative study was carried out using PVA-CNC and PVA-TA hydrogels containing the same amount of 1 wt% of additive. The whole of this work indicates that nanoparticle and molecular additives in PVA hydrogels prepared under the same conditions may give rise to very different properties, and that the H-bonds (number, nature, strength) between the additive and the matrix as well as their interfaces may be a determinant factor.

ACKNOWLEDGEMENTS

First of all, I want to thank my research supervisor, Prof. Yue Zhao, who was accepting me in his group and was always supporting me in all situations. I learnt so much from his academic knowledge and personality during my research work, which is so important for me in my educational progress and future development and will influence my whole life. I am also grateful for his financial aid for my research program which have provided me an educational situation without having any financial problem.

I have an especial thanks to my adorable parents and my lovely sister who were always beside me, trust on me, and support me even from long distance with their love and encouragement. I am so lucky to have them in my life.

Thanks so much to my committee, Prof. Céline Guéguen and Prof. Armand Soldera, who were always supporting and helpful in my studying time, with great advice and suggestions. I would like to thank Prof. Pierre Harvey for accepting being in my jury member and giving precious advice about my thesis. It is a genuine pleasure to express my sincere gratitude and respect to Prof. Jean Lessard and Prof. Patrick Ayotte for their kind support, like a family member, which is so priceless for me.

An especial thank to Jean-Marc Chapuzet, who helped me so much with great effort, patient, and care during my study years. He always tries so hard to solve all students' problems and find the solution to relive them to study well. He is formidable and it is my great honor to know such a wonderful person.

I wish to thank all personnel of the department of chemistry for helping me in all steps of my study: Solange Thériault, Sonia Gougeon, Josée Lamoureux, René Gagnon, Daniel Fortin, Michel Trottier, Philip Richter, Kirill Levin, Vincent St-Onge.

I want to thank my colleagues, Jie Jiang, Li Han, Meng Lui, Xinshi Chen, Amélie Auge, Shaoxia Zhang, Yaoyu Xiao, Yaru Ma, Ruidong Cheng, Junbo Hou, Yiming Chen, Feijie Ge, Zhichao Jiang, Lu Yin, Long Xu, Zeping Liu, who helped me so much and answered patiently all my questions.

Finally, thanks to the whole staffs of the university of Sherbrooke for providing me such a nice study and research environment. It was an honor for me to study in such a well-known and high-ranking university.

TABLE OF CONTENTS

LIST OF ABBREVIATIONS

PVA	Polyvinyl alcohol
CNC	Cellulose Nanocrystals
TA	Tannic acid
DSC	Differential scanning calorimetry
SMPs	Shape memory polymers
ATR-FTIR	Attenuated total reflectance- Fourier-transform infrared
H-bonds	Hydrogen bonds
XRD	X-ray diffraction
ATR-FTIR	Attenuated Total Reflectance Fourier Transform Infrared Spectroscopy
T_m	melting temperature
T_c	crystallization temperature
ΔH_m	heat of fusion
ΔH_c	heat of crystallisation

LIST OF TABLES

LIST OF FIGURES

LIST OF EQUATIONS

List of SCHEMES

I.1 What is Hydrogel

Hydrogels are three-dimensionally cross-linked, hydrophilic polymer networks, containing a large amount of water. They have been extensively over the past decades due to their applications in many fields including biomedicine.[1-3] Figure 1. shows various biomedical applications of antimicrobial hydrogels.[4]
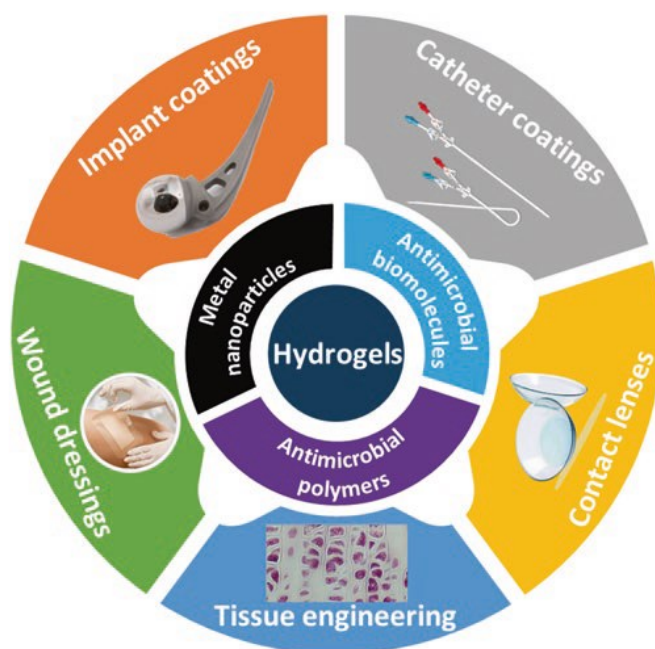
Figure 1. Different applications of hydrogels in biomedical area (Reprinted by permission from Springer Nature, Copyright 2020).[4]

Because of having physical and/or chemical cross-links, hydrogels are insoluble in water (no molecularly dissolved chains).[5] The physical cross-links can be crystallites, chain entanglements, or weak associations such as hydrogen bonds or Van der Waals forces which provide the network structure and physical integrity. In the case of using crosslinking agents to chemically form polymeric hydrogels some unwanted reactions with drugs or some toxic side effects may happen which is related to the residual cross-linking agents.[5]

The soft-and-wet nature and crosslinked-network structure of hydrogels are acknowledged to be important functional materials swollen with a large amount of water.[6, 7] Some special properties of the hydrogels such as high hydrophilicity, permeability, biocompatibility, and low friction coefficient are similar to the biological tissues, thus hydrogels have been widely employed as scaffolds for tissue engineering,[8] vehicles for drug delivery,[9] and model extracellular matrices for cell culture.[10] On the other sides, hydrogels have relatively poor mechanical properties,[11] because of their wet and soft nature with a high-water content, which may prevent using them for different applications, especially in load-bearing soft tissues.[12, 13]

In recent years, there have been many efforts to prepare mechanically tough hydrogels including double-network (DN) gel,[14] interpenetrating network gel,[15] topological sliding rings gel,[16] tetra-poly (ethylene glycol) (PEG) gel,[17] macromolecular microsphere gel,[18] and nanocomposite gel.[19] The most effective strategies to improve mechanical properties of hydrogels are incorporating energy dissipation mechanisms and tailoring homogeneously cross-linked structures.[20, 21] Based on the energy dissipation theory, Gong et al.,[22] designed and prepared a series of physically and/or chemically cross-linked hybrid DN gels which is composed of two asymmetric network structures. Utilising fully physically cross-linked networks without having covalent bonds in its structure is an ideal strategy for the fabrication of hydrogels with efficient self-healing property and good mechanical performance.[23]

Interpenetrating, hybrid, and double network (DN) are some complex networks prepared with dissipation-induced toughening theory,[11] which significantly enhances the mechanical strength and toughness of hydrogels.[24, 25] The water swelling property of hydrogels which weakens their toughness and mechanical strength, reduce the application of their hydrogels in different fields.[26] Therefore, it is highly challenging proposition to develop an equilibrated hydrogel with high mechanical strength and versatile functions.[27] Hydrogels form hydrogen bonds with water after adsorption which construct the second cross-link in hydrogel to form DC polymer network, and it would be suitable method for a broad range of hydrogel preparation.[4]

As already mentioned, hydrogels are among the category of soft biomaterials because of their biomimetic structure, application-dependent multifunctions, as well as tunable mechanical properties. To increase the applications of hydrogels, many efforts have been made to prepare hydrogels with different and flexible functionalities, such as photoluminescence (PL) by incorporating various photoluminescent substances into the polymer networks of hydrogels,[28] magnetic response,[29] thermosensitivity,[30] electroconductivity,[31] and biological response.[32]

A wide range of natural polymers including chitosan, sodium alginate and synthetic polymers like poly (vinyl alcohol) (PVA), or the mixture of both natural and synthetic polymers can be involved to prepare hydrogels.

Since last three decades, the mixture of natural and synthetic polymers as bioartificial or biosynthetic polymeric material have attracted more attention for biomedical applications because of their improved mechanical and thermal properties and biocompatibility compared to those of single polymer hydrogels.[33] Each polymer type gives different properties to the hydrogel. For instance, natural polymer has low toxicity, biodegradability, and biocompatibility, while synthetic polymers give good mechanical properties to the hydrogel.[34]

I.2 Smart Functions of Hydrogels: Self-healing and Shape memory

Stimuli-responsive hydrogels which are named smart hydrogels, are three-dimensional cross-linked hydrophilic polymer networks with the ability to change their properties in response to the external stimuli including temperature, chemical materials, and pH.[35]

In medicine and materials science fields there have been great attention to the functional medical materials because of the development of smart polymer materials.[36] In addition, polymers with functional groups can adjust their properties and structures to tolerate different and tough environmental conditions, which is impossible for traditional medical materials.[37, 38]

There are many biomedical applications[39] such as tissue engineering,[40] drug delivery,[41] and wound dressing,[42] because of their high-water content,[43] excellent biocompatibility,[44] flexibility, and stimulus response property[45] for dynamic crosslinked hydrogels. Dynamic intermolecular interactions or dynamic chemical bonds link the molecules in dynamic crosslinked hydrogel which provide the ability to the hydrogel to change its shape and self-heal easily.[46] Dynamic crosslinked hydrogel is an ideal candidate for wound dressing application because it can fully cover the irregular or deep wound surface to prevent more injuries and contaminations.[47]

Among smart materials, self-healing hydrogels are especially promising for different biomedical applications, such as biosensors,[48] drug delivery systems,[49] and wound healing,[50] due to their inherent biocompatibility and similar mechanical behavior to natural tissues.

Self-healing means the spontaneous new bonds formation after the breakage of old bonds within a material. New bond form through reconstructive covalent dangling side chain or non-covalent hydrogen bonding because of the dipole-dipole forces and the structure hydrogels. This property of hydrogel has motivated the research and development of self-healing hydrogels in fields such as reconstructive tissue engineering as scaffolding such as shown in Figure 2.[35]
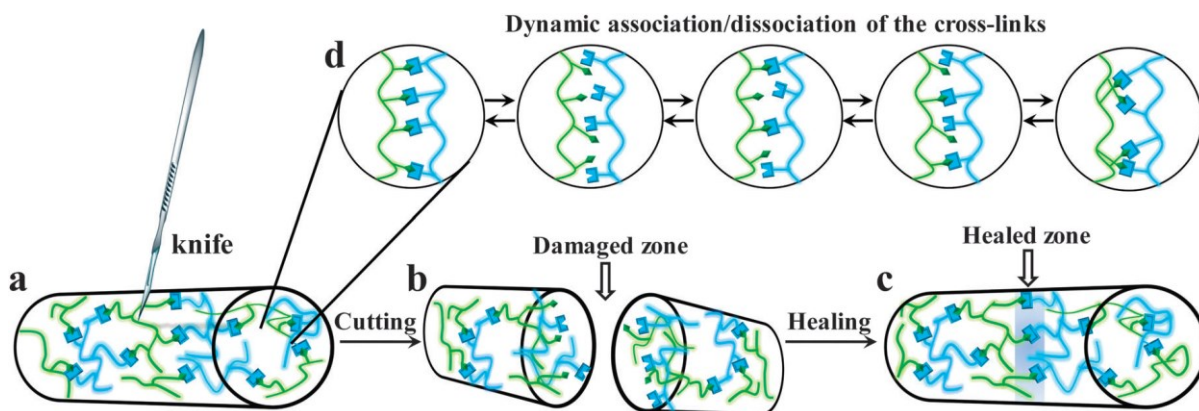
Figure 2. Schematic illustration of self-healing mechanisms of self-healing gels based on CDC.[35]

Because of the irreversibility and stability of the covalent crosslinked networks in the traditional chemical hydrogels, the reconstructing of intermolecular interactions for self-healing is disrupted.[51]

Two strategies have been developed for the preparation of hydrogel with self-healing property by:

(i)   Introduction of dynamic intermolecular interactions or other physical crosslinks such as hydrophobic interactions,[52] hydrogen bonds,[53] crystallization,[54] etc. which can develop self-healing property.[55] These physical interactions can help to obtain high strength for the healed hydrogel by re-establishing the intermolecular crosslinking networks. However, this self-healing process usually requires external stimulation or long time, which is unsuitable for simple and rapid operation of wound dressing.[56]

(ii)   Application of the dynamic chemical bonds in the structure of hydrogel,[51] including benzene boronic acid complexations,[57] disulfide bonds,[58] imine bonds,[57] acylhydrazone bonds,[59] etc. These dynamic chemical bonds are reformed easily and rapidly around the damaged part in the hydrogel[60] which bring the self-healing property to the hydrogels. Therefore, the formation of new chemical bonds between molecules which provide the self-healing process in damaged regions of the hydrogels is possible with the functional chemical structures or groups should exist in the cross-linking networks.

Physically crosslinked hydrogels, which are autonomously self-healable, stretchable, and deformable, are so attractive for the generation of artificial skin. The fabricating of self-healing hydrogels based on noncovalent reactions and dynamic covalent interactions are so popular in recent years.[61] Bao et al. reported preparation of a self-healable and elastic capacitive sensor with the combination of dynamic metal-coordinated bonds and hydrogen bonds in a multiphase separated network.[62] Figure 3 shows the ionic bonds between Fe^{3+} and carboxylic ions and hydrogen bonds between hydroxyl and carbonyl groups in preparation of KCl–Fe^{3+}/PAA supramolecular hydrogel electrolytes.
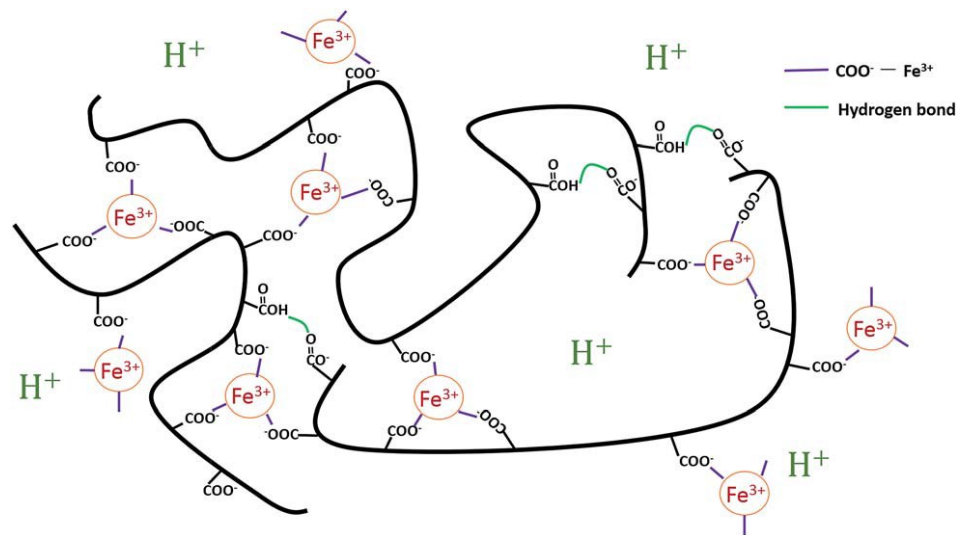
Figure 3. Schematic illustration of the internal crosslinking effect of the KCl–Fe^{3+}/PAA hydrogel.[62]

Self healing ability of physically crosslinked hydrogels increase the life service and reliability in certain applications because of restoring their functionalities and structure after being damaged. Without the external stimulus e.g., pH,[63] temperature,[64] or UV light,[35] physical hydrogels can realize self-healing process autonomously which is different than traditional self healing hydrogels based on covalent reactions. Nevertheless, the self-healable hydrogels with just one physically cross-linked network have the limitation in their practical applications for some fields due to their weak mechanical properties.[65]

Multiple noncovalent interactions in diverse types can improve the mechanical properties of self-healable hydrogels with noncovalent interactions. There are lots of natural or synthesis polymers for fabrication of self-healing hydrogels such as poly (acrylic acid),[66] poly (ethylene glycol),[67] poly (vinyl alcohol) (PVA),[68] hyaluronic acid,[69] guar gum,[70] chitosan,[71] and among all these polymers, PVA have been attracted more attention because of being water-soluble, nontoxic, highly crystalline, and biocompatible. Shape memory is another smart function for hydrogels. Such a hydrogel can be processed from a specific permanent shape to a stable temporary shape, and subsequently deform to recover the permanent shape by responding to a stimulus. There are different fields such as biomedicine, actuators, and so on which are interested to use shape memory hydrogels.[72] Generally, for these applications, three main issues must always consider. Fan et al. reported preparation of tough, self healable, and adhesive dual-cross-linked hydrogels with freeze-dry method. They immersed the freeze-dried aerogel in Tannic acid (TA) solutions as can be seen in Figure 4.[73]

Wang and co-workers reported effect of strong hydrogen bonding between PVA and TA as the permanent cross-link and the week hydrogen bonding between PVA chains as the temporary cross-link in preparation of tough PVA−TA hydrogel which has shape memory behaviour. It is mentioned that after 3h, the temporary shape of hydrogel was fixed at room temperature and recovered quickly in 2 s.[74]
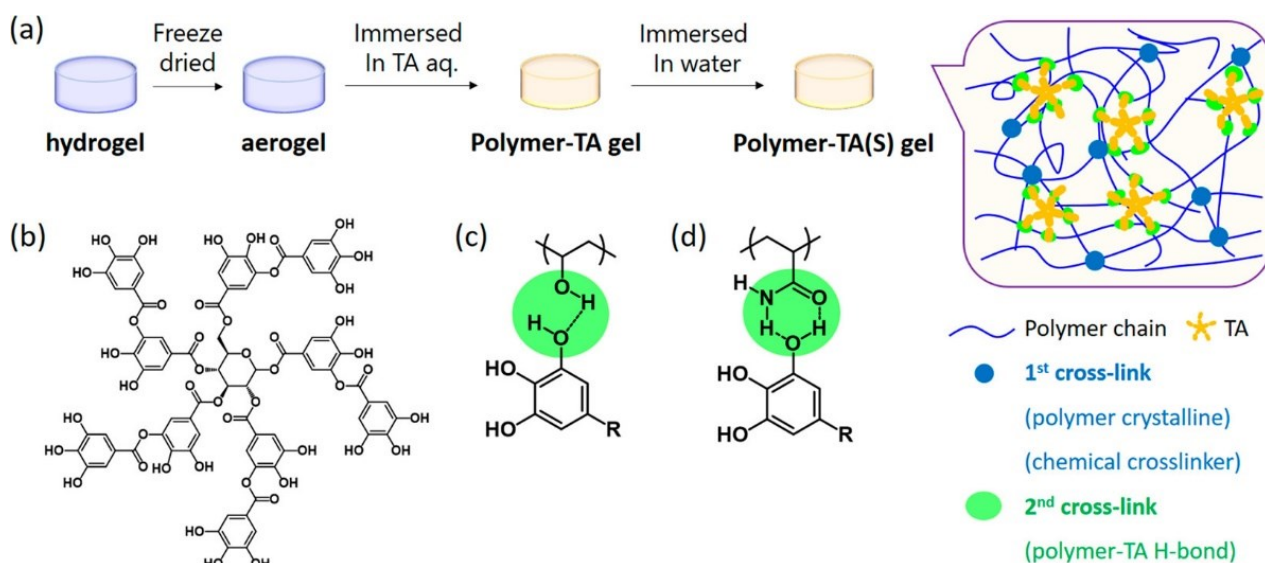
Figure 4. (a) Illustration of the preparation of polymer–TA DC hydrogels. (b) Chemical structure of TA. (c) The hydrogen bond between PVA and TA. (d) The hydrogen bond between PAAm and TA.[73]

Polymer with shape memory property should have two structural features: 1) For reversible transition which is fixing the temporary shape and its recovery, polymer must have a special segment which is capable for this transition. 2) For fixing the permanent shape, polymer must have a cross-linking network (chemically or physically cross-linked). Hydrogen bonding is often employed as a physically cross-linked noncovalent interaction. Furthermore, hydrogen bonding has been utilized to develop high modulus ratio shape memory polymers with excellent shape memory effects and stabilized shape memory complexes.[75] Shape memory hydrogels are kind of hydrogels which can response to the external stimuli such as temperature, pH, ultrasound, chemical materials, solvents, etc. by restoring the fix deformed shape to its original shape.

There are two networks that bring the shape memory effect to the hydrogel: (a) The strong fixing network which is difficult to be broken and is responsible for keeping the original shape. (b) The weak reversable network which is responsible to fix the temporary shape of hydrogels.[74]

This is a fact that self-healing effects of hydrogels can prolongs the lifetime of hydrogels because of their dynamic capability to restore the original structural of hydrogels after being damaged, which helps for great economy in the process of preparation and utilization of hydrogels. On the other hand, there are immense application in different fields including information storage and soft robotics for programmable shape memory hydrogels which can fix their temporary shape and recover their original shape.[76]

Highly meaningful progresses for preparing self healing hydrogels, with fast and efficient self-healable ability and robust mechanical strength have been made in recent years.[77] However, there is still a big

challenge to integrate self-healing and shape memory properties in a single hydrogel due to their potential structural incompatibility.

For example, to obtain a shape memory hydrogel, having a permanent cross-linking network which will prevent the exchange of component and keep the original structure, is a must.

All in all, it is of great interest to prepare a hydrogel with great self healing and shape memory behavior.

I.3 Poly (vinyl alcohol) (PVA) Hydrogels

Of the many self-healable and/or shape memory hydrogels reported in the literature, poly (vinyl alcohol) (PVA) based hydrogel is among the most studied.

There have been many reports which concern the development of shape memory polymers (SMPs) based on PVA.[78-81] However, in most of these reports, shape memory PVA networks are mainly connected with chemical cross-linking, which cannot be reprocessed. This behavior is in contrast with physically cross-linked SMPs, which are easy to reform their shape specially the hydrogen-bonding cross-linked ones. In Figure 5 three different linear Formula, molecular structure, and 3D ball representation of PVA is shown.[82]

a) $[-CH_2CHOH-]_n$

b)

c)
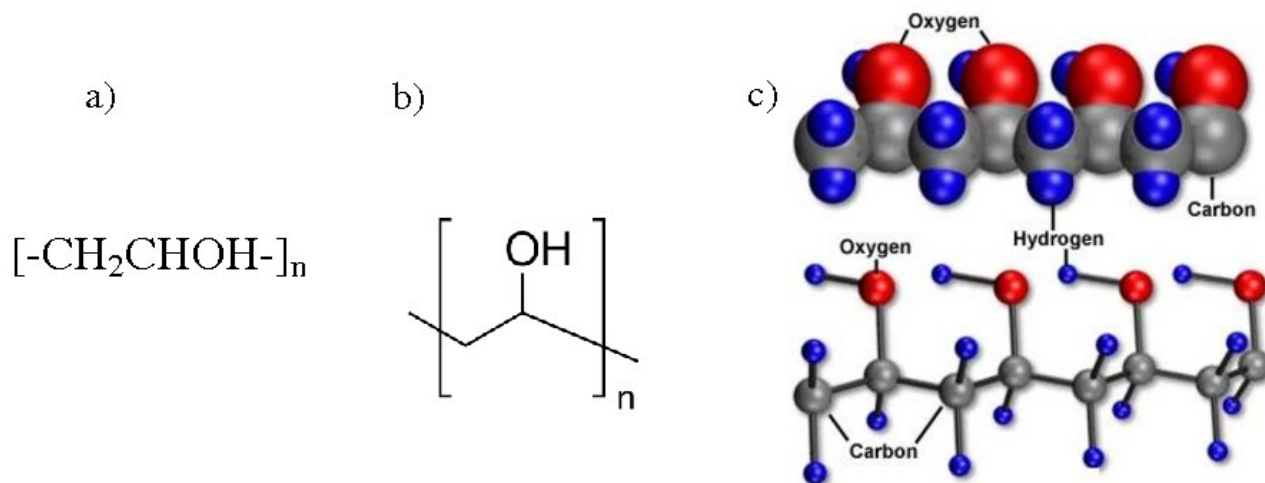
Figure 5. Linear formula (a), molecular structure (b) and 3D ball representation (c) of poly (vinyl alcohol).[82]

Hydrogels of PVA, which is a thermoplastic, high oxygen barrier polymer obtained by the hydrolysis of poly (vinyl acetate) (PVAc) and not by polymerization processes like some other synthetic polymers, have gained much attention in the last few decades. PVA is the most polar synthetic polymer, it is odorless, nontoxic, biocompatible, and soluble in water, acids, and high polar solvents. After hydrolysis, PVA still contains 1–2 mol% of acetyl groups. Its degree of polymerization (DP) depends primarily on the size of the PVAc macromolecular chain. The transformation of PVAc into PVA is obtained by the

base catalyzed alcoholysis or by the acid-initiated hydrolysis. Its molecular weight (MW) depends on PVAc MW and the degree of hydrolysis.[83]

PVA hydrogels has low cost, are biocompatibility and similar to the natural tissues, therefore they have been proposed extensive applications in tissue engineering and drug delivery.[84]

Because of being water insoluble, PVA is also well known in its application in the production of fibers including its use in tubing, transportation belts, artificial leather, gaskets with good stability to oil derivatives, rubber-like items, surgeries, emulsifiers, adhesives for paper and paperboard, and in general purpose adhesives for bonding leather, paper, textiles, and porous ceramic surfaces.[83]

Physically crosslinked semi-crystalline PVA hydrogel is generally prepared through a freeze-thaw process, which produce crystallized PVA chains and amorphous chains. A group of researchers studied the rheological behavior of the aqueous solution of PVA with different molecular weights and concentration subjected to freeze–thaw process. Their results suggest that during the freezing process, there is an augmentation in the number of PVA segments participating in the crystalline junction points, while decreases exponentially during thawing in the vicinity of the critical point.[85]

Due to the existence of crystalline microdomains and H-bonding between the hydroxyl side groups, PVA can behave like a hydrogel even before doing freezing/thawing process, which depends on the polymer concentration and its molecular weight.

Crystalline microdomains which act as cross-links, form stronger physical network's structure cross-links because of the increasing of the crystallization of PVA based on the freezing/thawing treatment.[86]

PVA is a hydrophilic polymer with excellent mechanical properties which is flexible in dry state. However, its properties have been reduced because of the presence of water molecules which act as plasticizer.[87] Thus, it is necessary to improve the properties of PVA such as mechanical performance or thermal resistance at high temperature, etc. with different possible ways such as incorporation of inorganic nanofillers.

Nanocellulose has been studied as a reinforcing agent for PVA films,[88] fibers,[89] and hydrogels,[90] to increase the ability of PVA in different applications requiring high mechanical toughness and stiffness.

The demerits of using reinforcing agents are their agglomeration specially at higher cellulose loads, which reduce their reinforcement effect;[91] therefore, a good interaction between the PVA matrix and fillers is necessary in preparation of hydrogels.

I.4 Additives in Hydrogels

The mechanical properties of hydrogels can be improved by addition of additives in many ways. For instance, for increasing the strength or elasticity of hydrogels, grafting or surface coating them onto a stronger/stiffer support can be one useful method or preparing super porous hydrogel (SPH) composites, in which a cross-linkable matrix swelling additive is added.[24] For significantly modify the toughness and gelation temperature of certain hydrogels used in biomedical applications, other additives including nanoparticles or microparticles have been used.

The absence of strong mechanical properties in hydrogels can limit their application in different fields specially in biomedical and industrial area. Topological hydrogels, nanocomposite hydrogels, and double network hydrogels are such great strategies which have been established to fabricate tough hydrogels by forming ideal hydrogel networks. In the nanocomposite hydrogels, various forms of nanoparticles including silica nanoparticles, montmorillonite, graphene oxide, and titanate nanosheet participate in the formation of strong nanocomposite hydrogels.[92]

By forming chemical bonds or having strong intermolecular interactions with hydrogel matrix, additives can also serve as cross linkers and facilitating reinforcement in the mechanical properties by increasing the extent of crosslinking the hydrogel network. For example, the performance of hydrogel actuators can be dramatically improved and/ or diversified by utilizing additives such as functional nanomaterials.[24] The limitations of stimuli-responsive hydrogel actuators, such as small deformation, slow response, and weak mechanical property can be reduced by using organic or inorganic additives into the hydrogels. As a result, additives are not only useful for improving the mechanical properties of hydrogels, but also act as stimuli- responsive mediators.

Dual chemically cross-linked hydrogels,[93] dual physically cross-linked hydrogels,[94] and hybrid cross-linked hydrogels[95] are kind of dual cross-linked hydrogels with excellent mechanical performance which attract more attention in recent years.

In the hydrogel networks, physical cross-linking points appears in various forms, such as ionic interactions, hydrogen bonds, hydrophobic associations, and host–guest interactions, crystalline domains whereas chemical cross-linking points form by covalent bonds that maintain the elasticity of hydrogels. Physical cross-linking points are reversible which is the opposite in chemical cross-linking points, allowing hydrogels to recover or self-heal after large deformation or disruption.[96]

Beside using nanoparticles as additives, various kind of small-molecule and polymeric additives have been utilized. For example, there will be numerous applications for hydrogels such as cells, proteins, and nucleic acids, with rational design of utilizing bioactive additives in preparation of hydrogels.[97] Cases of successful commercialization of such functional hydrogels are being reported, thus driving more translational research with hydrogels.

In addition, natural polymers, as it mentioned above, have been used in preparation of hydrogels with their properties such as energy saving and biocompatibility. Among these natural polymers such as alginate,[98] chitosan,[99] lignin and cellulose,[100] and starch,[101] cellulose nanocrystals (CNCs) are attracting more attention because of their special properties including high specific surface area ($800 \ m^2 \cdot g^{-1}$), excellent stabilizing effect on nanoparticles, widespread availability in the environment, high crystallinity ($\geq 90\%$) to prepare good mechanical and biocompatible hydrogels.[102] Generally, CNCs act as crosslinker, strengthening agent, and dispersant. Cellulose nanocrystals are achieved with acid treatment of cellulose as demonstrated in Figure 6.[103] In acid hydrolysis, which is the method to destroy the amorphous regions in cellulose, the crystalline regions in cellulose are unaltered and this treatment produce a rod-like structure which is named cellulose nanocrystals.
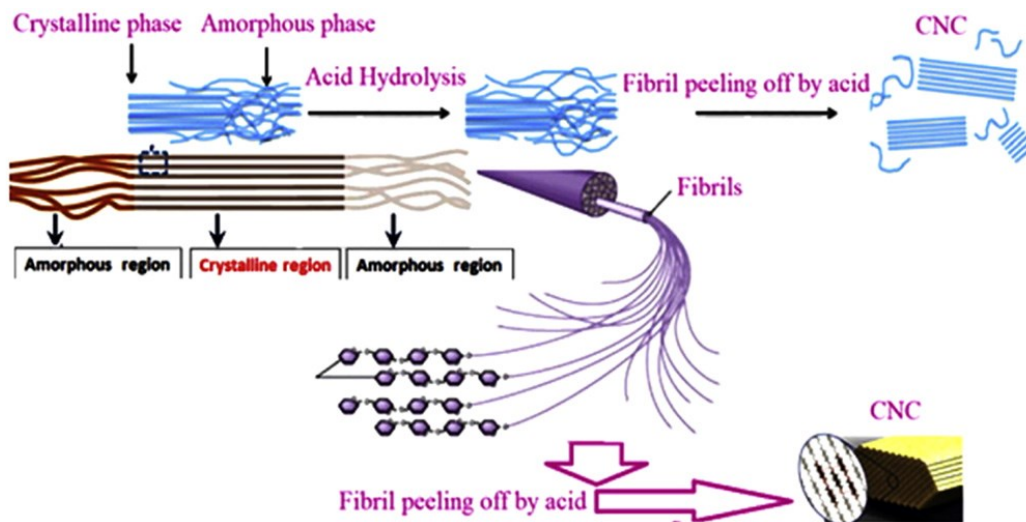
Figure 6. Scheme illustrating the extraction of cellulose nanocrystals.[103]

I.5 Objective of The Project

In the present study, we prepare and investigate the effect of two kinds of additives, CNC, which is a nanoparticle additive, and TA, which is a molecular additive, on PVA physical hydrogel. We compare the effects of nanoparticle and molecular additives with regard to the improvement of mechanical property, self-healing efficiency, and shape memory behavior of the hydrogel. The choice of CNC and TA is based on the consideration that they both, when surrounded by PVA chains, can develop multiple H-bonds with the polymer matrix through the hydroxyl groups on the PVA chains, which makes these two additives an effective physical cross-linker and modify the properties of the hydrogel.
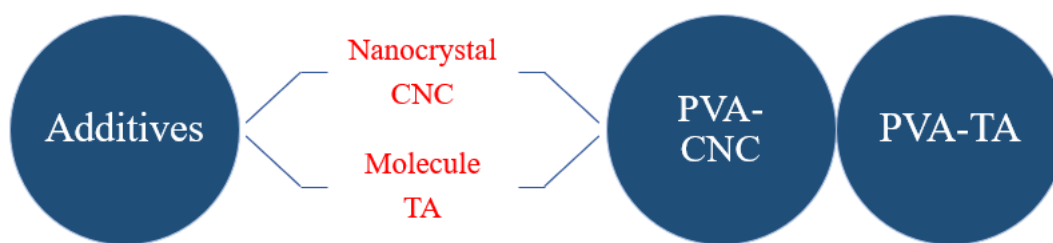
Scheme **I**.1

As mentioned above, there are many research concern with utilizing different additives to reinforce hydrogels such as PVA hydrogels.[5, 104] However, to the best of our knowledge, studies of physical PVA hydrogels containing CNC and TA, as two distinct types of additives with both forming multiple H-bonds with PVA, have not been done. This is the originality of the present project. Our studies aim to reveal how nanoparticle additive and molecular additive affect the properties of PVA hydrogel, and to find out if H-bonds linking PVA with the surface of CNC nanocrystals and with TA molecules contribute in a similar way to the mechanical properties of the hydrogel. A brief description of the two additives is given blow.

In one hand, Cellulose is a homopolysaccharide, highly crystalline and biodegradable natural polymer with the formula $(C_6H_{10}O_5)_n$, consisting of a linear chain of $(1 \rightarrow 4)$ linked d-glucose units, each of which has one primary hydroxy group(C_6–OH) and two secondary hydroxy groups (C_2–OH and C_3–OH).[105] Cellulose chains preparing with the assemblance of several glucose molecules via van der Waals and hydrogen bonds. These cellulose chains assemble to form three dimensional networks known as microfibrillated cellulose (MFC).

Cellulose nanocrystals (CNCs) are rod like particles or needle-shaped nanometric with at least one dimension <100 nm. The are stiff, with high aspect ratios (<100 nm length and 3-70 nm width) and high crystallinity (neat 90%), which depend on their condition and source of preparation.[106]

Some strong acids such as hydrochloric acid or sulfuric acid have been used to hydrolyze the cellulose by dissolving the amorphous part of cellulose presented in fiber, without effecting the crystalline parts of cellulose. Therefore, with hydrolysis of cellulose, we can separate the crystalline and amorphous parts of cellulose and prepare cellulose nanocrystals.[107, 108]

As a result, thanks to the complete crystalline structure of cellulose nanocrystals and high intermolecular bonding, CNC shows tough mechanical properties (Tensile strength of 7500 MPa and Young's modulus of 100–140 GPa).[109]
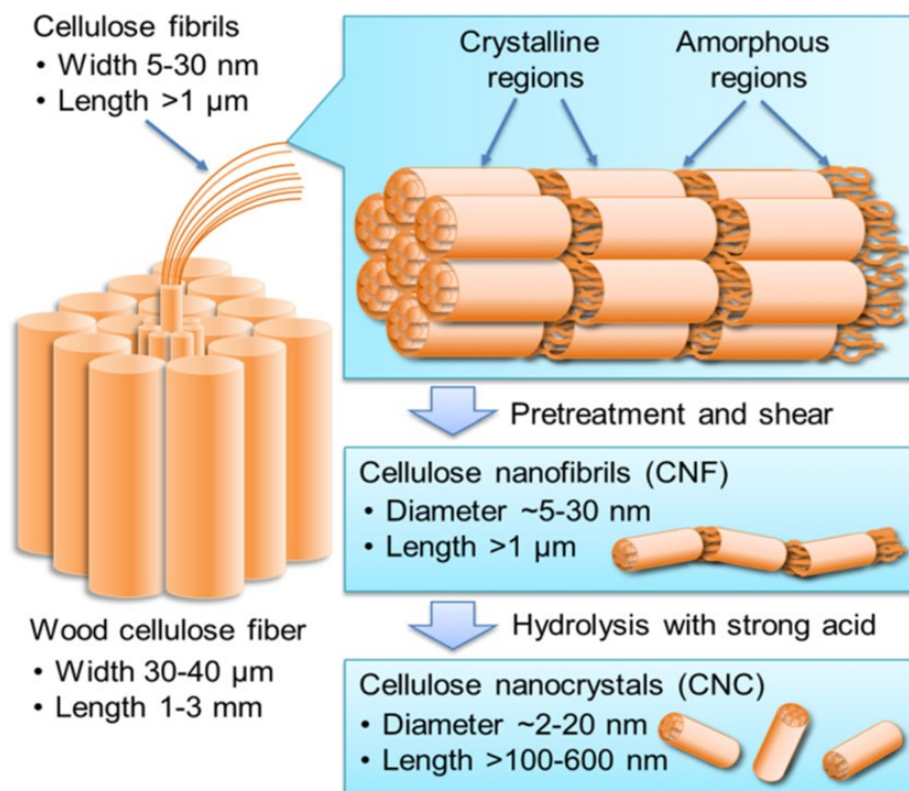
Figure 7. Schematic representation of nanocelluloses obtained from wood cellulose fibers.[110]

Thanks to the easily forming hydrogen bonding between polymers and the filler material, which enhance the mechanical properties, CNCs are recognized as effective fillers in polymer materials.[111]

On the other hand, tannic acid (TA) is a naturally produced polyphenolic compound with abundant catechol groups and catechol derivatives.

TA is a gallic ester of D-glucose with low cost, biodegradability, and nontoxicity, and can interact through several interactions such as hydrogen bonding and electrostatic interaction with macromolecules with catechol groups.[112]
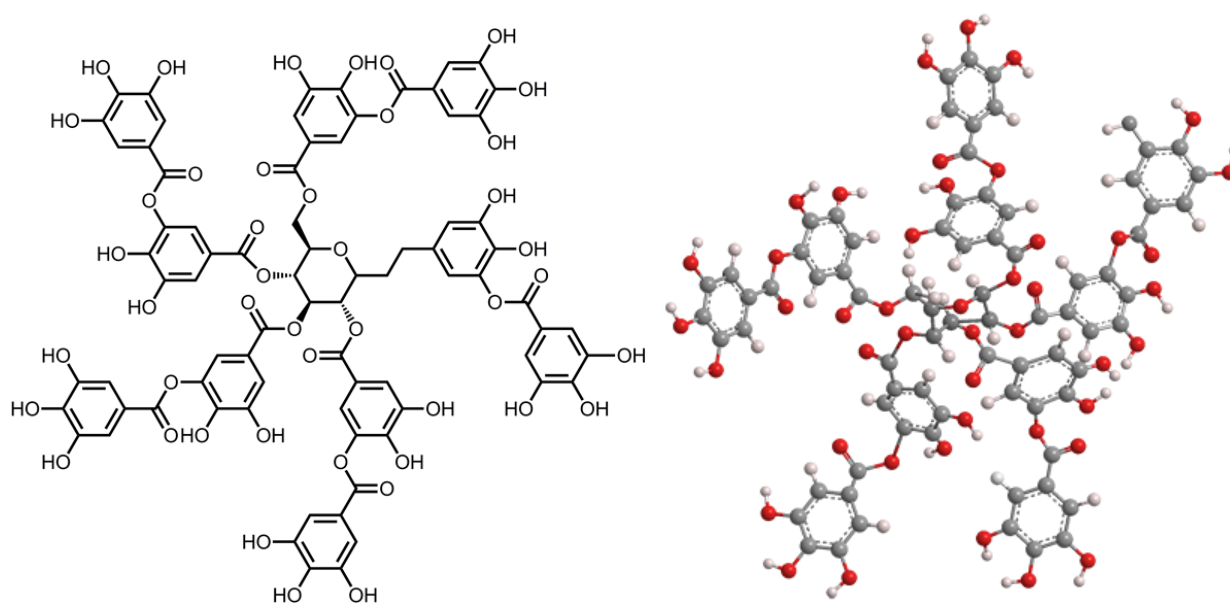
Figure 8. Molecular structure of tannic acid (TA) in a) structural formula b) ball-and-stick model.[113]

In addition, TA has been applied in the preparation of hydrogels. Thus, based on coordination interaction with metal ions,[114] polymers,[115] and other functional materials,[116] TA can form hydrogel networks. For example, PVA hydrogel with added TA was reported,[74] showing strong hydrogen bonding formed upon cooling a hot PVA solution.

Introduction of TA to the polymer matrix in hydrogen-bonded multilayers cause more stable systems due to the high pKa value of TA (8.5) and high density of hydrogen bonding because of catechol groups.[117]

On the other side, TA can act as a cross-linking agent because of its easily interact with some biopolymers such as chitosan,[118] and collagen,[119] gelatin[120]. For instance, it has been used as a crosslinker in gelatin films, enhancing the conjunction of the hydrogen bonding between gelatin and TA molecules.[117]

In addition, TA can act as a H-bonding based crosslinker, which form more stable structure due to the reorganization toward an anhydrous conformation.[120]

So, in this study, in principle tannic acid and cellulose nanocrystals is using as a minor additive cross-linker of PVA hydrogels.

CHAPTER 1. METHODOLOGY AND SYNTHESIS

1.1. Materials

Poly (vinyl alcohol) PVA (99+% hydrolyzed, Mw = 146000−186000 g/mol) were purchased from Sigma Aldrich. CNC with nominal dimensions of 100 by 5 by nm was purchased from CelluForce Inc., Canada. Tannic Acid (TA) (Mw = 1701.20 g/mol) was purchased from Fischer-Scientific. Deionized water was used throughout the experiments.

1.2. Instruments and Measurements

1.2.1 Test of self-healing

For self-healing experiments, the rectangular-shaped specimens were cut into halves using a blade. Immediately after, the two separate pieces were brought into contact without applied stress in air and were covered with silicon band and sealed at 25 °C for 12 h to prevent water evaporation. During the healing process, no stress or outside stimulation was applied to the interface during the 12 h self-healing process.

To better observe the self-healing, two pieces of original hydrogels, one of which contains a red pigment for visualization of the interface of cut surfaces, were prepared using PVA and one freezing/thawing cycle. They were cut into two pieces using scissors or blade and two halves taken from each of the original hydrogels were put together rapidly to have their freshly created fracture surfaces brought into contact. A single piece of hydrogel emerged quickly from the two halves without any stimulus or healing agent; The pigment molecules visibly diffuse from one-half to the other half. After 12 h, while the cut region on the surface was still visible, the interface in the bulk disappeared almost completely; and the self-healed, one-piece hydrogel could withstand almost all kinds of mechanical forces without failure at the interface, such as bending, twisting, compressing, and stretching to a large extension.

1.2.2 Swelling of hydrogel

The swelling ratios of PVA hydrogels in distilled water were determined as follows. Typically, a piece of hydrogel was dried completely at room temperature. Immediately after drying, the sample was soaked in distilled water at 25 °C for 2 days, during which, the hydrogel was weighed with various time intervals. In the end, after gentile removing the excess water on the surface of the swollen hydrogel, the hydrogel

in equilibrium with water was weighed. The degree of swelling was calculated using the following equation:

$$\text{Degree of swelling } W = \frac{(Ws-Wd)}{Wd} \times 100 \qquad \text{Equation 1.1}$$

where Wd, is final dry weight of the extracted PVA hydrogel and Ws is swollen weight of the same PVA hydrogel at immersion time (t) in distilled water.

The water content in the as-prepared PVA based hydrogels was also determined. To this end, the prepared hydrogels were weighed right after completing the freeze-thawing process (W_i). The hydrogels were then completely dried at room temperature for 72 h and their weights were measured immediately after (W_d). Finally, the water content is calculated according to:

$$\text{Water content (\%)} = \frac{(Wi-Wd)}{Wi} \times 100 \qquad \text{Equation 1.2}$$

1.2.3 DSC measurements

Differential scanning calorimetry (DSC) analysis was performed with a DSC Q200 calorimeter equipped with a liquid nitrogen cooling unit (Temperature precision: ±0.05 ˚C, Temperature accuracy: ±0.1 ˚C). DSC is used to determine the temperature and heat flow associated with material phase transitions as a function of temperature or, isothermally, over time. The instrument functions by measuring the difference in the heat flux required for maintaining the sample ($3-8$ mg, encapsulated in a pan) and a reference (an empty pan) at the same temperature. With the sample and reference pans sitting upon a thermoelectric disk surrounded by a furnace under nitrogen atmosphere, as the temperature of the furnace is changed by supplying heat in the temperature range 40–240 ˚C at a cooling/heating rate of 10 ˚C min^{-1}, the heat is transferred to the sample and the reference pan through the thermoelectric disk. The differential heat flow to the sample and reference is measured by using the thermal equivalent of Ohm's law.

From the DSC measurements, we can obtain qualitative and quantitative information including glass transitions in amorphous/semi crystalline materials, melting points, boiling points, crystallization time and temperature.

1.2.4 XRD

The crystallites of PVA in the hydrogels prepared using freezing-thawing are important because they play the role of crosslinks. They can be monitored and analyzed by means of X-ray diffraction (XRD). The samples were cut to approximately $1 \times 1 \times 1$ mm³, glued with silicone on the goniometer head and mounted at room temperature on a Bruker APEX DUO X-Ray diffractometer. A total of 6 correlated runs

with Phi Scan of 360 degrees and exposure times of 270 seconds were collected with the Cu micro-focus anode (1.54184 Å) and the CCD APEX II detector at 150 mm distance. These runs were then treated and integrated with the XRW^2 Eval Bruker software to produce wide-angle X-ray diffraction (WAXD) pattern from 2.5 to 82 degrees 2-theta. The crystallinity of PVA in the hydrogels, in terms of the crystallinity index (CrI), could be estimated using XRD according to the following Equation:

$$CrI = \frac{Ac}{(Ac-Aa)} \times 100 \qquad\qquad \text{Equation 1.3}$$

where Aa is experimental integrated intensity of amorphous phase and Ac is experimental integrated intensity of crystalline phase.

In general, we observe broad diffraction peak (halo) for an amorphous polymer and sharp diffraction X-ray peaks for crystallin regions of polymers.[121]

1.2.5 Infrared Spectroscopy

Attenuated Total Reflectance Fourier Transform Infrared Spectroscopy (ATR-FTIR) was utilized to characterize the obtained PVA based hydrogels, providing information on H-bonding, cross-linking and the chemical structures. An Agilent Cary 630 FTIR spectrometer was used to get IR spectra in the transmittance mode spectra at frequencies ranging from 4000-400 cm^{-1} with a resolution of 4 cm^{-1}, at room temperature.

1.2.6 Tensile Test

Depending on the type of application, PVA hydrogels may need improved mechanical and thermal properties. Tensile tests of the hydrogels were performed using an INSTRON 3366 universal testing machine with a 1000 N load cell at room temperature at a crosshead speed of 5 mm/min.

The samples placed between two clamps are rectangular bar with dimensions (25 mm (length) × 10 mm (width) × 5 mm (thickness)). Among the mechanical properties of interest for the hydrogels, the toughness was measured by calculating the area bounded by the stress-strain curve representing the energy absorbed by the specimen; the elastic (Young) modulus was calculated by the slope of initial linear region of the stress−strain curves (usually over 10−20% of strain); and the tensile stress σ, which is the force divided by the initial cross-sectional area of hydrogel sample, was taken as the highest stress on the stress-strain curve.

1.2.7 Shape memory Test

The hydrogel should be mechanically strong enough to keep the deformed state (temporary shape) by formation of physical network after being deformed, which is important part in shape memory effect. After releasing the external force, upon breaking the physical crosslinks, the shape recovery should occur and releases the strain energy stored in the deformation process. In the PVA hydrogel, as the crystalline domains of PVA act as the physical crosslinking to stabilize a temporary shape, the shape recovery is activated by the melting of the PVA crystallites.

To observe the shape memory effect of our PVA based hydrogels, the deformation of the sample was maintained with the external force while cooling down to -22 ˚C for PVA crystallization. After that, the recovery of the sample from temporary shape to the original shape was triggered by immersing the deformed specimen in distilled water with increasing temperature gradually to 60 ˚C.

1.3. Synthesis Section

1.3.1 Preparation of PVA physical hydrogel through "freeze-thawing"

Among the methods for preparing physically crosslinked PVA hydrogels, the process of freezing–thawing cycles of PVA aqueous solutions is attractive and produces strong hydrogels, even in the presence of biological species.[122] The absence of any chemicals, including co-solvents or cross-linking agents, as well as the absence of heating makes such process particularly suitable to prepare hydrogels for biomedical applications.[123]

The formation of physically crosslinked PVA hydrogels *via* the freeze-thawing method has been widely discussed in the literatures.[124, 125]

Hydrogels prepared by freeze-thawing from PVA aqueous solutions have shown many interesting properties. They have good mechanical strength, and are stable at room temperature, with no initiators or cross-linkers.

Significant contribution to the development of PVA hydrogels prepared by this method was made by Peppas et al.[126] Depending on the concentration of PVA, the freezing–thawing time, as well as on the number of freezing–thawing cycles, the crystallization degree of PVA can be adjusted. The hydrogel formation starts during the freezing step when the free water in the polymer solution freezes, which excludes the polymer chains from the ice regions and thus leads to supersaturated polymer regions where the formation of PVA crystallites is promoted. After the two steps of freezing and thawing, the ice regions melt to create pores which stabilize by crystalline walls.[123]

In the present study, a typical freezing-thawing cycle was performed as follows. A homogenous solution of PVA was obtained by dissolving PVA powder in distilled water at 85 °C under vigorous stirring and refluxing for 3 h. In order to remove trapped bubbles, the solution was placed in an ultrasonic water bath at 45 °C for 15 min without stirring. The aqueous solutions with same amount of PVA and various contents of CNC or/and TA were then cast into the mold of desired dimensions and cooled at -22 °C for 4 h, which was followed by thawing at room temperature for 4 h. The result is the formation of physically cross-linked PVA hydrogels.

The hydrogels investigated in this work were prepared at a PVA concentration of 15%, 20%, 25% and subjected to one and two cycle of freezing-thawing. The freeze-thawing cycle was varied to change the properties of the resulting PVA based hydrogels.

1.3.2 Preparation of additive enhanced PVA hydrogel

The method for preparing PVA-TA, PVA-CNC hydrogels is the same as for pure PVA hydrogel.

For preparation of PVA-CNC hydrogel, aqueous solutions of 1, 2, 3, 4, and 5 % wt CNC in distilled water were prepared separately by stirring the solutions. Then, a weighed amount of PVA powder was added to one of CNC dispersion at 85°C under refluxing for 3 h, under vigorous stirring, to obtain uniform PVA-CNC mixture. After being held at high temperature to remove the bubbles, the aqueous homogenous PVA-CNC solution was then cast into the mold of desired dimensions and subjected to cooling to -22 °C for 4 h, which was followed by thawing at room temperature for 4 h. The same method was used for preparing PVA-TA by adding (0.5,1,2,3,4,5) wt% of TA.

CHAPTER 2. PVA HYDROGELS ENHANCED BY CNC AND TA

2.1 Abstract

In this project, we carried out the preparation, characterization and comparison of PVA-TA, and PVA-CNC hydrogels with excellent mechanical properties, self-healing, and shape memory behaviors. In these hydrogels, H bonding in PVA and between PVA and additives (TA or CNC) contribute to cross-linking. More specifically, stronger H bonds between PVA and CNC, as well as PVA and TA could act as "permanent" cross-linking, while weaker H bonds between PVA chains as "temporary" cross-linking, and the latter can fix the deformed shape of the hydrogel.[127]

Figure 9 is a schematic of preparation of PVA based hydrogels after adding CNC and TA as two different additives.
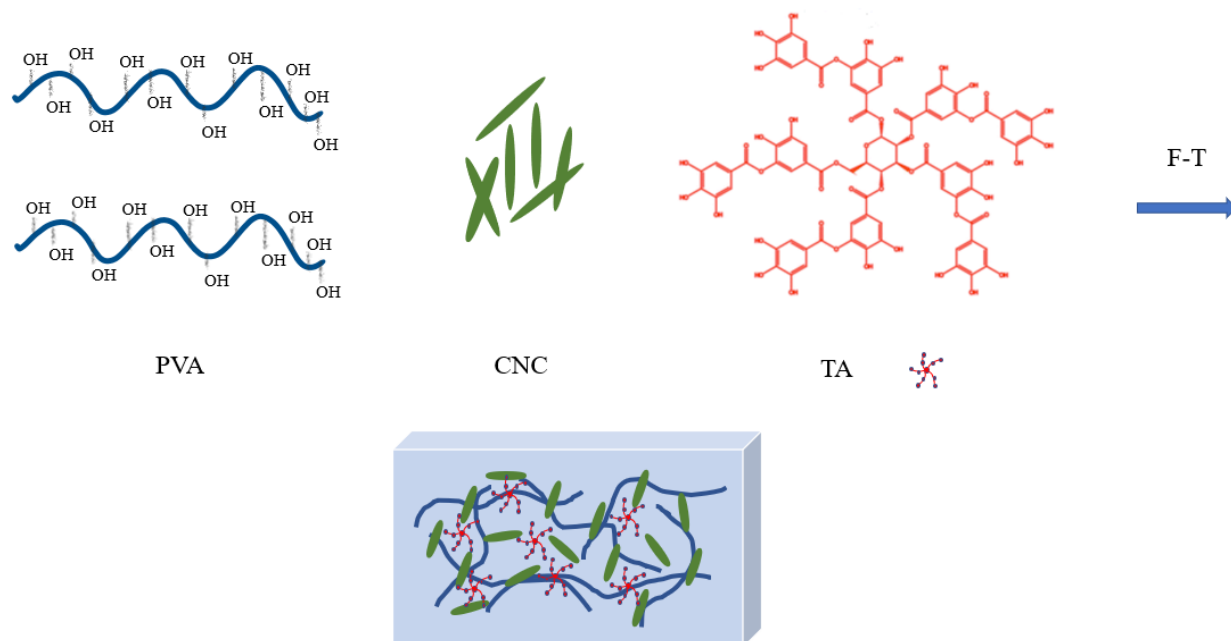
Figure 9. Illustration of the preparation of PVA hydrogels in the presence of CNC and TA additives.

2.2. Effect of Molecular Additive TA and Nanoparticle Additive CNC on PVA Hydrogels

2.2.1 Preparation of hydrogels

All hydrogels were prepared using the freezing-thawing method under the same conditions as detailed in Chapter 2. The prepared hydrogels are summarized in Table 1. At first, we prepared and evaluated PVA hydrogels without any additive. Several samples were obtained with various PVA contents (15%, 20%, and 25 wt% of PVA). Based on the obtained results, the mechanical strength of the hydrogel increases with increasing the PVA content, on one hand, in the 15% PVA hydrogel being weak while the 25% hydrogel is strong. However, with 25% PVA, it became difficult to obtain homogenous solution and remove the bubbles. Actually, the 20% PVA hydrogel shows the most effective shape recovery, better self-healing effect and retains good mechanical properties. Therefore, unless otherwise stated, the 20% PVA hydrogel was used for studying the effect of the two additives, and hydrogels loaded with different amounts of TA or CNC additives, as shown in Table 1.

Table 1. Different amount of PVA, CNC, or TA for preparation of hydrogels.

Input	PVA	CNC	TA
1	15% (1.5 g in 10ml water)	0	0
2	20% (2 g in 10ml water)	0	0
3	25% (2.5 g in 10ml water)	0	0
4	20%	1% (wt PVA) (0.02 g)	0
5	20%	2% (0.04 g)	0
6	20%	3% (0.06 g)	0
7	20%	4% (0.08 g)	0
8	20%	5% (0.1 g)	0
9	20%	0	0.5% (wt PVA) (0.01 g)
10	20%	0	1% (0.02 g)
11	20%	0	2% (0.02 g)

12	20%	0	3% (0.02 g)
13	20%	0	4% (0.02 g)
14	20%	0	5% (0.02 g)

2.2.2 Infrared spectroscopic analysis

The chemical structure and composition of all prepared samples were investigated using the ATR-FTIR. The presence of H-bonding between PVA and TA, or PVA and CNC, is noticeable in Figures 10,11, and 12, based on the presence of O-H bonding frequency. Following there are some figures that show the FTIR spectra of the prepared PVA, PVA-CNC, and PVA-TA hydrogels with different compositions.

In Figure 10, the broad bands of O-H stretching vibration for dry samples of pure PVA hydrogel of different contents (15%, 20%, 25%) are visible at 3248, 3257 and 3261 cm^{-1}, respectively. The characteristic peaks at 1080 cm^{-1} and 2914 cm^{-1} are related to stretching vibrations of the C-O and C-H, respectively. The bending vibration related to CH$_2$ groups is observed in the region of 1408 cm^{-1}, which is characteristic of semi-crystalline PVA.[128]

Figure 11 shows the ATR-IR spectra of the prepared PVA-CNC dry sample which indicates the characteristic peaks assigned to PVA and CNC structure. The spectra indicate interaction between CNC and PVA, with the −OH stretching peak of the PVA-CNC hydrogel shifted to a lower frequency of 3255 cm^{-1}. This band is subjected to the intermolecular (between PVA and CNC) and intramolecular (between PVA chains) H-bonding. The significant shifts of the absorption bands to lower frequencies suggest the formation of stronger H-bonding between PVA and CNC. It is well-known that the formation of intra- or intermolecular hydrogen bonding reduces the force constants of the chemical bonds, and hence their vibrational bands are shifted to lower frequencies.[129] Stronger hydrogen bonding leads to a more significant shift in vibrational frequency.

Figure 12 shows the ATR-IR spectra of PVA-TA dry sample which shows new peaks related to TA. Compared to PVA, the hydrogel containing TA displays new absorption peaks in 1705 cm^{-1} and 1559 cm^{-1}, which are assigned to the aromatic C=O stretching vibration mode of ester and aromatic C=C ring stretching. The band located at 1207 cm^{-1} attributed to the C-O stretching mode of ester, indicating the presence of the ester groups in the TA structure in the PVA-TA hydrogel.[134,135] The broad and strong absorption bands of symmetrical stretching vibration of hydroxyl groups (O–H) are shifted to a lower frequency of 3248 cm^{-1} after being treated with TA. The red shift of the peak is related to the reduction of the force constants of the chemical bonds and implies that hydrogen bond cross-linking is formed between PVA and TA. In addition, the ATR-IR spectra of PVA-CNC and PVA-TA hydrogels show no new peaks resulting from chemical reactions, indicating that the cross-linking system is exclusively enabled by physical effects.[119]

It can be deduced from this wavelength shift that the hydroxyl groups of PVA, TA and CNC are involved in the formation of extensive hydrogen bonds among them. These findings imply good mixing of TA and CNC in the PVA polymer matrix.
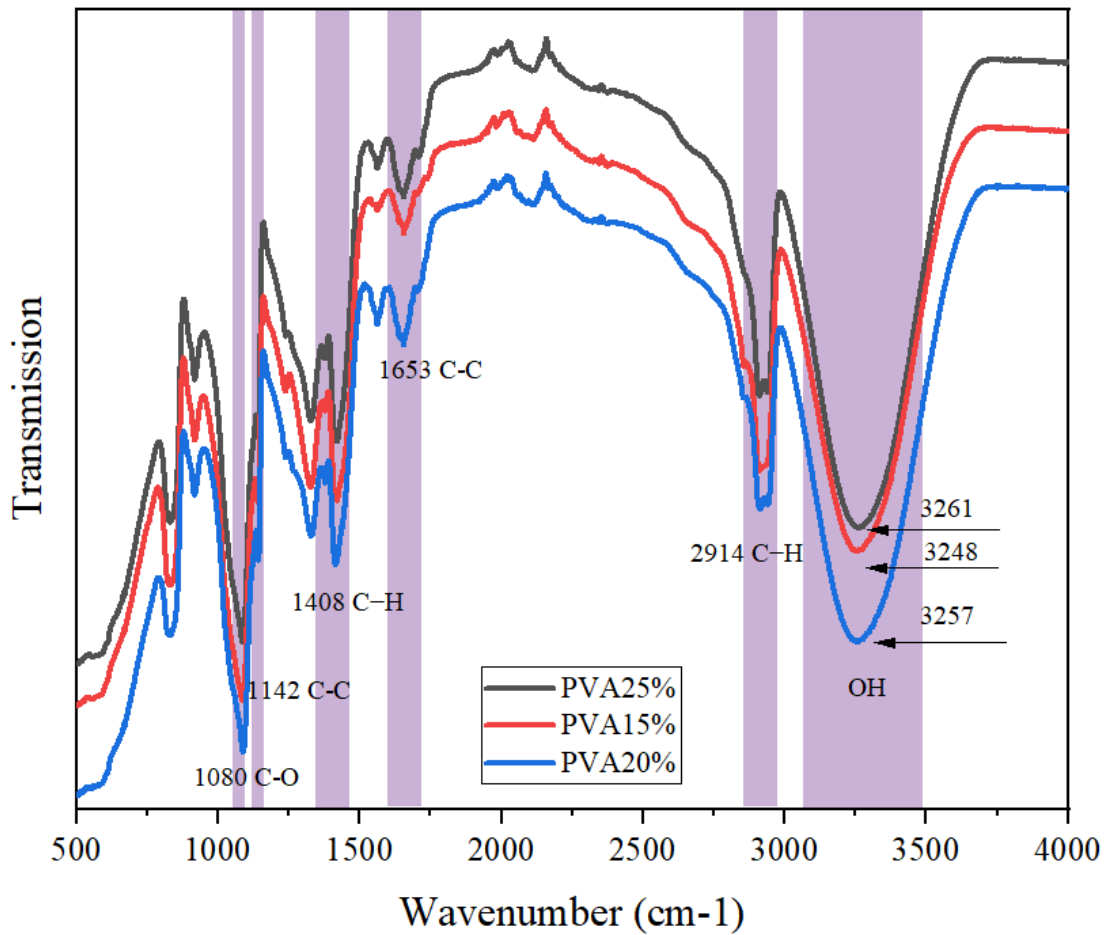
Figure 10. ATR-IR spectra of hydrogels with different PVA contents.
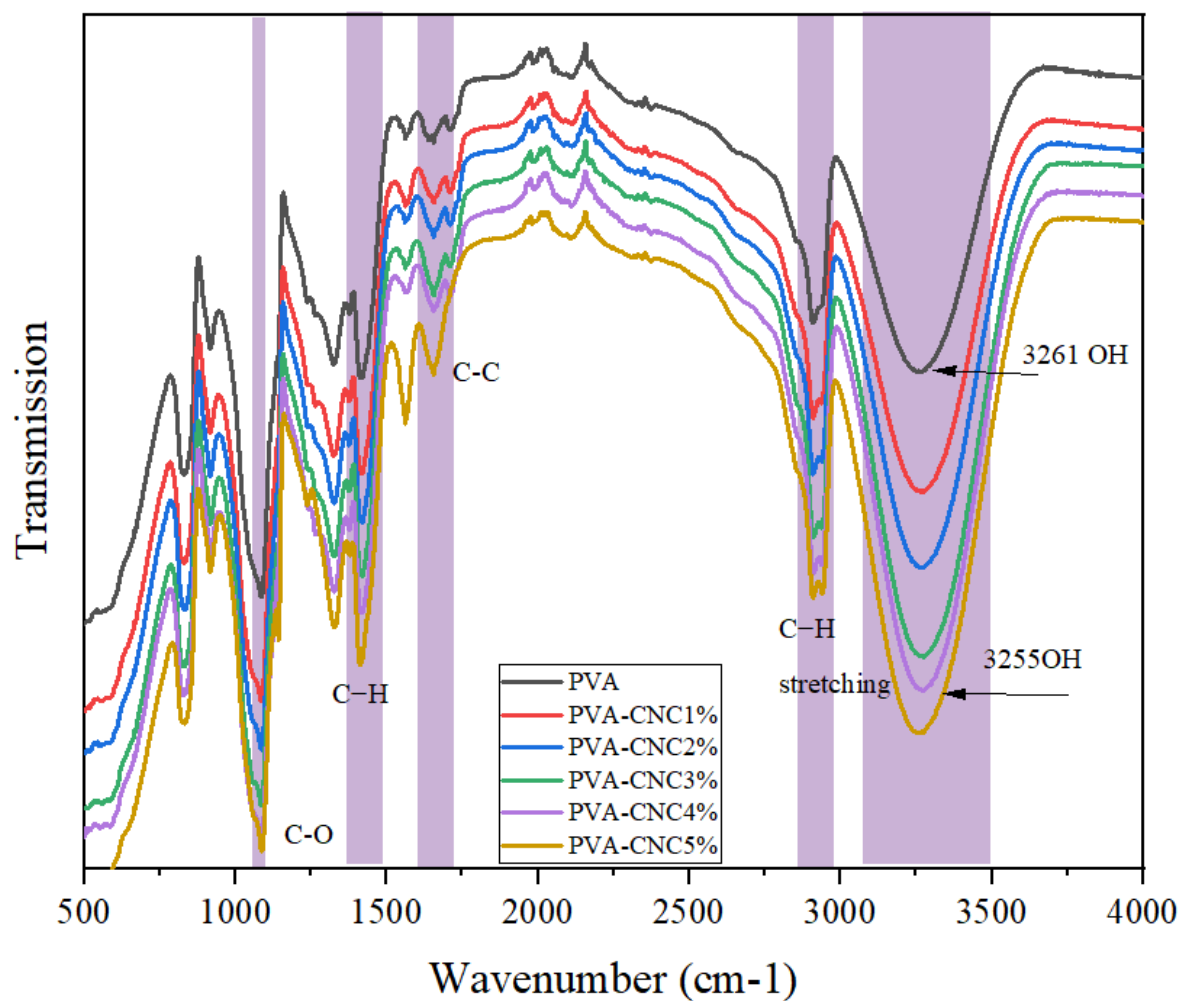
Figure 11. ATR-IR spectra of the 20% PVA hydrogels containing various amounts of CNC.
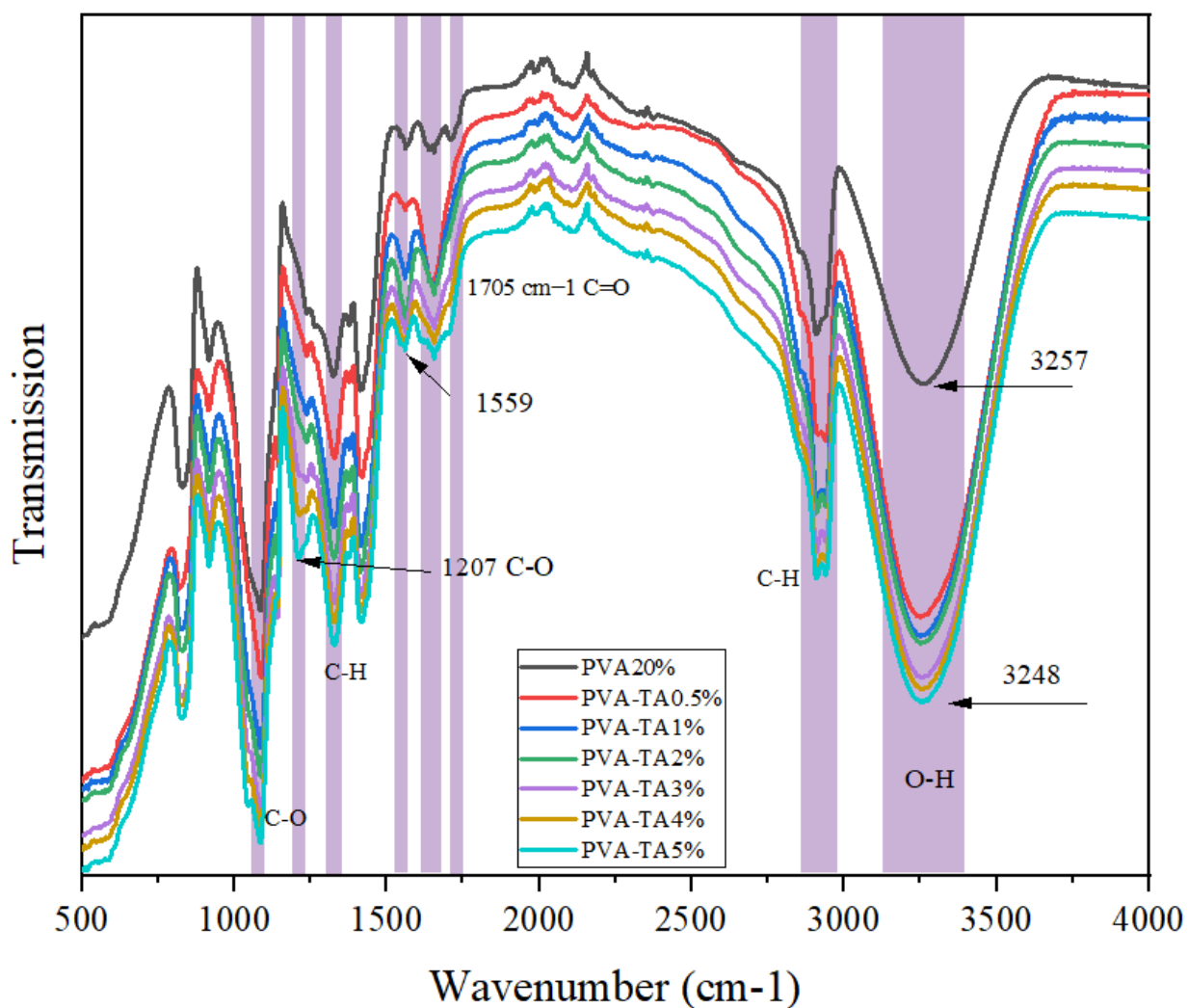
Figure 12. ATR-IR spectra of the 20% PVA hydrogels containing various amounts of TA.

2.2.3 Thermal properties

DSC measurements were carried out to study the influence of additives on the thermal phase transition behaviors of PVA hydrogels using dry samples. The results are shown in Figure 13 for the samples containing CNC and in Figure 14 for the samples with TA additive, while Tables 2 and 3 summarize the transition temperatures and the associated enthalpies. Figure 13 presents the heating and cooling DSC curves of PVA-CNC dry samples. As expected, neat PVA shows a high melting temperature (T_m) at 215 °C. Although removing the residual water in the PVA sample during the first heating run, the plasticization effect of water on PVA chains is still preserved at high temperature, leading to a decrease in the melting point of PVA. With increasing the content of CNC in the hydrogel, the melting peak of

PVA becomes increasingly weaker and broader, and gradually shifts to a lower temperature, from 223 ˚C for PVA-CNC (1%) to 216 ˚C for PVA-CNC (5%). Similar effects can be noticed for PVA-TA samples (Figure 14). The effect is due to the hydrogen bonding in PVA-TA and PVA-CNC samples, which disrupts the regular structure and improving the movement of PVA chains. In particular, T_c of the samples with 5% CNC and 5% TA decreases and the transition peak broadens most importantly. Obviously, the introduction of CNC and TA into the PVA matrix significantly disturbs the regularity of molecular chain arrangement in PVA upon cooling, thus hindering its crystallization.

PVA-TA and PVA-CNC hydrogels exhibit reduced crystallinity than pure PVA due to the presence of the molecular additive TA or the CNC nanoparticles in the polymer matrix. In fact, the presence of large numbers of additives could restrict the free motion of polymer chains. Therefore, after incorporation of TA or CNC, more energy is required for polymer chains to overcome the steric hindrance. This phenomenon occurs due to the hydrogen bonding between PVA and additives which could prevent the formation of PVA crystallites. On the other side, the exothermic peak on cooling reflects the capability of polymer chains to mobilize or re-arrange themselves into ordered crystals. The interacting TA or CNC exerts the same effect of hindering the crystallization of PVA chains.
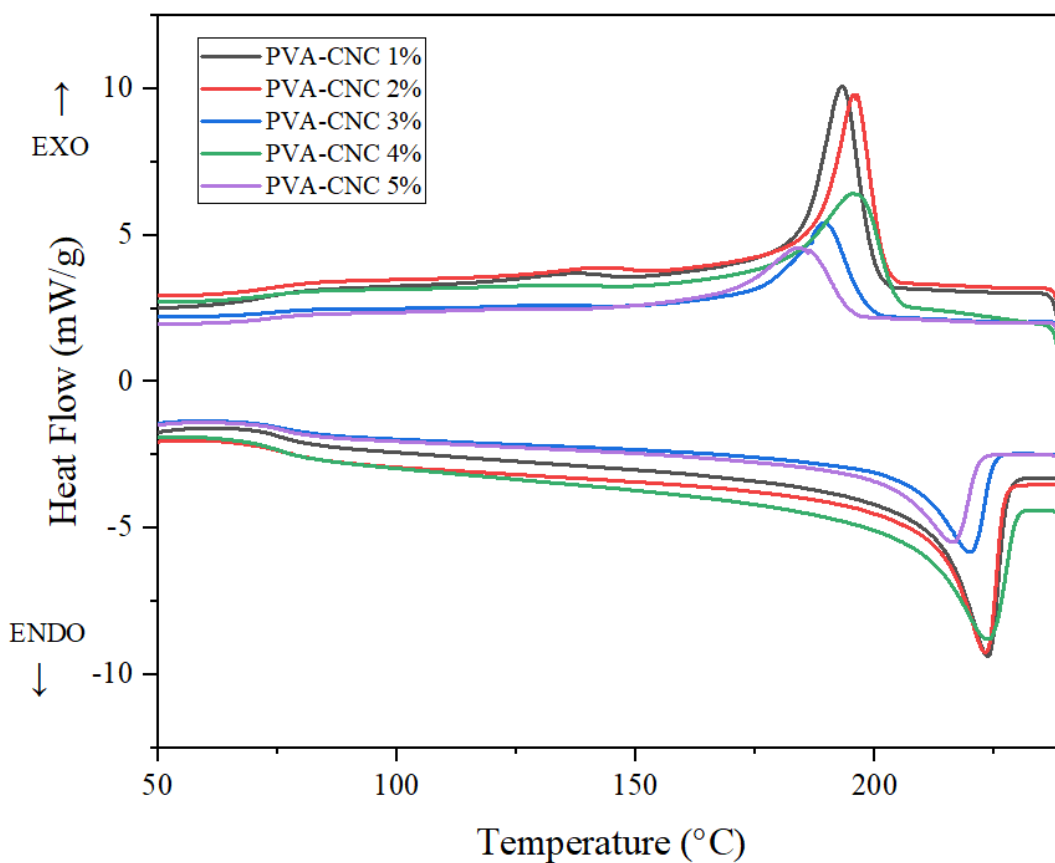
Figure 13. DSC heating and cooling curves of CNC-loaded PVA hydrogels (20% PVA).

Table 2. Thermal phase transition temperatures and enthalpies of CNC-loaded PVA hydrogels (20% PVA).

Input	Samples	T_m (°C)	ΔH_m (J/g)	T_c (°C)	ΔH_c (J/g)	% Crystallinity
1	PVA-CNC 1%	223.7	-39.7	193.7	41.9	26.20
2	PVA-CNC 2%	223.3	-53.9	196.3	47.0	29.4
3	PVA-CNC 3%	220.1	-48.5	189.6	38.7	24.2
4	PVA-CNC 4%	223.8	-42.0	196.4	31.7	19.9
5	PVA-CNC 5%	216.6	-35.7	184.9	25.6	16.0
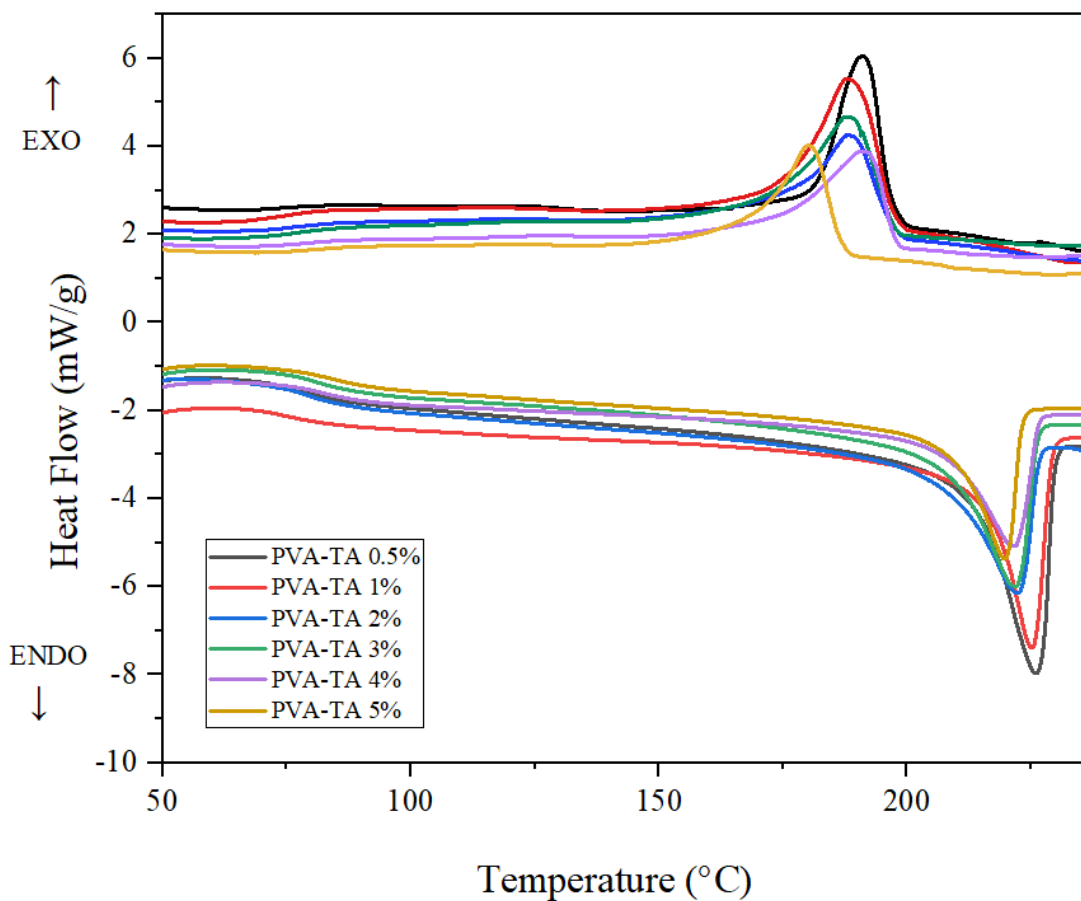
Figure 14. DSC heating and cooling curves of TA-loaded PVA hydrogels (20% PVA).

Table 3. Thermal phase transition temperatures and enthalpies of TA-loaded PVA hydrogels (20% PVA).

Input	Samples	Tm (°C)	ΔHm (J/g)	Tc (°C)	ΔHc (J/g)	% Crystallinity
1	PVA-TA 0.5%	225.9	-34.7	190.5	43.9	27.5
2	PVA-TA 1%	224.7	-30.9	188.1	35.7	22.3
3	PVA-TA 2%	222.6	-40.1	188.8	31.4	19.6
4	PVA-TA 3%	221.1	-44.9	188.3	31.0	19.4
5	PVA-TA 4%	221.7	-49.6	191.2	32	20.0

| 6 | PVA-TA 5% | 219.6 | -40.4 | 180.4 | 28.35 | 17.7 |

2.2.4 Self-healing

Our group reported the autonomously self-healed physically cross-linked PVA hydrogel at room temperature, prepared by using the freezing/ thawing method, without need for any stimulus or healing agent.[124] PVA with physical network is known to be self-healable due to a sufficient amount of free hydroxyl groups on the surface of the hydrogels which cause complete merging. The fractured PVA hydrogel can be healed spontaneously and rapidly without external treatment due to having multiple hydrogen bonds between PVA chains, which is much convenient compared with other self-healable tough hydrogels. This property can be seen in PVA-CNC and PVA-TA hydrogels too.
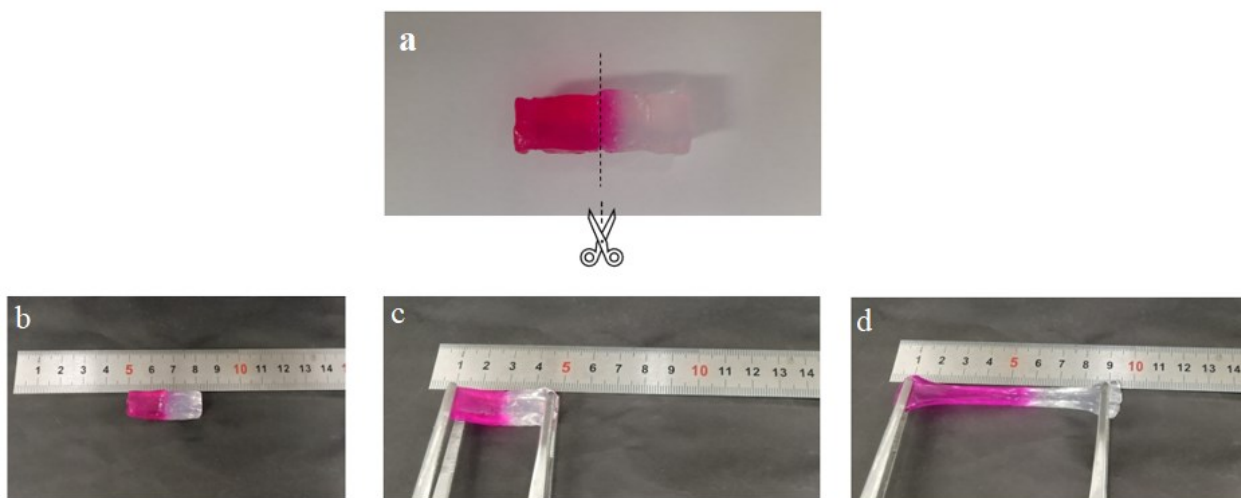
Figure 15. Photos showing the self-healing behavior of PVA hydrogel: a,b) two pieces of original hydrogels with and without rhodamine B for coloration are brought together; and c,d) stretching of the self-healed hydrogel.

This phenomenon is visually observable as shown by the photos in Figure 15. Two original PVA hydrogels with and without rhodamine B for coloration (for visualization in the interface of cut surfaces) were cut into two equal halves from the middle. The two separate pieces of hydrogels were brought into

contact, without hard pressing, for self-healing in a container for 12 h in air at room temperature without any external stimulus or addition of healing agents. Finally, the self-healed, one-piece hydrogel could withstand all kinds of mechanical force such as stretching.

The same self-healing experiment has been done for PVA-CNC and PVA-TA hydrogels with different percentage of additives. Based on the structures of the additives, the result of self-healing effect was different. At a small amount of additive, the self-healing effect was similar, which can be seen from the mechanical test of hydrogels (Section below). In PVA-TA hydrogel, self-healing effect decreases with increasing the content of TA. This is because although its polymer content is high and there are enough H bonds to regenerate the hydrogel network on the contacting interface, but the strength of the H bond formed between PVA is relatively weak and causes poor self-healing performance.[130]

2.2.5 Tensile tests

Regarding the self-healing property, the usual tensile testing was performed on the original and self-healed hydrogel samples to quantify the self-healing efficiency. We characterized the mechanical properties of the additive-enhanced PVA hydrogels, by measuring the stress-strain curves of the samples before and after self-healing.

Figure 16 shows the stretching ability of PVA, PVA-CNC 1%, and PVA-TA 1% hydrogels, respectively, at room temperature. As shown in these pictures, the self-healed hydrogels show good stretchability without being fractured from the cut part.

Figure 16. Tensile stress-strain measurements showing the stretching of self-healed hydrogel samples of PVA (a), PVA-CNC 1% (b) and PVA-TA 1% (c).

To get more insight into the self-healing behavior, the healing efficiencies of the hydrogels with different CNC contents were measured, and the results are shown in Figure 17. This figure shows tensile test of prepared samples of PVA and PVA-CNC with different amounts of CNC added to PVA solution to prepare hydrogels. The solid lines are for the original prepared hydrogels (sample acronym terminated with -O) and dashed lines for self-healed samples (acronym terminated with -SH).

Figure 17. Stress-strain curves of PVA, PVA-CNC 1%, PVA-CNC 2%, PVA-CNC 3%, PVA-CNC 4%, PVA-CNC 5%, for original (solid lines) and self-healed(dashed-lines) hydrogels.

It is evident that adding even a small number of additives, such as 1 wt % CNC to the PVA hydrogel can enhance the mechanical properties such as the Young's modulus, elongation at break, tensile strength, and, as a result, toughness. This beneficial effect is proportional to the content of additives over the range investigated. These results can be explained by the formation of a large amount of H-bonds between the CNC and PVA chains. The multiple H-bonded crosslinking in the hydrogel leads to a stable and mechanically strong physical network of PVA.[131]

With respect to pure PVA hydrogel, which displays a tensile strength of only 0.025 MPa at the ultimate elongation of 300%, the addition of physically cross-linked CNC improves much the tensile strength, and the increase becomes more prominent with increasing the CNC content. As can be seen, the hydrogels with 1, 2, 3, 4, and 5 wt % CNC have a tensile strength up to 0.03, 0.05, 0.06, 0.07, and 0.07 MPa, respectively, showing a strong reinforcement capability of CNC in PVA hydrogel.[129] Moreover, despite the increase in hardness, their ultimate elongation remains significant, decreasing from 298% for pure

PVA to 125% for PVA-CNC 5%, while the latter has greater toughness. Indeed, the elongation at break (ε) reduced gradually with the increase of CNC loading. On the other hand, it is no surprise to find that a higher CNC content results in a larger decrease in healing efficiency over the entire time. As mentioned above, the self-healing property of PVA hydrogel is related to the hydrogen bonding formed by hydroxyl groups of polymer chains, and the addition of CNC network reduces the PVA chain mobility in the hydrogel. These effects become more important by increasing the content of CNC.

On the other side, we observe the same trend of results for self-healing hydrogels, which show reduction in tensile strain from 251% to 151% and increase in tensile stress from 0.013 MPa to 0.049 MPa for pure PVA hydrogel and PVA-CNC 5% hydrogel respectively.

Table 4 collects the data of mechanical properties, including Young's modulus, elongation at break and tensile strength, for pure PVA and CNC-loaded PVA hydrogels, for both original and self healed samples.

Table 4. Tensile stress, elongation at break, and Young's modulus for PVA, PVA-CNC (1%,2%,3%,4%, and 5%) original and self-healed hydrogels.

Input	Samples	Tensile stress (MPa)	Elongation at break (%)	Young's modulus (MPa)
1	PVA-O	0.026	229.5	0.0051
2	PVA-CNC 1%-O	0.030	159.1	0.0196
3	PVA-CNC 2%-O	0.046	148.2	0.0291
4	PVA-CNC 3%-O	0.063	135.1	0.0356
5	PVA-CNC 4%-O	0.066	109.1	0.0634
6	PVA-CNC 5%-O	0.065	125.4	0.0409
7	PVA-SH	0.018	251.1	0.0051
8	PVA-CNC1 %-SH	0.026	148.1	0.0215
9	PVA-CNC 2%-SH	0.041	126.8	0.0357
10	PVA-CNC 3%-SH	0.050	124.1	0.0324
11	PVA-CNC 4%-SH	0.037	65.1	0.0620
12	PVA-CNC 5%-SH	0.033	79.8	0.0431

Figure 18 shows the tensile strain-stress curve of PVA-TA original and self-healed hydrogels with different amounts of TA as an additive. Same as adding CNC to prepare PVA hydrogel, adding TA to PVA can keep the self healing effect and enhance the mechanical properties of PVA hydrogel at the same time due to the multiple H-bonding between the two constituents. However, increasing the amount of TA reduces more importantly the self-healing capability of the hydrogel even though the tensile stress and strain continue to increase. Interestingly, the ultimate elongation also increases with increasing the amount of TA, suggesting that with respect to a relatively weak physical network of PVA, an enhanced physical network structure due to hydrogen bonding with TA can better sustain the stress arising from chain extension in the double-network hydrogel, making the failure occur at a greater elongation of the sample.
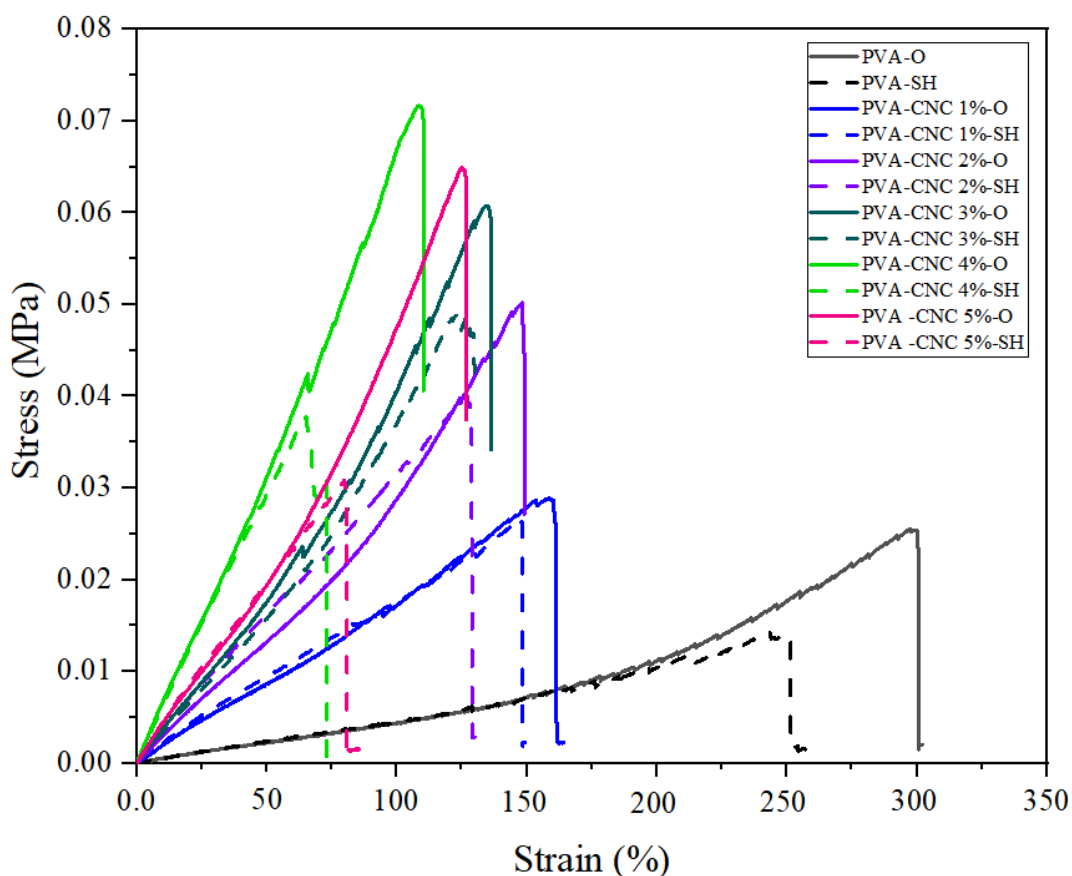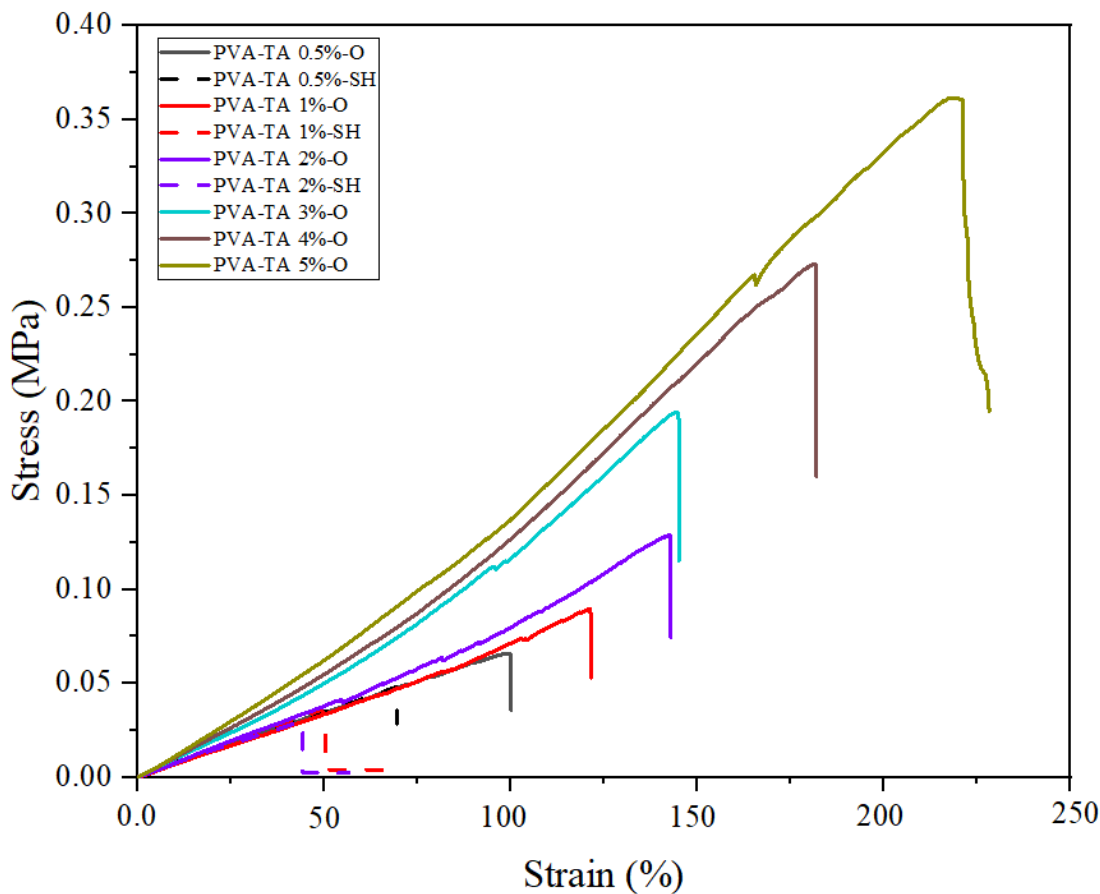

Figure 18. Stress-strain curves of PVA-TA 0.5%, PVA-TA 1%, PVA-TA 2%, PVA-TA 3%, PVA-TA 4%, PVA-TA 5%, for original (solid lines) and self-healed(dashed-lines) hydrogels.

Likewise, the data of the mechanical properties for all investigated PVA-TA hydrogels, both original and after self-healing, are summarized in Table 5.

Table 5. Tensile tress, elongation at break, and Young's modulus calculation for PVA, PVA-TA (0.5%,1%,2%,3%,4%, and 5%) original and self-healed hydrogels.

Input	Samples	Tensile stress (MPa)	Elongation at break (%)	Young's modulus (MPa)
1	PVA-TA 0.5%-O	0.071	100.0	0.0758
2	PVA-TA 1%-O	0.089	121.3	0.0695
3	PVA-TA 2%-O	0.107	142.6	0.0785
4	PVA-TA 3%-O	0.183	144.9	0.0954
5	PVA-TA 4%-O	0.228	181.5	0.1068
6	PVA-TA 5%-O	0.386	220.4	0.1204
7	PVA-TA 0.5%-SH	0.038	44.5	0.0754
8	PVA-TA 1%-SH	0.035	50.0	0.0785
9	PVA-TA 2%-SH	0.025	69.9	0.0731
10	PVA-TA 3%-SH	-	-	-
11	PVA-TA 4%-SH	-	-	-
12	PVA-TA 5%-SH	-	-	-
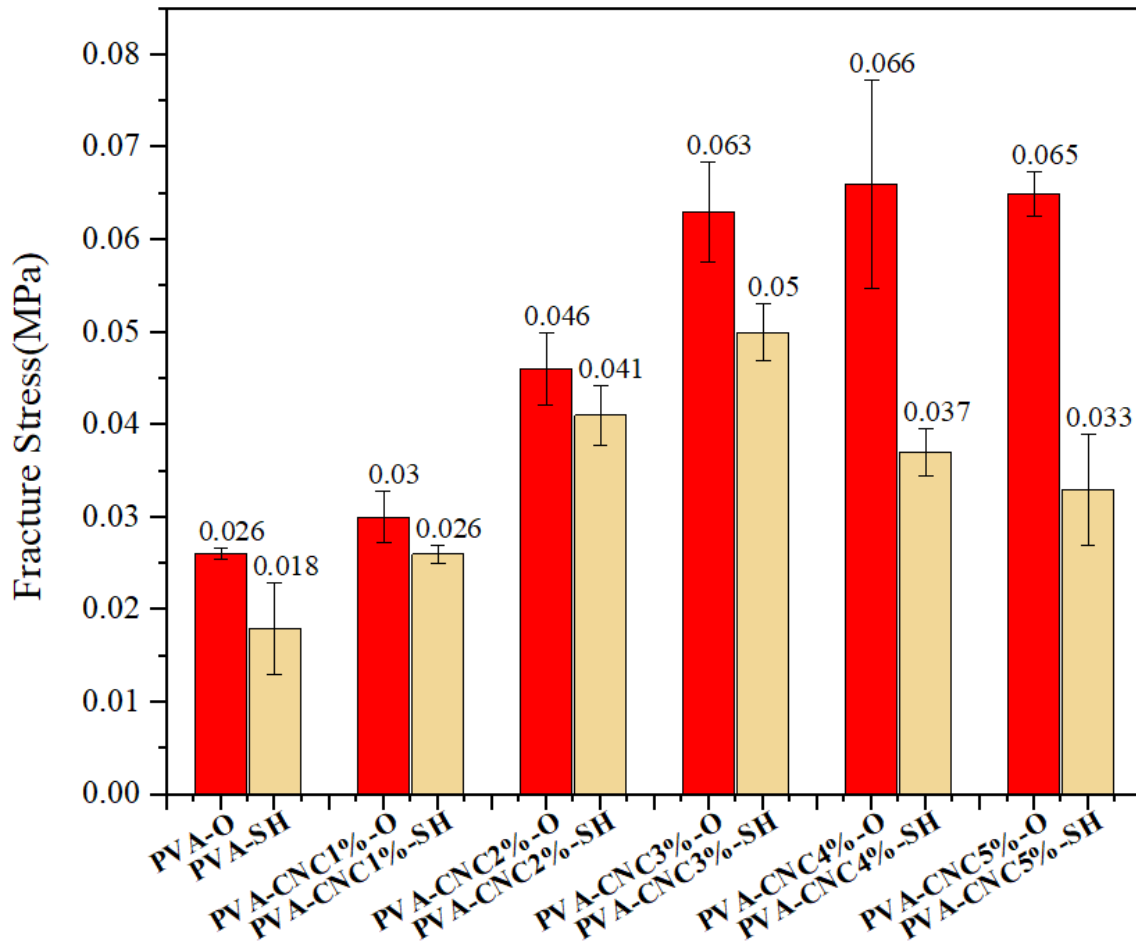
Figure 19. Fracture stress of PVA, PVA-CNC (1%, 2%, 3%, 4%, and 5%) original and self-healed hydrogels.

For both PVA-CNC and PVA-TA hydrogels, the tensile strength, defined as the highest stress that can be sustained by a sample before breaking, turns to be the stress at the breaking, i.e., the fracture stress. Figures 19 and 20. show the fracture stress of prepared samples of PVA-CNC and PVA-TA hydrogels, respectively. The results show that with increasing the content of CNC or TA, the fracture stress increases. For PVA-CNC, the fracture stress is plateaued after 3% CNC, and the self-healing effect starts to diminish.
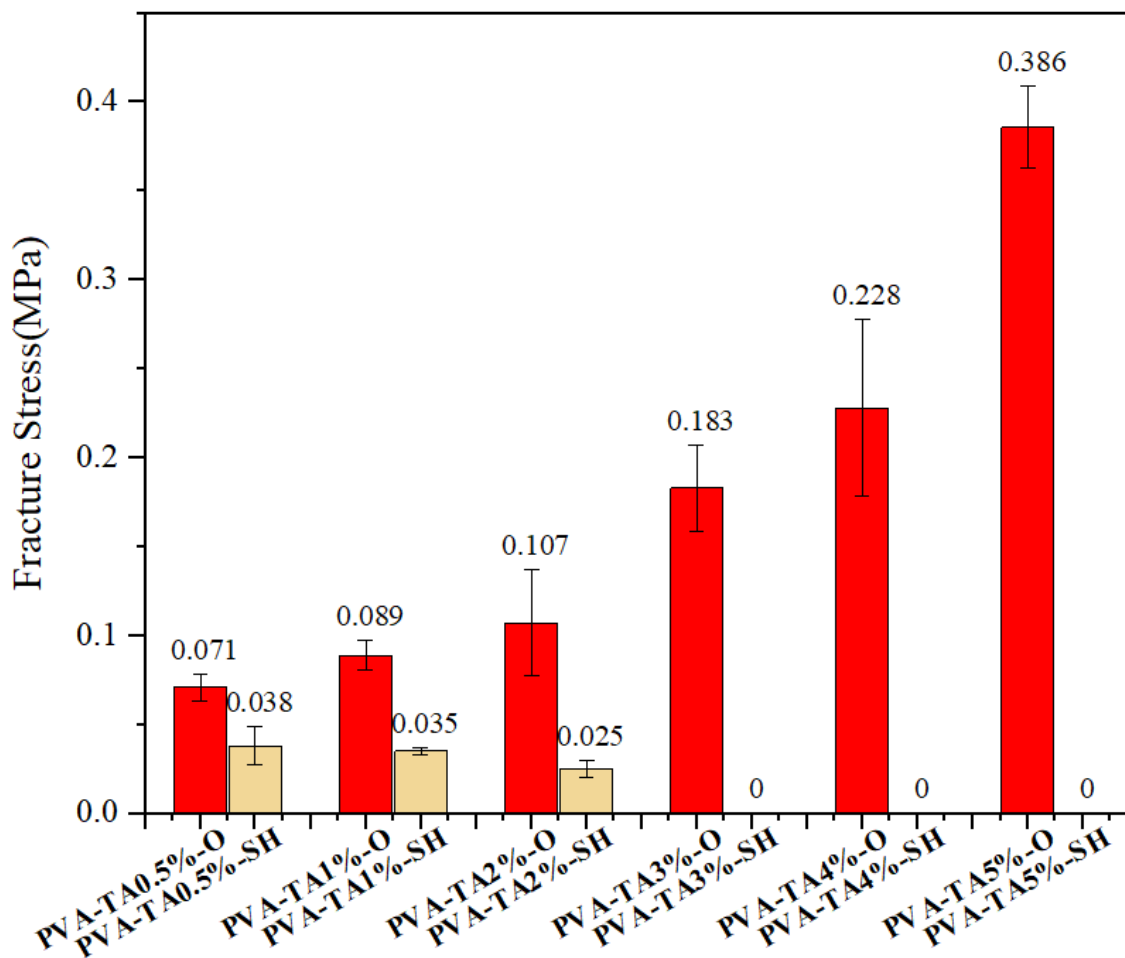
Figure 20. Fracture stress of PVA, PVA-TA (0.5%,1%, 2%, 3%, 4%, and 5%) original and self-healed hydrogels.

In the case of PVA/TA, with the increase of TA content and the freezing time during the hydrogel preparation, the mechanical strength of the hydrogel increases significantly, while the self-healing efficiency decreases. This is because with more TA molecules forming multiple H-bonds with PVA chains or with more crystallized PVA (longer freezing time), the mobility of PVA chains is reduced, which causes the increase of the mechanical strength of the hydrogel. As a result, the diffusion of polymer chains and the reconstruction of H-bonds are restricted, and poor self-healing performance appears. Therefore, there will be a balance point where the PVA-TA hydrogel has both high mechanical strength and good self-healing properties.[132]

The whole of the results indicate that the addition of either CNC or TA in PVA hydrogel presents a significant positive effect on enhancing both the mechanical strength (tensile strength) and the stiffness (Young's modulus) of the obtained hydrogels. However, the effect of the molecular additive TA is much stronger than the effect of the nanoparticle additive CNC. The most important difference can be noticed

by comparing the tensile test results in Figure 19 for PVA-CNC and in Figure 20. for PVA-TA. With increasing the CNC content, the hydrogel becomes mechanically stronger, but the achievable elongation-at-break diminishes quickly. By contrast, with increasing the TA content, the hydrogel not only becomes harder, but also more stretchable, breaking at larger elongation. In other words, the PVA-TA hydrogels are much tougher than the PVA-CNC hydrogels. TA contains many functional groups and form hydrogen bonds, i.e., physical cross-links, with PVA chains, which are sacrificial crosslinking bonds because of the dynamic nature of H-bonding. The breaking and reformation of these sacrificial bonds upon elongation gives rise to the toughness of PVA hydrogel. In other words, when a mechanical force is applied to deform the PVA-TA hydrogel, hydrogen bonds between TA molecules and PVA chains can dissociate and reassociate, accompanying polymer chain extension, which dissipates a large amount of elastic energy (internal stress) and thus results in increased toughness.[133]

2.3. Comparison of PVA-CNC and PVA-TA Hydrogels Containing the Same Amount of Additive

The results presented in Section 2.3. revealed some different effects of CNC and TA as enhancing additive in PVA physically crosslinked hydrogel prepared through freezing-thawing. In an attempt to have a better understanding on the different effects of the two types of additives, we performed a number of additional experiments on the 20% PVA hydrogel containing the same amount of one additive, i.e., 1% CNC in PVA or 1% TA in PVA, i.e., 1% CNC and 1% TA in the same PVA hydrogel. The two hydrogels are denoted as PVA-CNC 1%, and PVA-TA 1%, respectively. In what follows, we present the main results.

2.3.1 ATR-IR

In Section 2.3, it was found that the addition of CNC appeared to have a smaller negative impact on the hydrogel's self-healing efficiency than TA. ATR-IR spectra were recorded on a fracture surface to see how H-bonds involving the hydroxyl groups on PVA change over time. At first, we cut the hydrogel and immediately the IR spectrum is recorded for one cut surface, and then repeated the spectral recording from the surface of the hydrogel with a 5 min interval. The results obtained with PVA-CNC 1% and PVA-TA 1% hydrogels are shown in Figures 21 and 22, respectively.

The general trend is the same for both hydrogels. On one hand, in both cases, the spectral change shows a reduction in the intensity of the absorption peak in the 3250-3300 cm^{-1} region from free hydroxyl groups, indicting a decrease in the number of free hydroxyl groups on the cut surface of hydrogel over time. On the other side, in all IR spectra, as time goes on, the peaks show a red shift in frequency, which means that more hydroxyl groups form H-bonds on the surface of hydrogel. However, upon closer inspection of the spectra, the decrease in the number of free hydroxyl groups on the cut surface is faster for PVA-TA 1% than PVA-CNC 1%. After 15 min, the absorption peak of free hydroxyl groups decreases

by about 40% in intensity for PVA-CNC 1% as compared by about 65% for PVA-TA 1%. This result implies that in the latter case there are less free hydroxyl groups available and, consequently, when two fracture surfaces are brought into contact, fewer H-bonds can be formed across the interface, which is required for self-healing. Therefore, a fast depletion of free hydroxyl groups on cut surfaces would be, at least partly, the reason for which the presence of TA in PVA hydrogel reduces drastically the self-healing capability.
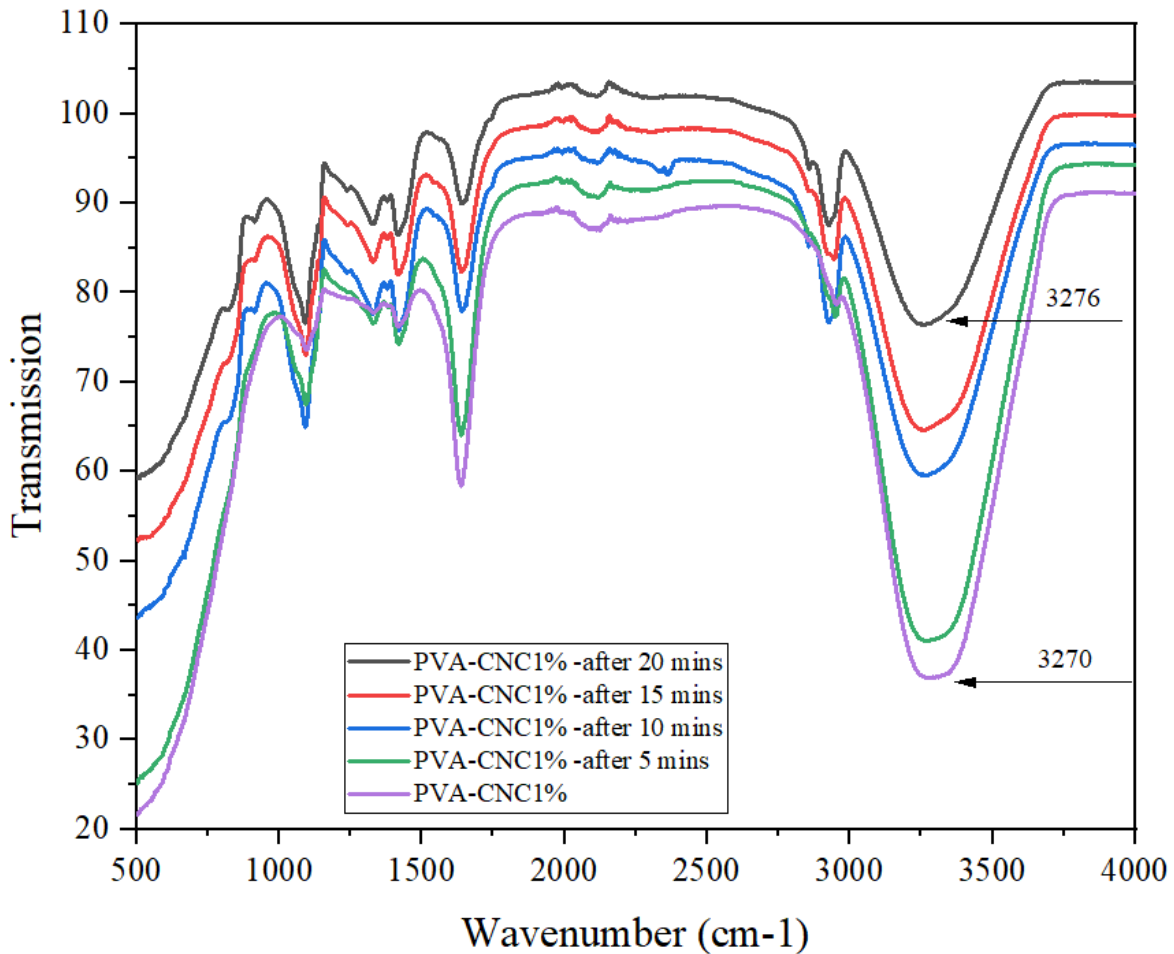
Figure 21. ATR-IR spectra of PVA-CNC 1% hydrogel recorded from a cut surface immediately after cutting and after different times.
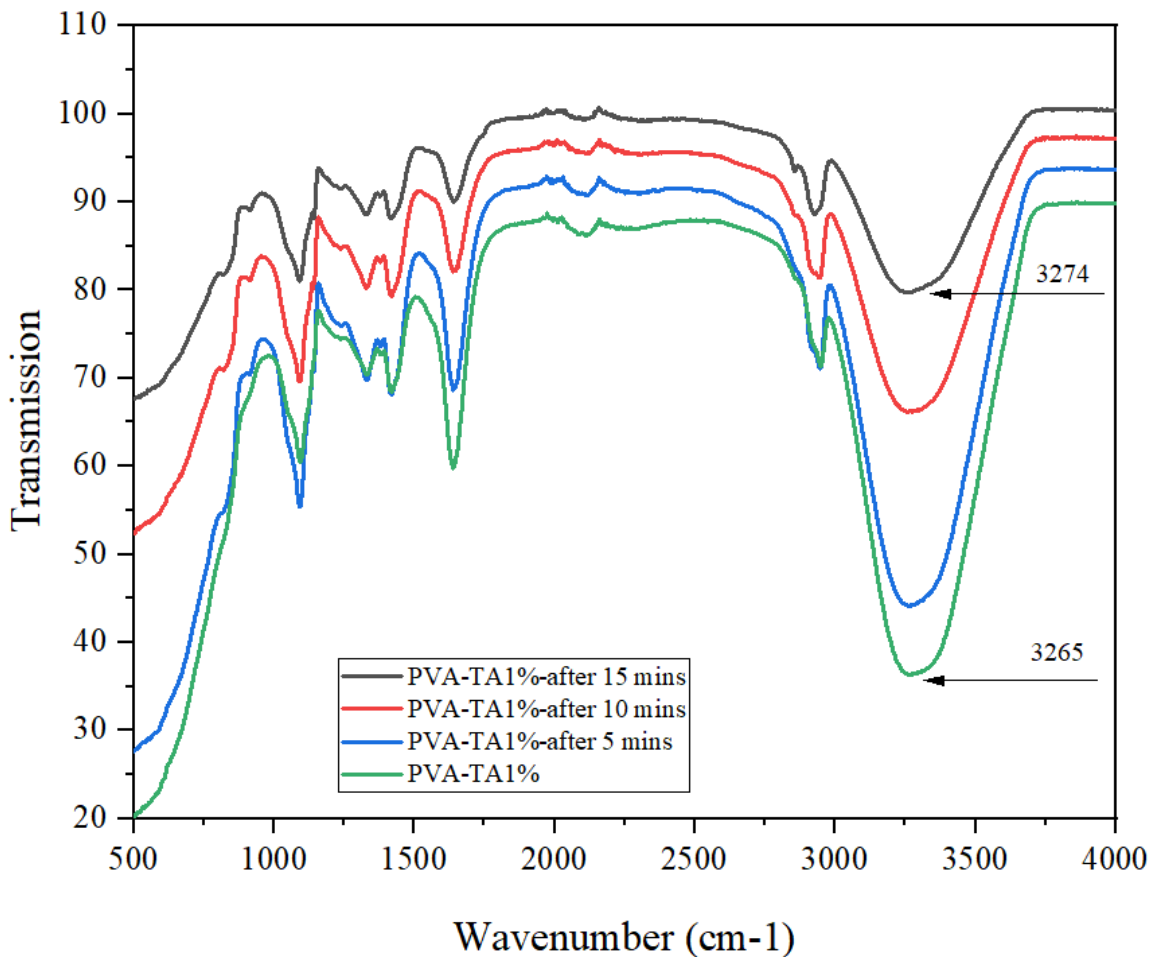
Figure 22. ATR-IR spectra of PVA-TA 1% hydrogel recorded from a cut surface immediately after cutting and after different times.

2.3.2 DSC result

DSC measurements were performed on wet hydrogel samples, recording two heating and cooling runs. Figures 23 and 24. compare the DSC curves of PVA, PVA-CNC 1% and PVA-TA 1% hydrogels, for the first and second cooling/heating cycles, respectively. On the first heating, two endothermic peaks can be observed for all samples, in which the lower-temperature peak is attributed to the evaporation of water and the one at higher temperature belongs to the melting of PVA. The temperature ranges from 100°C to 150°C shows broad endothermic peaks due to the evaporation of water confined in the hydrogel sample. This is because the stronger hydrogen bonds between water and PVA than the interaction between, which results in higher water evaporation temperature (T_p) compared to bulk water (approximately 100 °C). The

results show that the addition of 1% CNC or 1% TA has limited effect on the melting and crystallization temperatures of PVA, especially for the first heating and cooling cycle. The effect becomes more important for the second cycle, especially on the second cooling, where the CNC and TA additive broadens the crystallization temperature region and shifts them to lower temperatures.

The melting and crystallisation temperatures and their associated enthalpies as well as the crystallinity obtained from the heating and cooling curves are summarised in Tables 6 and 7. Both the heat of fusion (ΔH_m) and heat of crystallisation (ΔHc) decreased with filler loading. Based on the results of DSC in this Table, the heat of crystallization (ΔH_c) decreased from 10.97 J/g to 8.86 J/g with 1% CNC, and to 10.41 J/g with 1% TA. The reason for this phenomenon is that TA and CNC form strong hydrogen bonding cross-linking between PVA chains, which reduces the PVA chain mobility required for crystallization. On the other side, the presence of CNC can also decrease the crystallinity of PVA by hindering the spherulite formation.[134]

Please notice that in DSC Figures, the heating and cooling peaks show separately because of having large peaks of water evaporation in heating curves, which were disturbing in showing the melting and crystallization temperatures at the same curve.
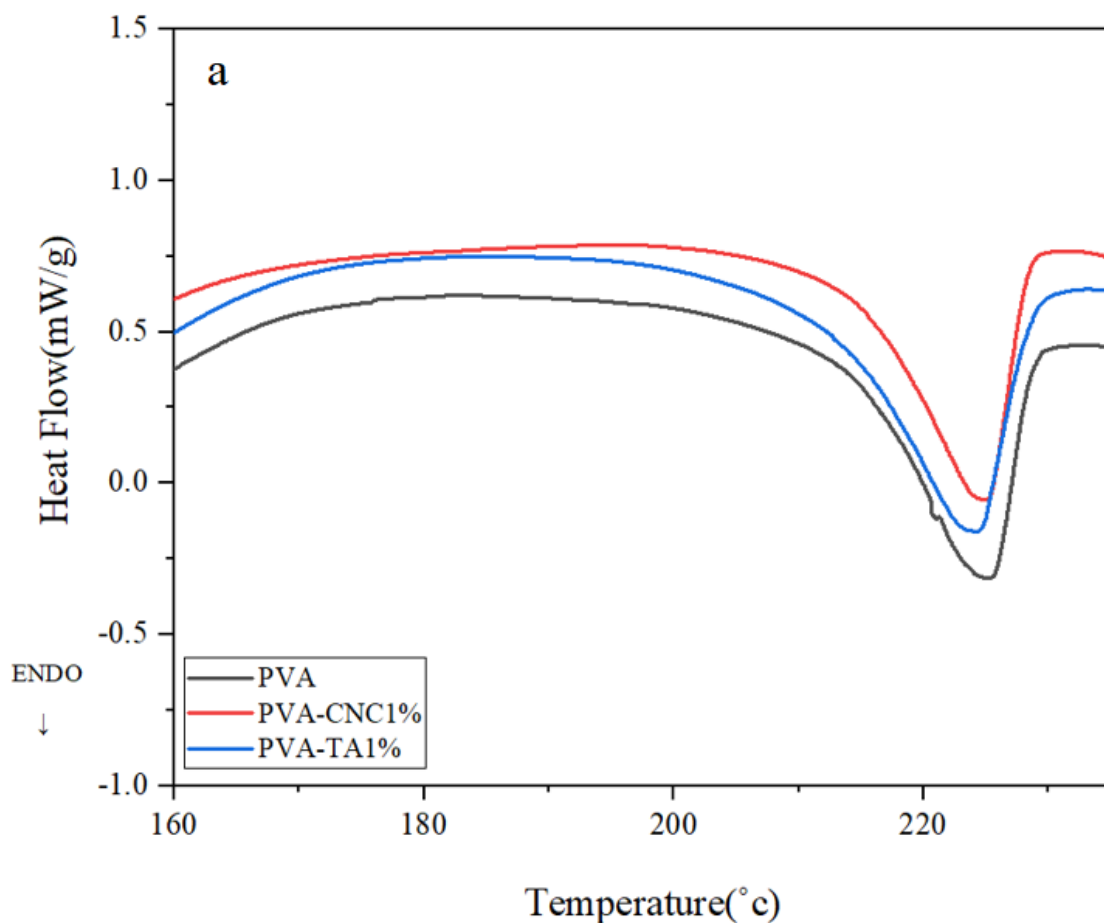
Figure 23. DSC heating (a) and cooling curves (b) of wet PVA, PVA-CNC 1% and PVA-TA 1% hydrogels for the first heating and cooling cycle.

Table 6. DSC-determined melting and crystallization temperatures, enthalpies and crystallinity for PVA, PVA-CNC1%, and PVA-TA1% hydrogels upon the first heating and cooling cycle.

Input	Samples	T_m (°C)	ΔH_m (J/g)	T_c (°C)	ΔH_c (J/g)	% Crystallinity
1	PVA	225.2	-8.5	192.7	11.0	34.3
2	PVA-CNC 1%	225.0	-7.6	188.8	8.9	27.7
3	PVA-TA 1%	223.2	-8.9	193.1	10.4	32.5

These results further confirm that the hydrogen bond crosslinking from TA limited the PVA crystallization process. Based on the results on the Table 6, the crystallinity of PVA hydrogel is different after adding TA or CNC as additives, with a greater effect of CNC. Basically, the same observation can be made with the data obtained from the second heating and cooling scan (see Table 7).
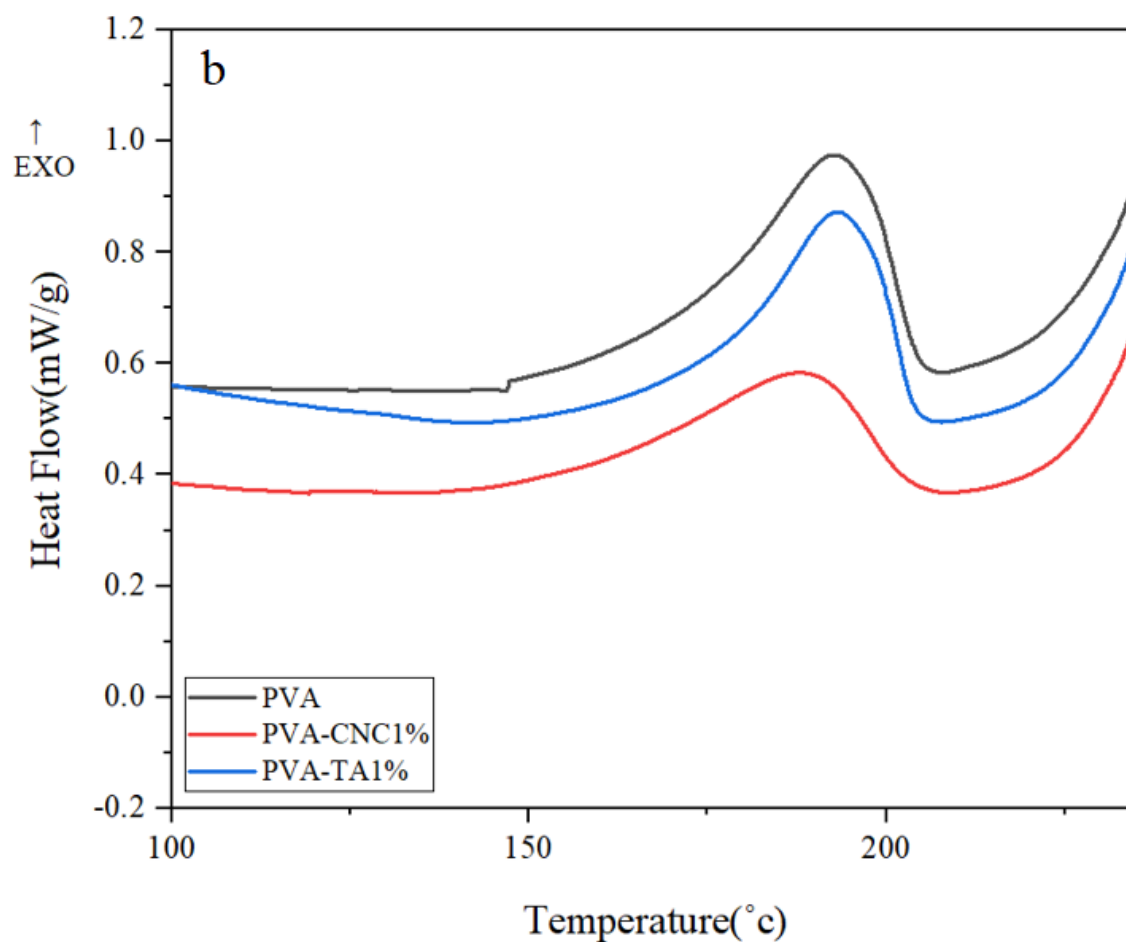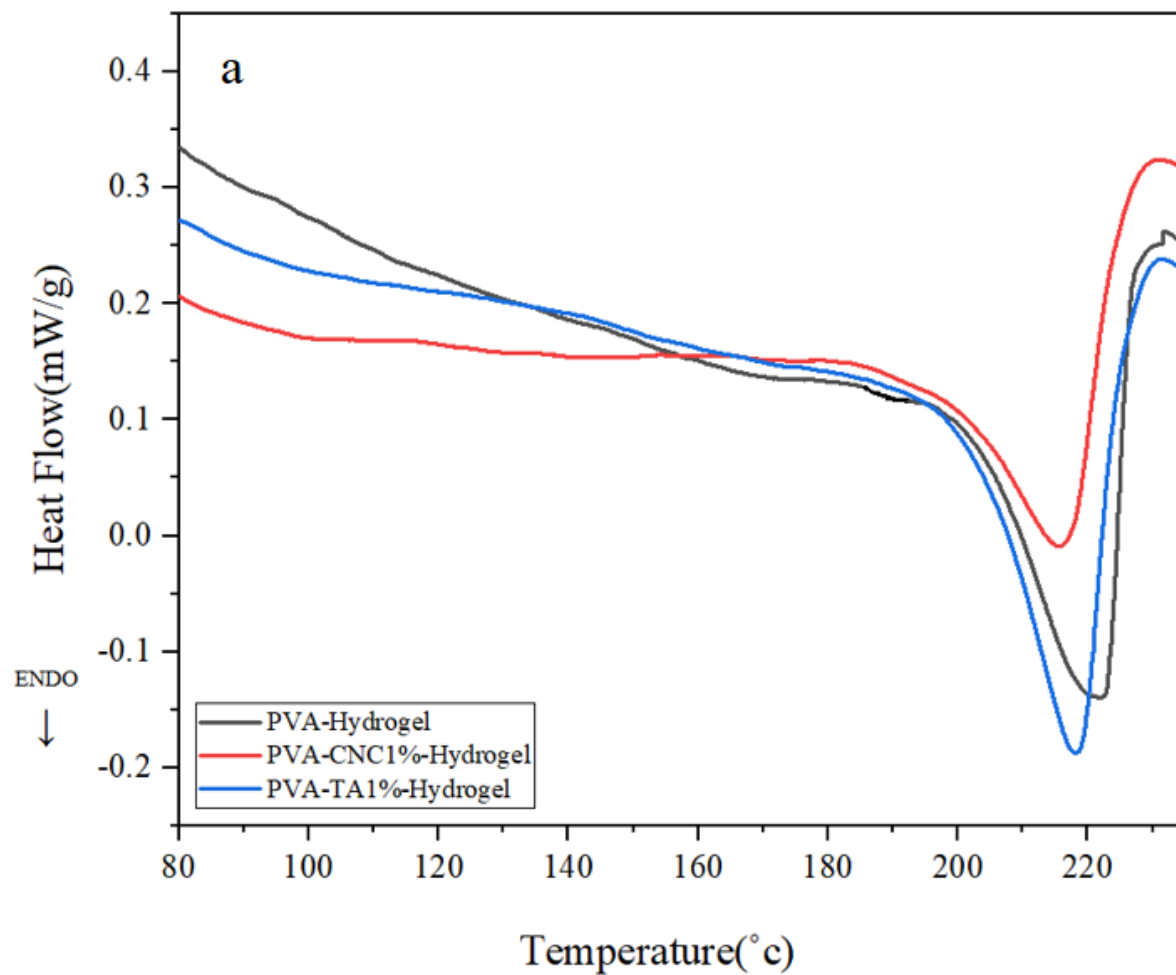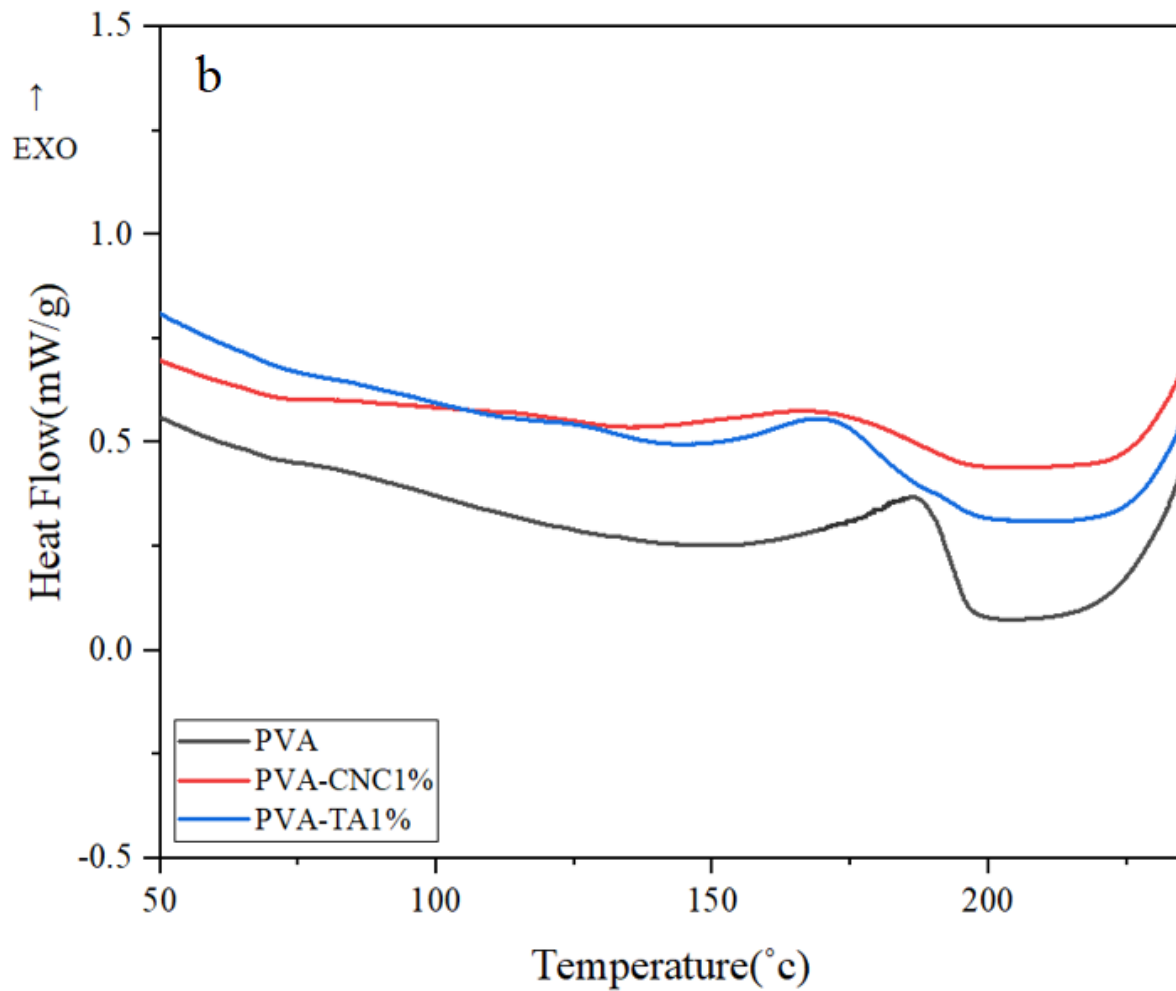
Figure 24. DSC heating (a) and cooling curves (b) of wet PVA, PVA-CNC 1% and PVA-TA 1% hydrogels for the second heating and cooling cycle.

Table 7. DSC-determined melting and crystallization temperatures, enthalpies and crystallinity for PVA, PVA-CNC 1%, and PVA-TA 1% hydrogels upon the second heating and cooling cycle.

Input	Samples	T_m (°C)	ΔH_m (J/g)	T_c (°C)	ΔH_c (J/g)	% Crystallinity
1	PVA	222.4	-6.7	186.7	6.4	20.0
2	PVA-CNC 1%	216.1	-6.1	173.2	3.3	10.3
3	PVA-TA 1%	218.4	-6.0	171.4	4.0	12.3

2.3.3 XRD Result

PVA typically shows a strong and sharp peak at $2\theta = 19.4°$ with a shoulder peak at $2\theta = 22.3°$ and a weak peak at $2\theta = 40.7°$, corresponding to the (101), (200), and (102) planes of PVA crystallites.[135] Figure 25 shows the XRD patterns of the pure PVA, PVA-CNC 1%, and PVA-TA1% hydrogels prepared by the freeze-thawing process. Sharp crystalline reflection with very high intensity at around 19.4° and 22.30° was observed in the pure PVA hydrogel. It is well known that PVA is semi-crystalline due to the strong intermolecular interaction between the PVA chains through intermolecular hydrogen bonding. The crystalline degree in PVA is determined by the number of PVA chains which are packed together. However, the crystallinity of the PVA phase decreased with the presence of 1% of TA or CNC in the hydrogel (the crystallinity decreased from about 31.8% for pure PVA to 31.0% for PVA-TA 1% and to 29.3% for PVA-CNC 1%). This is likely due to cross-linking which formed between the PVA polymer chains, consequently setting the PVA polymer components apart from each other and disturbing the PVA crystalline formation process.
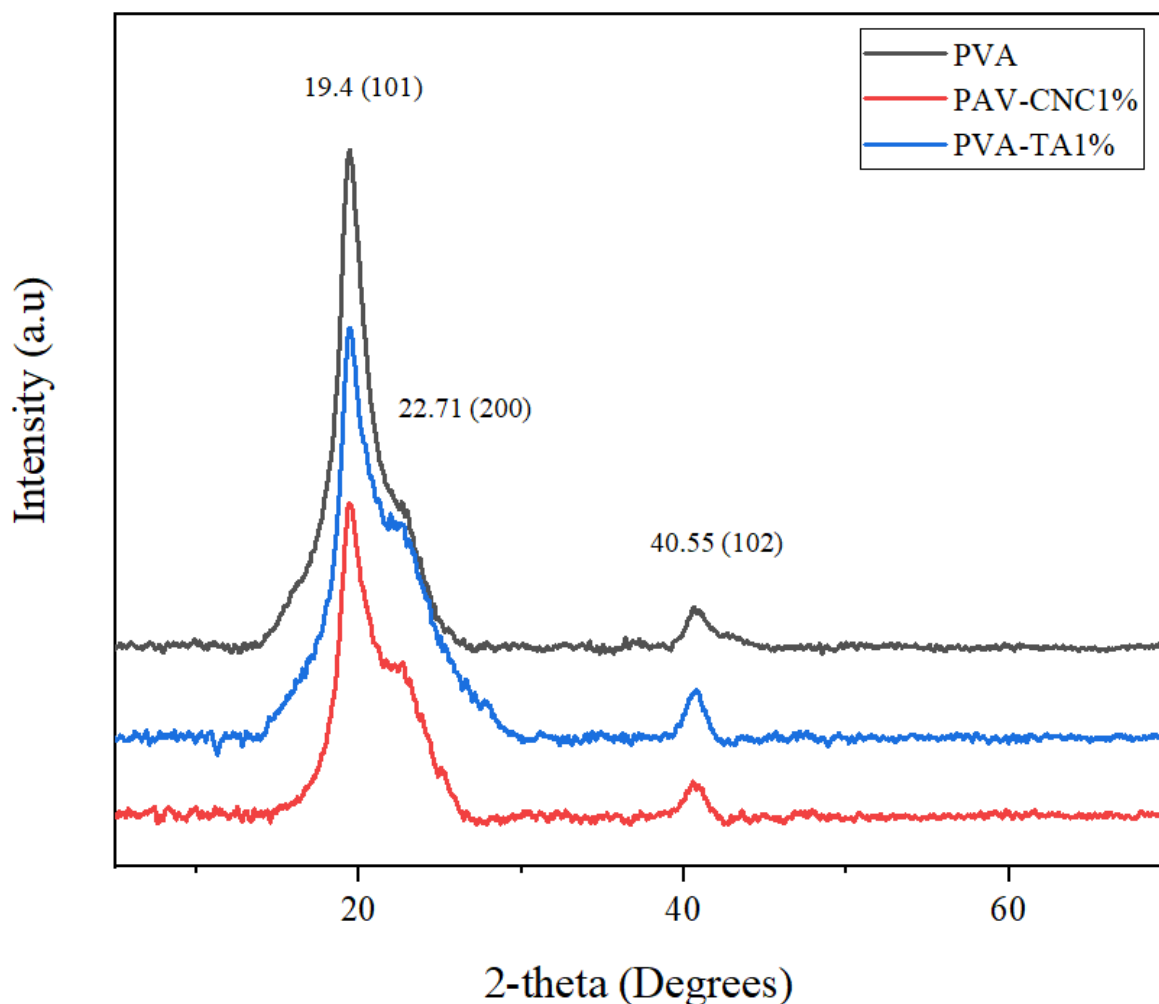
Figure 25. X-ray diffraction patterns of PVA, PVA-CNC 1%, and PVA-TA 1% hydrogels

TA mainly displayed a broad peak at around $2\theta = 25°$ with some sharp shoulder peaks. The characteristic crystalline peaks at around $2\theta=19.4°$, $22.30°$, and $40.70°$ are related to PVA. The absence of characteristic peak of TA (at $2\theta = 25°$) illustrated their homogenous dissipation in PVA matrix and strong interactions among them.[136]

TA is amorphous polysaccharides; therefore, the existence of TA in the PVA-TA hydrogel resulted in the decrease of the crystallinity of PVA. For the PVA-CNC sample the crystallinity is lower than crystallinity of the PVA-TA sample due to the less relative intensity. This happens due to the formation of more inter and intra molecular hydrogen bond. As a result, its crystallinity was less than another prepared sample.

Based on the result of XRD, the crystallinity of PVA shows the reduction after addition of additives. This reduction appears to be more obvious after the addition of CNC than TA, showing a clear difference between TA and CNC as an additive on PVA hydrogel. The greater decrease of crystallinity of PVA

hydrogel after adding CNC is related to the strong hydrogen bonding between PVA chains and CNC which reduces the mobility of PVA chains required for forming crystallites during the freezing process. On the other side, CNC nanoparticles might also disrupt the ordered structure of the crystallizing PVA chains as revealed by the reduced intensity of the peak at 19.4°. The result of XRD is consistent with the result of DSC regarding the crystallinity.

2.3.4 Swelling Behavior

The influence of TA and CNC on the water absorption ability of the PVA hydrogel was investigated and the results are shown in Figure 26. As can be seen from the change in swelling degree over immersion time, after introducing TA or CNC into PVA matrix, the obtained hydrogel displayed a notable decrease in water absorption. However, the decrease seems to be similar for the hydrogels containing 1% CNC and TA, respectively. The water absorption of cross-linked PVA networks decreased with an increase of the cross-linker content.
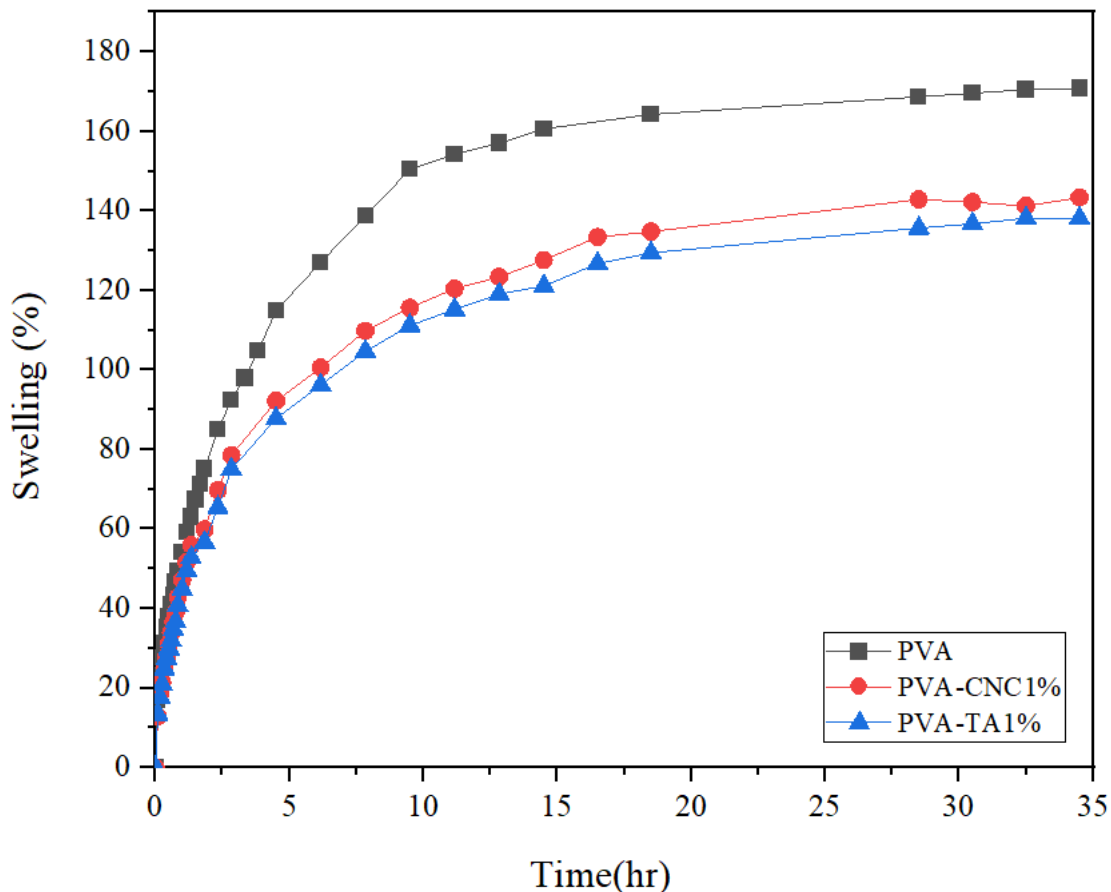
Figure 26. Swelling ratio for PVA, PVA-CNC1%, and PVA-TA1%.

The reason for the lower swelling ratio of the hydrogels with 1% TA and 1% CNC is again due to H-bonding. As the additive molecules form efficient H-bonding with PVA chains, they reduce the probability for the O-H groups to interact with water molecules. These multiple hydrogen interactions among PVA, CNC, and TA can also serve as physical cross-linking sites that limit the absorption of water molecules by diffusion. So, the presence of TA and CNC additives provides more compact hydrogels with less pores and less hydroxyl groups available for hydrogen bonding with water, and, as a result, the amount of water retained by the hydrogel decreases.

2.3.5 Shape Memory Effect

In Figure 27, the PVA-CNC 1% and PVA-TA 1% hydrogels were utilized to investigate their thermally activated shape memory effect. For this experiment, after preparation of the hydrogels using freezing-thawing, physically crosslinked, additive-loaded PVA hydrogels (80 wt % water), a hydrogel strip was deformed to a new shape (spiral or twisted) and, under deformation, subjected to another freezing (at -22 ˚C) – thawing cycle to fix the deformed state. After the treatment, the retained deformed state of the hydrogel can be seen in Figure 27.

Figure 27. Photos showing the initial shape of PVA-CNC or PVA-TA hydrogel (strip), and the deformed state retained by one freezing-thawing cycle (twist, spiral).

Afterward, the external force was removed, and the initial shape can be recovered by disrupting the physical network of PVA through melting of the crystalline microdomains by heating the temperature of water in which the samples were placed.

The shape recovery process was recorded with a digital camera, from which images of the hydrogel could be extracted. The photos in Figure 28 show the thermos-responsive shape memory behavior of the prepared hydrogels.
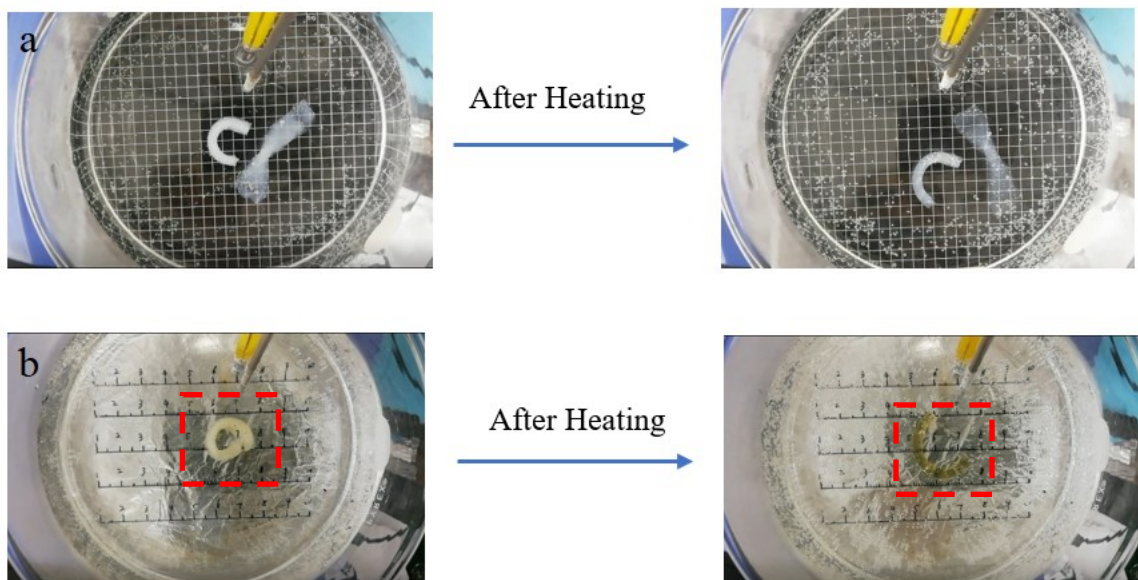
Figure 28. Photos showing the fast thermally activated shape recovery of a) PVA-CNC 1% and b) PVA-TA1 % hydrogel

Shape recovery is due to the melting of the crystalline microdomains formed by the PVA chains in the presence of CNC or TA during the F-T treatment. Crystallized domains act as the cross-linking points that are melted by heating which mainly disturb the second physical network of the hydrogel. As can be seen in Figure 28, after heating the hydrogel changes from opaque to transparent which implies crystal melting. These results clearly indicate that the shape memory effect of PVA can be realized after the introduction of either TA or CNC additive. The behaviors of PVA-CNC 1% and PVA-TA 1% hydrogels are similar to this regard.

2.4. Effect of the Number of Freezing/Thawing Cycles

In an attempt to know the effect of the freezing-thawing process on the properties of prepared hydrogels, we performed measurements and compared PVA, PVA-CNC 1%, and PVA-TA 1% hydrogels prepared using one and two freezing/thawing cycles, respectively. The main findings and data are presented below.

Figure 29 shows ATR-IR spectra of all hydrogel samples. In all cases, changes in absorption peaks from free and H-bonded OH groups, as discussed above, are visible. No clear difference between the hydrogels prepared using either one or two freezing-thawing cycles.
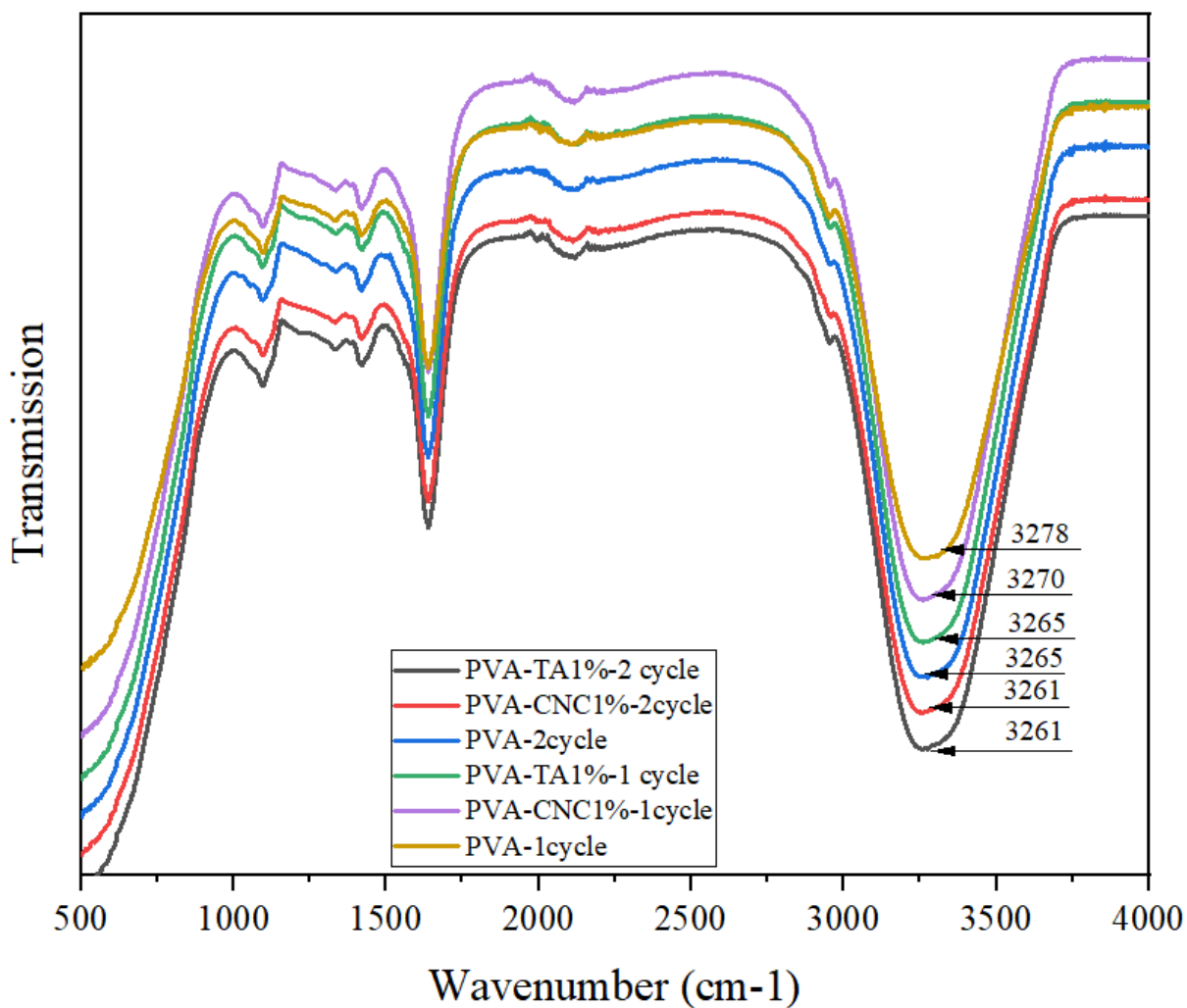
Figure 29. ATR-IR spectra of PVA, PVA-CNC 1%, and PVA-TA 1% prepared using one and two freezing-thawing cycles, respectively.

Thermal phase behaviors of all hydrogel samples were investigated using DSC, and data obtained from the first run heating and cooling scans are collected in Table 8. (DSC heating and cooling curves are in supplementary).

Table 8. DSC-determined melting and crystallization temperatures, enthalpies and crystallinity for PVA, PVA-CNC 1%, and PVA-TA 1% hydrogels prepared using one and two freezing-thawing cycles, respectively.

Input	Samples	T_m (°C)	ΔH_m (J/g)	T_c (°C)	ΔH_c (J/g)	% Crystallinity
1	PVA-1cycle F-T	225.2	-8.5	196.4	11.1	34.3
2	PVA-2cycle F-T	223.8	-7.0	185.1	7.7	24.0
3	PVA-CNC1 %-1cycle F-T	225.0	-7.6	193.0	8.9	27.7
4	PVA-CNC1 %-2cycle F-T	222.8	-7.1	188.3	7.8	23.9
5	PVA-TA 1%-1cycle F-T	224.2	-8.9	198.6	10.4	32.5
6	PVA-TA 1%-2cycle F-T	222.8	-7.4	192.1	9.6	30.0

The results in Table 8 show that the crystallinity of PVA not only decreases after the addition of 1% CNC and 1% TA, it also further decreases after the second freezing-thawing cycle. This observation is a bit surprising, because more freezing-thawing cycles normally result in an increase in PVA crystallinity.[137,138] The lower crystallinity of PVA in the PVA-CNC 1% and PVA-TA 1% hydrogels prepared using two cycles of freezing-thawing was confirmed by XRD measurements, as can be seen from Figures 30, 31, 32.
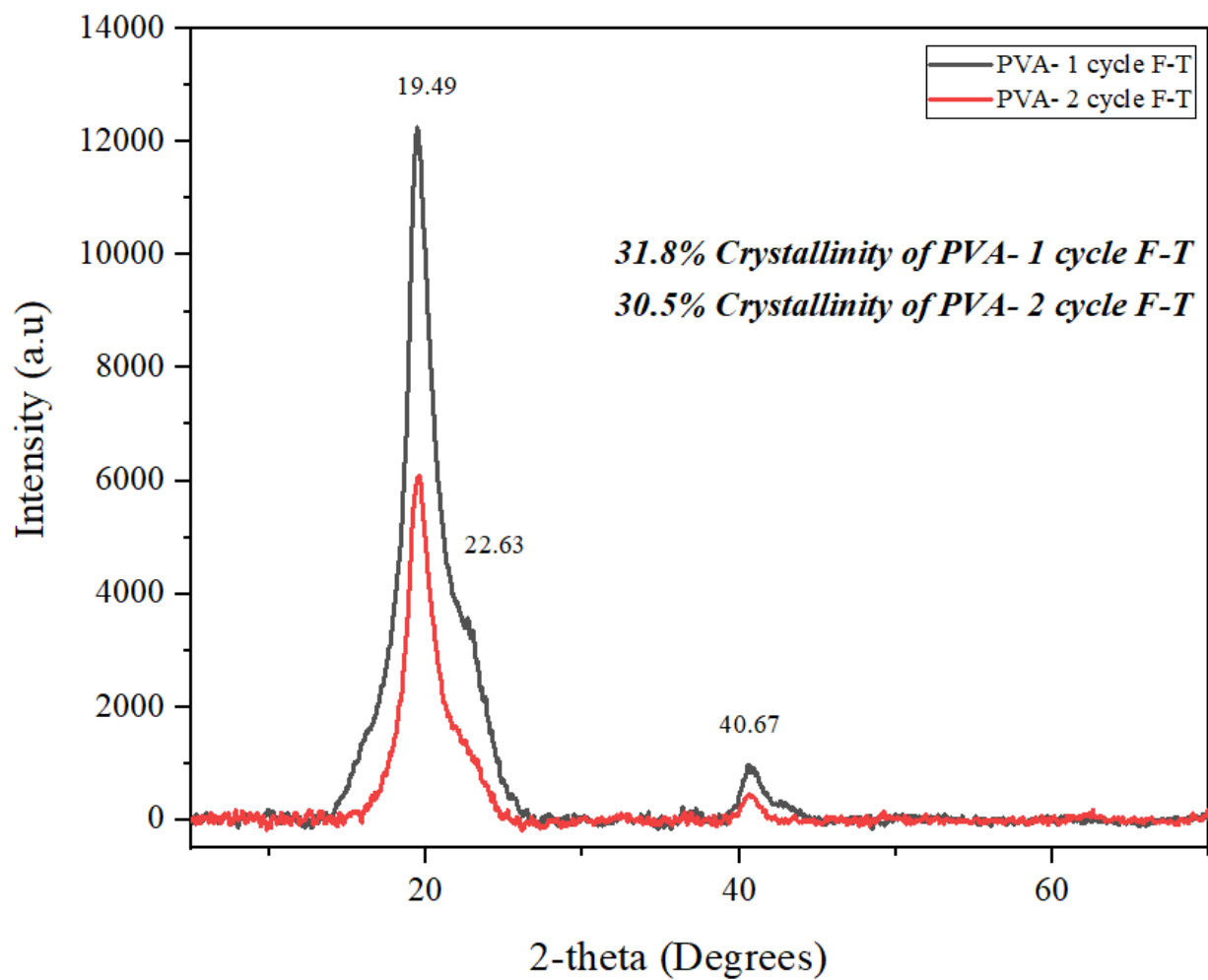
Figure 30. X-ray diffraction patterns for PVA hydrogel prepared using one and two freezing-thawing cycles, respectively.
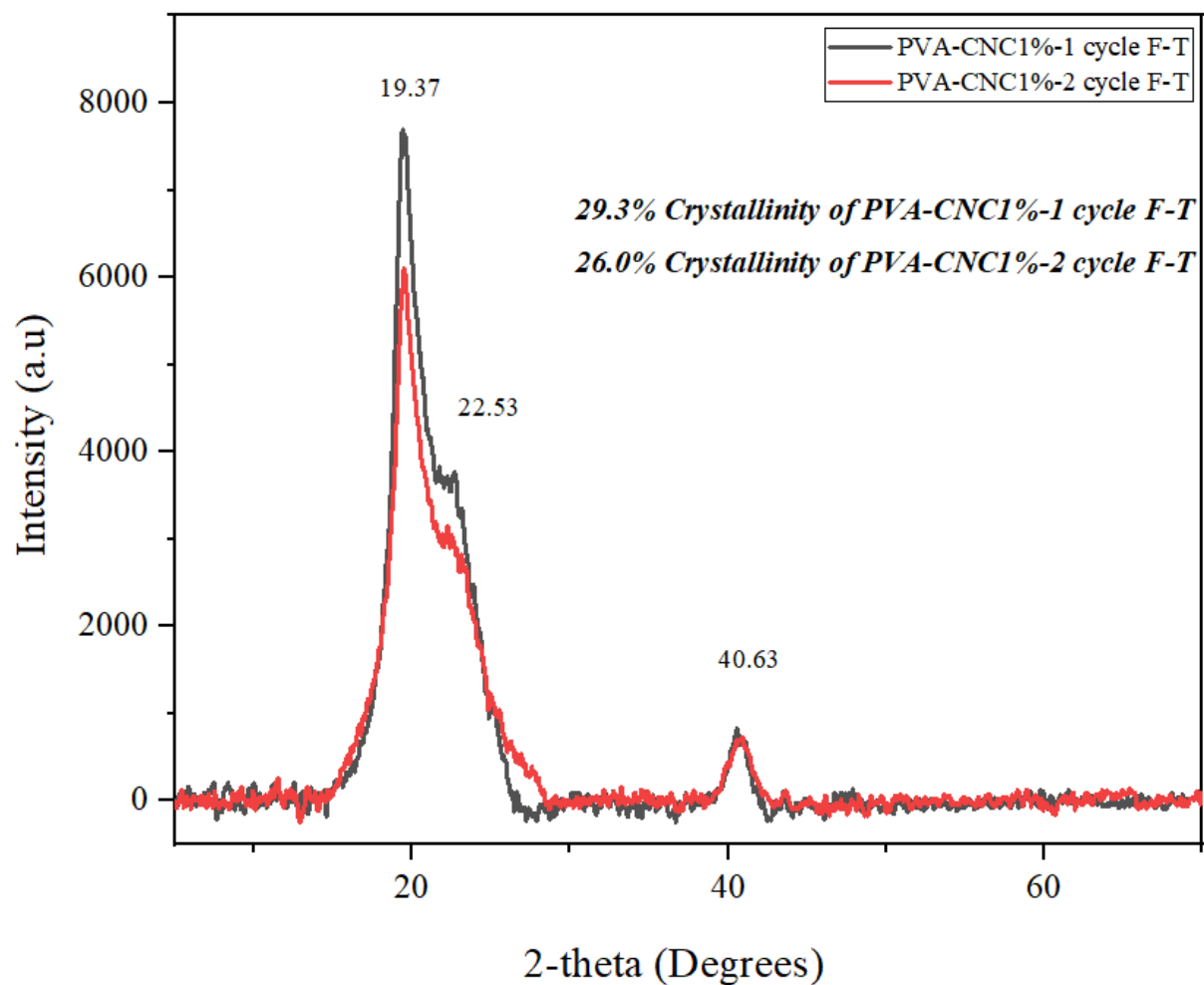
Figure 31. X-ray diffraction patterns for PVA-CNC 1% hydrogel prepared using one and two freezing-thawing cycles, respectively.
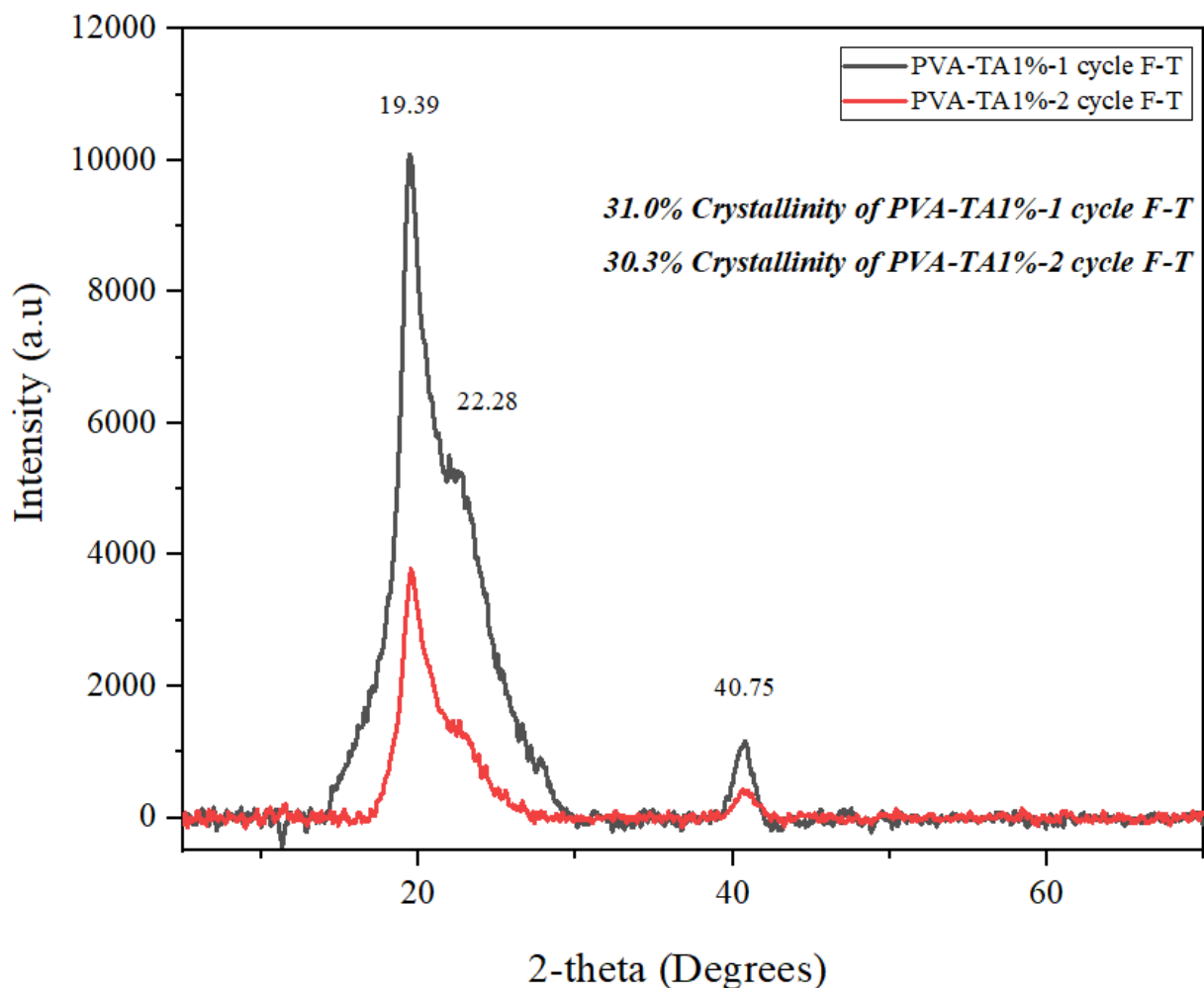
Figure 32. X-ray diffraction patterns for PVA-TA 1% hydrogel prepared using one and two freezing-thawing cycles, respectively.

Moreover, the hydrogels prepared using one or two freezing-thawing cycles also display some differences in swelling degree in water (see Figure S4 in supplementary).

Finally, increasing the number of freezing-thawing cycle from one to two was found to have an interesting effect on realizing the shape memory. For hydrogels, the fixation of a temporary shape (deformed state) is often challenging. We found that applying two consecutive freezing-thawing cycles can better retain the deformation of the hydrogel (either PVA or PVA-CNC 1% or PVA-TA 1%) after removal of external force, and that subsequent heating allows the shape recovery to take place.

For investigating the shape memory effect, we prepared the PVA, PVA-CNC 1%, and PVA-TA 1% hydrogels with F-T method and with initial straight rod shape; then we stretched it and put it (under strain) in the refrigerator to get temporary shape. After the thawing step, we repeated this process to get the second freeze-thawing cycle. After the external force was removed, the elongation ratio (the retained length over the initial length), which corresponds to the fixed temporary shape of the hydrogel, was measured, followed by placing the sample in a water bath to undergo heating at a rate of 10 °C/min while recording the change in the elongation ratio. The results are shown in Figure S5 in supplementary by plotting the elongation ratio vs temperature for PVA, PVA-CNC 1% and PVA-TA 1% hydrogels. For each hydrogel, two stretched samples subjected to one and two freezing-thawing cycles, respectively, were utilized for the tests.

Several observations can be made from Figure 33. First, more cycles of freezing/ thawing resulted in a better shape fixation, with the elongation ratio increased from 54% (1 cycle) to 80% (2 cycles) for PVA hydrogel, from 30% (1 cycle) to 60% (2 cycles) for PVA-CNC 1%, and from 40% (1 cycle) to 60% (2 cycles) for PVA-TA 1% hydrogel. The stronger physical cross-linking in the 2-cycle samples preserves better the deformed state of the wet hydrogel after removal of the external force. Secondly, pure PVA hydrogel has a greater temporary shape fixation than PVA-TA 1% and PVA-CNC 1% hydrogels. The reduction of crystallinity upon addition of additives may weaken the ability of hydrogel to keep the deformed shape. Thirdly, while for the 1-cycle samples, PVA-TA 1% hydrogel shows a better temporary shape fixation than PVA-CNC 1% hydrogel, with 2 freezing-thawing treatments, the two additive-loaded PVA hydrogels display a similar temporary shape fixation. Finally, for all hydrogels, a significant shape recovery (contraction of the hydrogel rods) starts in a similar range of temperatures, 45-50 °C, and increases on further heating. Data on the shape memory effect of the different hydrogels are summarized in Table 9.

The deformed ratio was calculated using the following equation:

Deformed ratio $Dr = \frac{(L2-L1)}{L1} \times 100$ Equation 2.1

Where L_2, is final length of hydrogel after removing the stretching force (after freezing/thawing process) and L_1 is initial length of hydrogel while stretching (before freezing process).

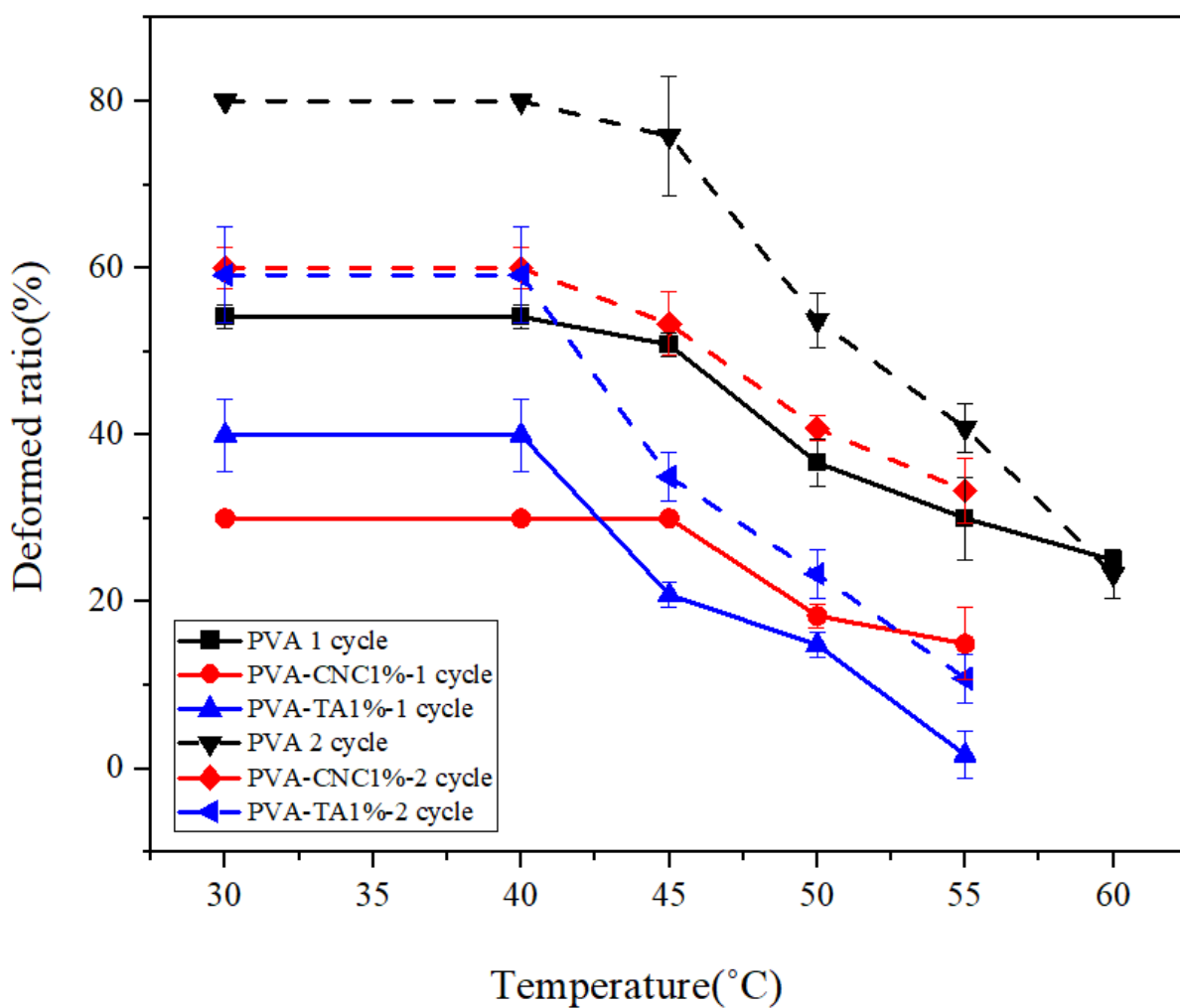**Figure 33.** Plots of deformation ratio vs. temperature for PVA, PVA-CNC 1% and PVA-TA 1% hydrogels prepared using one and two freezing-thawing cycles, respectively. The initial ratio at 30 °C corresponds to the fixation efficiency of the temporary shape of the hydrogel and the decrease in deformation ratio with increasing temperature indicates the thermally activated shape recovery.

Table 9. Temporary shape fixing and shape recovery ratio of PVA, PVA-CNC 1% and PVA-TA 1% hydrogels prepared using one and two freezing-thawing cycles, respectively.

Input	Samples	Shape fixing ratio (%)	Shape recovery ratio (%)
1	PVA-1 cycle	24.2	53.9
2	PVA-CNC 1%-1 cycle	4.4	50.2
3	PVA-TA 1%-1 cycle	16.8	94.9
4	PVA-2 cycle	44.2	70.8
5	PVA-CNC 1%-2 cycle	20.6	44.5
6	PVA-TA 1%- 2 cycle	30.4	76.6

Finally, a number of PVA hydrogels loaded with both CNC and TA of varying composition were also prepared under the same conditions and characterized with the same techniques of ATR-IR, DSC, XRD. Basically, similar results as described in Sections 3.1 and 3.2 were obtained, reflecting simultaneous contributions of the two additives, with the effect of each additive weighed by its relative content. The characterization data are presented in supplementary.

2.5. Summary

The research in this thesis focuses on the design, synthesis and fabrication of PVA-based hydrogels by examining the different aspects of their fabrication and properties, such as self-healing, toughness, and shape memory. The principal reason to utilize PVA to produce hydrogels is their ability to self-heal spontaneously. However, their relatively week mechanical strength reduces their application in many different fields. Interest in the most abandoned and bio-based organic materials, cellulose nanocrystals and tannic acids has increased notably over recent decades. Mainly due to their high mechanical reinforcement ability, these additives have been used to increase the mechanical properties of PVA hydrogels. Thanks to the hydrogen bonding between PVA chains and these additives, the polymer matrix is bonded strongly with CNC and TA, and high stiffness for PVA hydrogel arises. In our project, we prepared a number of PVA-CNC and PVA-TA hydrogels that exhibited different mechanical, shape memory and self-healing properties. The characterization results suggest that different H-bonding between PVA chains and the CNC or TA additive could be determining factor. The obtained multifunctional hydrogels with high mechanical strength could be an attractive candidate for a wide variety of applications.

GENERAL CONCLUSION

Poly(vinyl alcohol) (PVA) hydrogels produced by freeze-thaw method, which is a simple water-based processing method without the aid of harmful chemical additives, have attracted attention for a long time, due to their interesting properties such as spontaneous self-healing capability and biocompatibility suitable for biomedical applications.

The availability of free hydroxyl groups and formation of hydrogen bonding between PVA chains promotes self-healing effect in the hydrogel. However, such physically crosslinked PVA hydrogel has relatively weak mechanical strength, which may be an issue for applications.

Therefore, in this study, we added two types of additives, CNC (nanoparticle) and TA (molecule) in PVA hydrogel to increase the mechanical strength while keeping the self-healable property. Adding different additives shows different effects on hydrogel which can be seen from different measurements such as ATR-IR, DSC, XRD, mechanical test, self-healing, and shape memory tests.

This study focused on hybrid hydrogels, produced by using the same concentration of PVA (20% with respect to water) and different concentrations of CNC or TA (1 and 5 wt.%).

Our main objective is to determine the impact of both types of additives on thermal, mechanical, self-healing, shape memory, and water absorption properties of hydrogels as well as on crystallinity. Our results found that CNC and TA as reinforcing agents could have a reinforcing effect on PVA hydrogels, but their effects were both concentration-dependent and freezing-thawing cycle-dependent. As a general result, the addition of additives decreases the crystallinity of PVA, decreases self-healing effect, increases the mechanical effect, but the magnitude of increase or decrease is different with different additives. The performance of PVA hydrogels prepared using different numbers of freezing-thawing cycles was also investigated. The results show greater reduction in crystallinity and self-healing effect, but greater improvement in mechanical properties.

As the most noticeable difference between the two additives, the tensile tests found that the presence of CNC retains largely the self-healing property of the hydrogel better than TA, while the addition of TA improves the mechanical properties of the hydrogel more than CNC. This difference is probably due to different numbers, strengths of H-bonds between PVA chains and the additive in the hydrogels, as well as the interfaces between the matrix and additive. All additive loadings also resulted in a decrease in the crystallinity of PVA in the hydrogel and a decrease in water uptake. Moreover, the preparation conditions in preparing the hydrogels, including the freezing and thawing.

REFERENCES

1. Annabi, N.; Tamayol, A.; Uquillas, J. A.; Akbari, M.; Bertassoni, L. E.; Cha, C.; Camci-Unal, G.; Dokmeci, M. R.; Peppas, N. A.; Khademhosseini, A., 25th anniversary article: Rational design and applications of hydrogels in regenerative medicine. *Adv Mater* **2014,** *26* (1), 85-123.

2. Wang, H.; Heilshorn, S. C., Adaptable hydrogel networks with reversible linkages for tissue engineering. *Adv Mater* **2015,** *27* (25), 3717-36.

3. Webber, M. J.; Appel, E. A.; Meijer, E. W.; Langer, R., Supramolecular biomaterials. *Nat Mater* **2016,** *15* (1), 13-26.

4. Joshi Navare, K.; Eggermont, L. J.; Rogers, Z. J.; Mohammed, H. S.; Colombani, T.; Bencherif, S. A., Antimicrobial hydrogels: Key considerations and engineering strategies for biomedical applications. *Racing for the Surface* **2020**, 511-542.

5. Hu, C.; Wang, M. X.; Sun, L.; Yang, J. H.; Zrínyi, M.; Chen, Y. M., Dual-Physical Cross-Linked Tough and Photoluminescent Hydrogels with Good Biocompatibility and Antibacterial Activity. *Macromolecular Rapid Communications* **2017,** *38* (10), 1600788.

6. Nam, C.; Zimudzi, T. J.; Geise, G. M.; Hickner, M. A., Increased Hydrogel Swelling Induced by Absorption of Small Molecules. *ACS Applied Materials & Interfaces* **2016,** *8* (22), 14263-14270.

7. Du, X.; Zhou, J.; Shi, J.; Xu, B., Supramolecular Hydrogelators and Hydrogels: From Soft Matter to Molecular Biomaterials. *Chemical Reviews* **2015,** *115* (24), 13165-13307.

8. Lee, K. Y.; Mooney, D. J., Hydrogels for Tissue Engineering. *American Chemical Society* **2001,** *101* (7), 1869-1880.

9. Secret, E.; Kelly, S. J.; Crannell, K. E.; Andrew, J. S., Enzyme-responsive hydrogel microparticles for pulmonary drug delivery. *ACS Appl Mater Interfaces* **2014,** *6* (13), 10313-21.

10. Discher, D. E.; Mooney, D. J.; Zandstra, P. W., Growth Factors, Matrices, and Forces Combine and Control Stem Cells. *Science.* **2009,** *324* (5935), 1673-1677.

11. Zhao, X., Multi-scale multi-mechanism design of tough hydrogels: building dissipation into stretchy networks. *Soft Matter* **2014,** *10* (5), 672-687.

12. Seliktar, D., Designing cell-compatible hydrogels for biomedical applications. *Science* **2012,** *336 (6085)*, 1124-1128.

13. Wang, Q.; Mynar, J. L.; Yoshida, M.; Lee, E.; Lee, M.; Okuro, K.; Kinbara, K.; Aida, T., High-water-content mouldable hydrogels by mixing clay and a dendritic molecular binder. *Nature* **2010,** *463* (7279), 339-343.

14. Chen, Q.; Zhu, L.; Huang, L.; Chen, H.; Xu, K.; Tan, Y.; Wang, P.; Zheng, J., Fracture of the Physically Cross-Linked First Network in Hybrid Double Network Hydrogels. *Macromolecules* **2014,** *47* (6), 2140-2148.

15. Menyo, M. S.; Hawker, C. J.; Waite, J. H., Rate-Dependent Stiffness and Recovery in Interpenetrating Network Hydrogels through Sacrificial Metal Coordination Bonds. *ACS Macro Lett* **2015,** *4* (11), 1200-1204.

16. Okumura, Y.; K., I., The Polyrotaxane Gel: A Topological Gel by Figure-of-Eight Cross-links. *Advanced materials* **2001,** *13* (7), 485-487.

17. Yang, J.; Han, C.-R.; Duan, J.-F.; Xu, F.; Sun, R.-C., Mechanical and Viscoelastic Properties of Cellulose Nanocrystals Reinforced Poly(ethylene glycol) Nanocomposite Hydrogels. *ACS Applied Materials & Interfaces* **2013,** *5* (8), 3199-3207.

18. Hou, J.; Ren, X.; Guan, S.; Duan, L.; Gao, G. H.; Kuai, Y.; Zhang, H., Rapidly recoverable, anti-fatigue, super-tough double-network hydrogels reinforced by macromolecular microspheres. *Soft Matter* **2017,** *13* (7), 1357-1363.

19. Yang, J.; Han, C.-R.; Duan, J.-F.; Xu, F.; Sun, R.-C., Insitu grafting silica nanoparticles reinforced nanocomposite hydrogels. *Nanoscale* **2013,** *5* (22), 10858-10863.

20. Yang, J.; Han, C.-R.; Zhang, X.-M.; Xu, F.; Sun, R.-C., Cellulose Nanocrystals Mechanical Reinforcement in Composite Hydrogels with Multiple Cross-Links: Correlations between Dissipation Properties and Deformation Mechanisms. *Macromolecules* **2014,** *47* (12), 4077-4086.

21. Yang, J.; Ma, M.; Zhang, X.; Xu, F., Elucidating Dynamics of Precoordinated Ionic Bridges as Sacrificial Bonds in Interpenetrating Network Hydrogels. *Macromolecules* **2016,** *49* (11), 4340-4348.

22. Gong, J. P., Why are double network hydrogels so tough? *Soft Matter* **2010,** *6* (12), 2583-2590.

23. Rybtchinski, B., Adaptive Supramolecular Nanomaterials Based on Strong Noncovalent Interactions. *ACS nano.* **2011,** *5 (9)*, 6791-6818.

24. Gong, J. P.; Katsuyama, Y.; Kurokawa, T.; Osada, Y., Double-Network Hydrogels with Extremely High Mechanical Strength. *Advanced Materials* **2003,** *15* (14), 1155-1158.

25. Rauner, N.; Meuris, M.; Zoric, M.; Tiller, J. C., Enzymatic mineralization generates ultrastiff and tough hydrogels with tunable mechanics. *Nature* **2017,** *543* (7645), 407-410.

26. Kamata, H.; Akagi, Y.; Kayasuga-Kariya, Y.; Chung, U. I.; T., S., "Nonswellable" hydrogel without mechanical hysteresis. *Science.* **2014,** *343* (6173), 873-875.

27. Chen, H.; Yang, F.; Hu, R.; Zhang, M.; Ren, B.; Gong, X.; Ma, J.; Jiang, B.; Chen, Q.; Zheng, J., A comparative study of the mechanical properties of hybrid double-network hydrogels in swollen and as-prepared states. *Journal of Materials Chemistry B* **2016,** *4* (35), 5814-5824.

28. Wang, X.; Dong, L.; Zhang, H.; Yu, R.; Pan, C.; Wang, Z. L., Recent Progress in Electronic Skin. *Advanced Science* **2015,** *2* (10), 1500169.

29. Liu, H.; Dong, M.; Huang, W.; Gao, J.; Dai, K.; Guo, J.; Zheng, G.; Liu, C.; Shen, C.; Guo, Z., Lightweight conductive graphene/thermoplastic polyurethane foams with ultrahigh compressibility for piezoresistive sensing. *Journal of Materials Chemistry C* **2017,** *5* (1), 73-83.

30. Liu, S.; Zheng, R.; Chen, S.; Wu, Y.; Liu, H.; Wang, P.; Deng, Z.; Liu, L., A compliant, self-adhesive and self-healing wearable hydrogel as epidermal strain sensor. *Journal of Materials Chemistry C* **2018,** *6* (15), 4183-4190.

31. Hu, C.; Li, Z.; Wang, Y.; Gao, J.; Dai, K.; Zheng, G.; Liu, C.; Shen, C.; Song, H.; Guo, Z., Comparative assessment of the strain-sensing behaviors of polylactic acid nanocomposites: reduced graphene oxide or carbon nanotubes. *Journal of Materials Chemistry C* **2017,** *5* (9), 2318-2328.

32. Li, Y.; Zhou, B.; Zheng, G.; Liu, X.; Li, T.; Yan, C.; Cheng, C.; Dai, K.; Liu, C.; Shen, C.; Guo, Z., Continuously prepared highly conductive and stretchable SWNT/MWNT synergistically composited electrospun thermoplastic polyurethane yarns for wearable sensing. *Journal of Materials Chemistry C* **2018,** *6* (9), 2258-2269.

33. Lin, C. C.; Metters, A. T., Hydrogels in controlled release formulations: network design and mathematical modeling. *Adv Drug Deliv Rev* **2006,** *58* (12-13), 1379-408.

34. Sionkowska, A., Current research on the blends of natural and synthetic polymers as new biomaterials: Review. *Progress in Polymer Science* **2011,** *36* (9), 1254-1276.

35. Wei, Z.; Yang, J. H.; Zhou, J.; Xu, F.; Zrinyi, M.; Dussault, P. H.; Osada, Y.; Chen, Y. M., Self-healing gels based on constitutional dynamic chemistry and their potential applications. *Chem Soc Rev* **2014,** *43* (23), 8114-31.

36. Lin, Y.; Li, G., An intermolecular quadruple hydrogen-bonding strategy to fabricate self-healing and highly deformable polyurethane hydrogels. *J Mater Chem B* **2014,** *2* (39), 6878-6885.

37. Deng, Z.; Wang, H.; Ma, P. X.; Guo, B., Self-healing conductive hydrogels: preparation, properties and applications. *Nanoscale* **2020,** *12* (3), 1224-1246.

38. Yan, X.; Wang, F.; Zheng, B.; Huang, F., Stimuli-responsive supramolecular polymeric materials. *Chem Soc Rev* **2012,** *41* (18), 6042-65.

39. Xia, S.; Song, S.; Ren, X.; Gao, G., Highly tough, anti-fatigue and rapidly self-recoverable hydrogels reinforced with core-shell inorganic-organic hybrid latex particles. *Soft Matter* **2017,** *13* (36), 6059-6067.

40. Zhang, C.-M.; Qin, S.-Y.; Cheng, Y.-J.; Zhang, A.-Q., Construction of poly(dopamine) doped oligopeptide hydrogel. *RSC Adv.* **2017,** *7* (80), 50425-50429.

41. Wutzel, H.; Richter, F. H.; Li, Y.; Sheiko, S. S.; Klok, H.-A., Poly[N-(2-hydroxypropyl)methacrylamide] nanogels by RAFT polymerization in inverse emulsion. *Polym. Chem.* **2014,** *5* (5), 1711-1719.

42. Sun, T.; Zhu, C.; Xu, J., Multiple stimuli-responsive selenium-functionalized biodegradable starch-based hydrogels. *Soft Matter* **2018,** *14* (6), 921-926.

43. Zhu, S.; Gu, Z.; Xiong, S.; An, Y.; Liu, Y.; Yin, T.; You, J.; Hu, Y., Fabrication of a novel bio-inspired collagen–polydopamine hydrogel and insights into the formation mechanism for biomedical applications. *RSC Advances* **2016,** *6* (70), 66180-66190.

44. Willocq, B.; Odent, J.; Dubois, P.; Raquez, J. M., Advances in intrinsic self-healing polyurethanes and related composites. *RSC Adv* **2020,** *10* (23), 13766-13782.

45. Ding, X.; Wang, Y., Weak Bond-Based Injectable and Stimuli Responsive Hydrogels for Biomedical Applications. *J Mater Chem B* **2017,** *5* (5), 887-906.

46. Li, Y.; Zhou, T.; Yu, Z.; Wang, F.; Shi, D.; Ni, Z.; Chen, M., Effects of surfactant and ionic concentration on properties of dual physical crosslinking self-healing hydrogels by hydrophobic association and ionic interactions. *New Journal of Chemistry* **2020,** *44* (10), 4061-4070.

47. Lewis, C. L.; Anthamatten, M., Synthesis, swelling behavior, and viscoelastic properties of functional poly(hydroxyethyl methacrylate) with ureidopyrimidinone side-groups. *Soft Matter* **2013,** *9* (15).

48. Ahn, S. K.; Kasi, R. M.; Kim, S. C.; Sharma, N.; Zhou, Y., Stimuli-responsive polymer gels. *Soft Matter* **2008,** *4* (6), 1151-1157.

49. Cheng, C.; Convertine, A. J.; Stayton, P. S.; Bryers, J. D., Multifunctional triblock copolymers for intracellular messenger RNA delivery. *Biomaterials* **2012,** *33* (28), 6868-6876.

50. Loo, Y.; Wong, Y. C.; Cai, E. Z.; Ang, C. H.; Raju, A.; Lakshmanan, A.; Koh, A. G.; Zhou, H. J.; Lim, T. C.; Moochhala, S. M.; Hauser, C. A., Ultrashort peptide nanofibrous hydrogels for the acceleration of healing of burn wounds. *Biomaterials* **2014,** *35* (17), 4805-14.

51. Appel, E. A.; del Barrio, J.; Loh, X. J.; Scherman, O. A., Supramolecular polymeric hydrogels. *Chem Soc Rev* **2012,** *41* (18), 6195-214.

52. Datta, S.; Bhattacharya, S., Multifarious facets of sugar-derived molecular gels: molecular features, mechanisms of self-assembly and emerging applications. *Chem Soc Rev* **2015,** *44* (15), 5596-637.

53. Bae, K. H.; Wang, L. S.; Kurisawa, M., Injectable biodegradable hydrogels: progress and challenges. *J Mater Chem B* **2013,** *1* (40), 5371-5388.

54. Hu, W.; Wang, Z.; Xiao, Y.; Zhang, S.; Wang, J., Advances in crosslinking strategies of biomedical hydrogels. *Biomater Sci* **2019,** *7* (3), 843-855.

55. Fichman, G.; Guterman, T.; Adler-Abramovich, L.; Gazit, E., Synergetic functional properties of two-component single amino acid-based hydrogels. *CrystEngComm* **2015,** *17* (42), 8105-8112.

56. Dzhardimalieva, G. I.; Yadav, B. C.; Singh, S.; Uflyand, I. E., Self-healing and shape memory metallopolymers: state-of-the-art and future perspectives. *Dalton Trans* **2020,** *49* (10), 3042-3087.

57. Perera, M. M.; Ayres, N., Dynamic covalent bonds in self-healing, shape memory, and controllable stiffness hydrogels. *Polymer Chemistry* **2020,** *11* (8), 1410-1423.

58. De, P.; Gondi, S. R.; Roy, D.; Sumerlin, B. S., Boronic Acid-Terminated Polymers: Synthesis by RAFT and Subsequent Supramolecular and Dynamic Covalent Self-Assembly. *Macromolecules* **2009,** *42* (15), 5614-5621.

59. Deng, C. C.; Brooks, W. L. A.; Abboud, K. A.; Sumerlin, B. S., Boronic Acid-Based Hydrogels Undergo Self-Healing at Neutral and Acidic pH. *ACS Macro Lett* **2015,** *4* (2), 220-224.

60. Hui, Y.; Wen, Z.-B.; Pilate, F.; Xie, H.; Fan, C.-J.; Du, L.; Liu, D.; Yang, K.-K.; Wang, Y.-Z., A facile strategy to fabricate highly-stretchable self-healing poly(vinyl alcohol) hybrid hydrogels based on metal–ligand interactions and hydrogen bonding. *Polymer Chemistry* **2016,** *7* (47), 7269-7277.

61. Zhang, Q.; Niu, S.; Wang, L.; Lopez, J.; Chen, S.; Cai, Y.; Du, R.; Liu, Y.; Lai, J. C.; Liu, L.; Li, C. H.; Yan, X.; Liu, C.; Tok, J. B.; Jia, X.; Bao, Z., An Elastic Autonomous Self-Healing Capacitive Sensor Based on a Dynamic Dual Crosslinked Chemical System. *Adv Mater* **2018,** *30 (33),* 1801435.

62. Guo, Y.; Zhou, X.; Tang, Q.; Bao, H.; Wang, G.; Saha, P., A self-healable and easily recyclable supramolecular hydrogel electrolyte for flexible supercapacitors. *Journal of Materials Chemistry A* **2016,** *4* (22), 8769-8776.

63. Krogsgaard, M.; Hansen, M. R.; Birkedal, H., Metals & polymers in the mix: fine-tuning the mechanical properties & color of self-healing mussel-inspired hydrogels. *J Mater Chem B* **2014,** *2* (47), 8292-8297.

64. Xu, Z.; Zhao, Y.; Wang, X.; Lin, T., A thermally healable polyhedral oligomeric silsesquioxane (POSS) nanocomposite based on Diels-Alder chemistry. *Chem Commun (Camb)* **2013,** *49* (60), 6755-7.

65. Tuncaboylu, D. C.; Sahin, M.; Argun, A.; Oppermann, W.; Okay, O., Dynamics and Large Strain Behavior of Self-Healing Hydrogels with and without Surfactants. *Macromolecules* **2012,** *45* (4), 1991-2000.

66. Shao, C.; Wang, M.; Meng, L.; Chang, H.; Wang, B.; Xu, F.; Yang, J.; Wan, P., Mussel-Inspired Cellulose Nanocomposite Tough Hydrogels with Synergistic Self-Healing, Adhesive, and Strain-Sensitive Properties. *Chemistry of Materials* **2018,** *30* (9), 3110-3121.

67. Li, G.; Zhang, H.; Fortin, D.; Xia, H.; Zhao, Y., Poly(vinyl alcohol)-Poly(ethylene glycol) Double-Network Hydrogel: A General Approach to Shape Memory and Self-Healing Functionalities. *Langmuir* **2015,** *31* (42), 11709-16.

68. Lu, B.; Lin, F.; Jiang, X.; Cheng, J.; Lu, Q.; Song, J.; Chen, C.; Huang, B., One-Pot Assembly of Microfibrillated Cellulose Reinforced PVA–Borax Hydrogels with Self-Healing and pH-Responsive Properties. *ACS Sustainable Chemistry & Engineering* **2016,** *5* (1), 948-956.

69. Yu, F.; Cao, X.; Du, J.; Wang, G.; Chen, X., Multifunctional Hydrogel with Good Structure Integrity, Self-Healing, and Tissue-Adhesive Property Formed by Combining Diels-Alder Click Reaction and Acylhydrazone Bond. *ACS Appl Mater Interfaces* **2015,** *7* (43), 24023-31.

70. Pan, X.; Wang, Q.; Ning, D.; Dai, L.; Liu, K.; Ni, Y.; Chen, L.; Huang, L., Ultraflexible Self-Healing Guar Gum-Glycerol Hydrogel with Injectable, Antifreeze, and Strain-Sensitive Properties. *ACS Biomater Sci Eng* **2018,** *4* (9), 3397-3404.

71. Qu, J.; Zhao, X.; Ma, P. X.; Guo, B., pH-responsive self-healing injectable hydrogel based on N-carboxyethyl chitosan for hepatocellular carcinoma therapy. *Acta Biomater* **2017,** *58*, 168-180.

72. Yang, S.; Zhang, Y.; Zhang, C.; Wang, T.; Sun, W.; Tong, Z., Combinational Hydrogel and Xerogel Actuators Showing NIR Manipulating Complex Actions. *Macromol Rapid Commun* **2019,** *40* (18), e1900270.

73. Fan, H.; Wang, J.; Jin, Z., Tough, Swelling-Resistant, Self-Healing, and Adhesive Dual-Cross-Linked Hydrogels Based on Polymer–Tannic Acid Multiple Hydrogen Bonds. *Macromolecules* **2018,** *51* (5), 1696-1705.

74. Chen, Y. N.; Peng, L.; Liu, T.; Wang, Y.; Shi, S.; Wang, H., Poly(vinyl alcohol)-Tannic Acid Hydrogels with Excellent Mechanical Properties and Shape Memory Behaviors. *ACS Appl Mater Interfaces* **2016,** *8* (40), 27199-27206.

75. Chen, H.; Li, Y.; Tao, G.; Wang, L.; Zhou, S., Thermo- and water-induced shape memory poly(vinyl alcohol) supramolecular networks crosslinked by self-complementary quadruple hydrogen bonding. *Polymer Chemistry* **2016,** *7* (43), 6637-6644.

76. Sun, T. L.; Kurokawa, T.; Kuroda, S.; Ihsan, A. B.; Akasaki, T.; Sato, K.; Haque, M. A.; Nakajima, T.; Gong, J. P., Physical hydrogels composed of polyampholytes demonstrate high toughness and viscoelasticity. *Nature materials* **2013,** *12* (10), 932-937.

77. Yang, W.; Shao, B.; Liu, T.; Zhang, Y.; Huang, R.; Chen, F.; Fu, Q., Robust and Mechanically and Electrically Self-Healing Hydrogel for Efficient Electromagnetic Interference Shielding. *ACS Appl Mater Interfaces* **2018,** *10* (9), 8245-8257.

78. Hirai, T.; Maruyama, H.; Suzuki, T.; Hayashi, S., Shape Memorizing Properties of a Hydrogel of Poly (vinyl Alcohol). *Journal of applied polymer science.* **1992,** *45* (10), 1849-1855.

79. Hirai T.; Maruyama H.; Suzuki T.;, H. S., Effect of Chemical Cross-linking under Elongation on Shape Restoring of Poly (vinyl alcohol) Hydrogel. *Journal of applied polymer science.* **1992,** *46* (8), 1449-1451.

80. Du, H.; Zhang, J., Solvent induced shape recovery of shape memory polymer based on chemically cross-linked poly(vinyl alcohol). *Soft Matter* **2010,** *6* (14), 3370-3376.

81. Qi, X.; Yao, X.; Deng, S.; Zhou, T.; Fu, Q., Water-induced shape memory effect of graphene oxide reinforced polyvinyl alcohol nanocomposites. *J. Mater. Chem. A* **2014,** *2* (7), 2240-2249.

82. Akduman, C.; Perrin, E.; Kumabasar, A.; Çay, A., Effect of molecular weight on the morphology of electrospun poly (vinyl alcohol) nanofibers. *XIIIth International Izmir Textile and Apparel Symposium* **2014**, 2-5.

83. Feldman, D., Poly(Vinyl Alcohol) Recent Contributions to Engineering and Medicine. *Journal of Composites Science* **2020,** *4* (4), 175.

84. Sirvio, J. A.; Honkaniemi, S.; Visanko, M.; Liimatainen, H., Composite Films of Poly(vinyl alcohol) and Bifunctional Cross-linking Cellulose Nanocrystals. *ACS Appl Mater Interfaces* **2015,** *7* (35), 19691-19699.

85. Joshi, N.; Suman, K.; Joshi, Y. M., Rheological Behavior of Aqueous Poly(vinyl alcohol) Solution during a Freeze–Thaw Gelation Process. *Macromolecules* **2020,** *53* (9), 3452-3463.

86. Fergg, F.; Keil, F. J.; Quader, H., Investigations of the microscopic structure of poly (vinyl alcohol) hydrogels by confocal laser scanning microscopy. *Colloid and Polymer Science* **2001,** *279* (1), 61-67.

87. Korsmeyer, R. W.; Peppas, N. A., Effect of the morphology of hydrophilic polymeric matrices on the diffusion and release of water soluble drugs. *Journal of membrane Science* **1981,** *9* (3), 211-227.

88. Kvien, I.; Oksman, K., Orientation of cellulose nanowhiskers in polyvinyl alcohol. *Applied Physics A* **2007,** *87* (4), 641-643.

89. Peresin, M. S.; Habibi, Y.; Vesterinen, A. H.; Rojas, O. J.; Pawlak, J. J.; Seppala, J. V., Effect of moisture on electrospun nanofiber composites of poly (vinyl alcohol) and cellulose nanocrystals. *Biomacromolecules* **2010,** *11* (9), 2471-2477.

90. Abitbol, T.; Johnstone, T.; Quinn, T. M.; Gray, D. G., Reinforcement with cellulose nanocrystals of poly(vinyl alcohol) hydrogels prepared by cyclic freezing and thawing. *Soft Matter* **2011,** *7* (6), 2373-2379.

91. Paralikar, S. A.; Simonsen, J.; Lombardi, J., Poly(vinyl alcohol)/cellulose nanocrystal barrier membranes. *Journal of Membrane Science* **2008,** *320* (1-2), 248-258.

92. Liu, M.; Ishida, Y.; Ebina, Y.; Sasaki, T.; Aida, T., Photolatently modulable hydrogels using unilamellar titania nanosheets as photocatalytic crosslinkers. *Nature Communications* **2013,** *4* (1), 1-7.

93. Zawko, S. A.; Suri, S.; Truong, Q.; Schmidt, C. E., Photopatterned anisotropic swelling of dual-crosslinked hyaluronic acid hydrogels. *Acta Biomater* **2009,** *5* (1), 14-22.

94. Cui, W.; Zhang, Z.-J.; Li, H.; Zhu, L.-M.; Liu, H.; Ran, R., Robust dual physically cross-linked hydrogels with unique self-reinforcing behavior and improved dye adsorption capacity. *RSC Advances* **2015,** *5* (65), 52966-52977.

95. Lin, P.; Ma, S.; Wang, X.; Zhou, F., Molecularly engineered dual-crosslinked hydrogel with ultrahigh mechanical strength, toughness, and good self-recovery. *Adv Mater* **2015,** *27* (12), 2054-2059.

96. Zhang, T.; Zuo, T.; Hu, D.; Chang, C., Dual Physically Cross-Linked Nanocomposite Hydrogels Reinforced by Tunicate Cellulose Nanocrystals with High Toughness and Good Self-Recoverability. *ACS Appl Mater Interfaces* **2017,** *9* (28), 24230-24237.

97. Bae, S. W.; Kim, J.; Kwon, S., Recent Advances in Polymer Additive Engineering for Diagnostic and Therapeutic Hydrogels. *International Journal of Molecular Sciences.* **2022,** *23* (6), 2955.

98. Hong, K. H.; Oh, K. W.; Kang, T. J., Preparation of conducting nylon-6 electrospun fiber webs by thein situ polymerization of polyaniline. *Journal of Applied Polymer Science* **2005,** *96* (4), 983-991.

99. Luo, C.; Zhao, Y.; Sun, X.; Luo, F., Fabrication of antiseptic, conductive and robust polyvinyl alcohol/chitosan composite hydrogels. *Journal of Polymer Research* **2020,** *27* (9), 1-9.

100. Cao, J.; Lu, C.; Zhuang, J.; Liu, M.; Zhang, X.; Yu, Y.; Tao, Q., Multiple Hydrogen Bonding Enables the Self-Healing of Sensors for Human-Machine Interactions. *Angew Chem Int Ed Engl* **2017,** *56* (30), 8795-8800.

101. Gonzalez, K.; Garcia-Astrain, C.; Santamaria-Echart, A.; Ugarte, L.; Averous, L.; Eceiza, A.; Gabilondo, N., Starch/graphene hydrogels via click chemistry with relevant electrical and antibacterial properties. *Carbohydr Polym* **2018,** *202*, 372-381.

102. Wu, X.; Lu, C.; Zhou, Z.; Yuan, G.; Xiong, R.; Zhang, X., Green synthesis and formation mechanism of cellulose nanocrystal-supported gold nanoparticles with enhanced catalytic performance. *Environmental Science: Nano* **2014,** *1* (1), 71-79.

103. Mishra, R. K.; Sabu, A.; Tiwari, S. K., Materials chemistry and the futurist eco-friendly applications of nanocellulose: Status and prospect. *Journal of Saudi Chemical Society* **2018,** *22* (8), 949-978.

104. Jiang, X.; Xiang, N.; Zhang, H.; Sun, Y.; Lin, Z.; Hou, L., Preparation and characterization of poly(vinyl alcohol)/sodium alginate hydrogel with high toughness and electric conductivity. *Carbohydr Polym* **2018,** *186*, 377-383.

105. Emsley, A. M.; Stevens, G. C., Kinetics and mechanisms of the low-temperature degradation of cellulose. *Cellulose* **1994,** *1* (1), 26-56.

106. Trache, D.; Hussin, M. H.; Haafiz, M. K.; Thakur, V. K., Recent progress in cellulose nanocrystals: sources and production. *Nanoscale* **2017,** *9* (5), 1763-1786.

107. Hemmati, F.; Jafari, S. M.; Taheri, R. A., Optimization of homogenization-sonication technique for the production of cellulose nanocrystals from cotton linter. *Int J Biol Macromol* **2019,** *137*, 374-381.

108. Hemmati, F.; Jafari, S. M.; Kashaninejad, M.; Barani Motlagh, M., Synthesis and characterization of cellulose nanocrystals derived from walnut shell agricultural residues. *Int J Biol Macromol* **2018,** *120* (Pt A), 1216-1224.

109. Isogai, A.; Hänninen, T.; Fujisawa, S.; Saito, T., Review: Catalytic oxidation of cellulose with nitroxyl radicals under aqueous conditions. *Progress in Polymer Science* **2018,** *86*, 122-148.

110. Rajala, S.; Siponkoski, T.; Sarlin, E.; Mettanen, M.; Vuoriluoto, M.; Pammo, A.; Juuti, J.; Rojas, O. J.; Franssila, S.; Tuukkanen, S., Cellulose Nanofibril Film as a Piezoelectric Sensor Material. *ACS Appl Mater Interfaces* **2016,** *8* (24), 15607-14.

111. Rubentheren, V.; Ward, T. A.; Chee, C. Y.; Nair, P., Physical and chemical reinforcement of chitosan film using nanocrystalline cellulose and tannic acid. *Cellulose* **2015,** *22* (4), 2529-2541.

112. Chen, C.; Yang, H.; Yang, X.; Ma, Q., Tannic acid: a crosslinker leading to versatile functional polymeric networks: a review. *RSC Adv* **2022,** *12* (13), 7689-7711.

113. Jin, Y.-N.; Yang, H.-C.; Huang, H.; Xu, Z.-K., Underwater superoleophobic coatings fabricated from tannic acid-decorated carbon nanotubes. *RSC Advances* **2015,** *5* (21), 16112-16115.

114. Ejima, H.; Richardson, J. J.; Liang, K.; Best, J. P.; van Koeverden, M. P.; Such, G. K.; Cui, J.; Caruso, F., One-step assembly of coordination complexes for versatile film and particle engineering. *Science* **2013,** *341* (6142), 154-157.

115. Fan, H.; Wang, J.; Zhang, Q.; Jin, Z., Tannic Acid-Based Multifunctional Hydrogels with Facile Adjustable Adhesion and Cohesion Contributed by Polyphenol Supramolecular Chemistry. *ACS Omega* **2017,** *2* (10), 6668-6676.

116. Bjornmalm, M.; Wong, L. M.; Wojciechowski, J. P.; Penders, J.; Horgan, C. C.; Booth, M. A.; Martin, N. G.; Sattler, S.; Stevens, M. M., In vivo biocompatibility and immunogenicity of metal-phenolic gelation. *Chem Sci* **2019,** *10* (43), 10179-10194.

117. Hong, K. H., Polyvinyl alcohol/tannic acid hydrogel prepared by a freeze-thawing process for wound dressing applications. *Polymer Bulletin* **2016,** *74* (7), 2861-2872.

118. Vickers, N. J., Animal Communication: When I'm Calling You, Will You Answer Too? *Curr Biol* **2017,** *27* (14), R713-R715.

119. Sionkowska, A.; Kaczmarek, B.; Lewandowska, K., Modification of collagen and chitosan mixtures by the addition of tannic acid. *Journal of Molecular Liquids* **2014,** *199*, 318-323.

120. Zhang, X.; Do, M. D.; Casey, P.; Sulistio, A.; Qiao, G. G.; Lundin, L.; Lillford, P.; Kosaraju, S., Chemical modification of gelatin by a natural phenolic cross-linker, tannic acid. *J Agric Food Chem* **2010,** *58* (11), 6809-15.

121. Kim, J. H.; Lee, Y. M., Gas permeation properties of poly (amide-6-b-ethylene oxide)–silica hybrid membranes. *Journal of Membrane Science* **2001,** *193* (2), 209-225.

122. Paranhos, C. M.; Soares, B. G.; Oliveira, R. N.; Pessan, L. A., Poly(vinyl alcohol)/Clay-Based Nanocomposite Hydrogels: Swelling Behavior and Characterization. *Macromolecular Materials and Engineering* **2007,** *292* (5), 620-626.

123. Hassan, C. M.; Peppas, N. A., Structure and morphology of freeze/thawed PVA hydrogels. *Macromolecules* **2000,** *33* (7), 2472-2479.

124. Zhang, H.; Xia, H.; Zhao, Y., Poly(vinyl alcohol) Hydrogel Can Autonomously Self-Heal. *ACS Macro Lett* **2012,** *1* (11), 1233-1236.

125. Hassan, C. M.; Peppas, N. A., Structure and applications of poly (vinyl alcohol) hydrogels produced by conventional crosslinking or by freezing/thawing methods. *Biopolymers· PVA hydrogels, anionic polymerisation nanocomposites* **2000**, 37-65.

126. Peppas, N. A.; Stauffer, S. R., Reinforced uncrosslinked poly (vinyl alcohol) gels produced by cyclic freezing-thawing processes: a short review. *Journal of Controlled Release* **1991,** *16* (3), 305-310.

127. Chan, G. G.; Koch, C. M.; Connors, L. H., Blood Proteomic Profiling in Inherited (ATTRm) and Acquired (ATTRwt) Forms of Transthyretin-Associated Cardiac Amyloidosis. *J Proteome Res* **2017,** *16* (4), 1659-1668.

128. Kumar, A.; Lee, Y.; Kim, D.; Rao, K. M.; Kim, J.; Park, S.; Haider, A.; Lee, D. H.; Han, S. S., Effect of crosslinking functionality on microstructure, mechanical properties, and in vitro cytocompatibility of cellulose nanocrystals reinforced poly (vinyl alcohol)/sodium alginate hybrid scaffolds. *Int J Biol Macromol* **2017,** *95*, 962-973.

129. Han, L.; Cui, S.; Yu, H. Y.; Song, M.; Zhang, H.; Grishkewich, N.; Huang, C.; Kim, D.; Tam, K. M. C., Self-Healable Conductive Nanocellulose Nanocomposites for Biocompatible Electronic Skin Sensor Systems. *ACS Appl Mater Interfaces* **2019,** *11* (47), 44642-44651.

130. Ihsan, A. B.; Sun, T. L.; Kurokawa, T.; Karobi, S. N.; Nakajima, T.; Nonoyama, T.; Roy, C. K.; Luo, F.; Gong, J. P., Self-Healing Behaviors of Tough Polyampholyte Hydrogels. *Macromolecules* **2016,** *49* (11), 4245-4252.

131. Song, P.; Xu, Z.; Guo, Q., Bioinspired Strategy to Reinforce PVA with Improved Toughness and Thermal Properties via Hydrogen-Bond Self-Assembly. *ACS Macro Lett* **2013,** *2* (12), 1100-1104.

132. Wei, Z.; Yang, J. H.; Liu, Z. Q.; Xu, F.; Zhou, J. X.; Zrínyi, M.; Osada, Y.; Chen, Y. M., Novel Biocompatible Polysaccharide-Based Self-Healing Hydrogel. *Advanced Functional Materials* **2015,** *25* (9), 1352-1359.

133. Guo, W.; Yang, M.; Liu, S.; Zhang, X.; Zhang, B.; Chen, Y., Chitosan/polyvinyl alcohol/tannic acid multiple network composite hydrogel: preparation and characterization. *Iranian Polymer Journal* **2021,** *30* (11), 1159-1168.

134. Huang, R.; Zhang, Y.; Xiang, A.; Ma, S.; tian, h.; Ouyang, Y.; Rajulu, A. V., Crystallization behavior of polyvinyl alcohol with inorganic nucleating agent talc and regulation mechanism analysis. *Journal of Polymers and the Environment* **2022**, 1-11.

135. Peng, M.; Xiao, G.; Tang, X.; Zhou, Y., Hydrogen-Bonding Assembly of Rigid-Rod Poly(p-sulfophenylene terephthalamide) and Flexible-Chain Poly(vinyl alcohol) for Transparent, Strong, and Tough Molecular Composites. *Macromolecules* **2014,** *47* (23), 8411-8419.

136. Dai, H.; Huang, Y.; Huang, H., Enhanced performances of polyvinyl alcohol films by introducing tannic acid and pineapple peel-derived cellulose nanocrystals. *Cellulose* **2018,** *25* (8), 4623-4637.

137. Holloway, J. L.; Lowman, A. M.; Palmese, G. R., The role of crystallization and phase separation in the formation of physically cross-linked PVA hydrogels. *Soft Matter* **2013,** *9* (3), 826-833.

138. Zhang, Y.; Song, M.; Diao, Y.; Li, B.; Shi, L.; Ran, R., Preparation and properties of polyacrylamide/polyvinyl alcohol physical double network hydrogel. *RSC Advances* **2016,** *6* (113), 112468-112476.

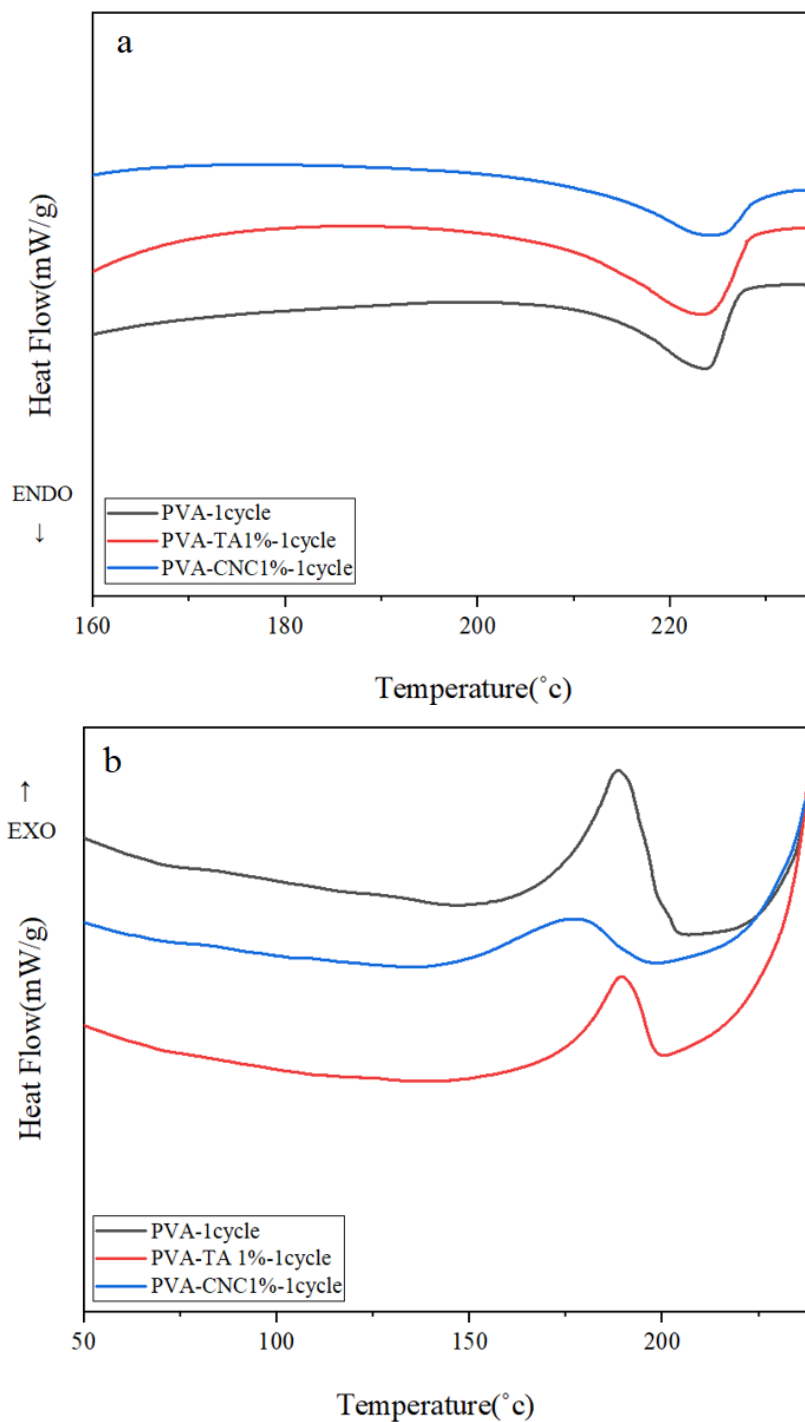**Figure S1.** DSC measurements of PVA, PVA-CNC 1%, and PVA-TA 1% for one cycle of F-T process for first cycle of a) heating and b) cooling.
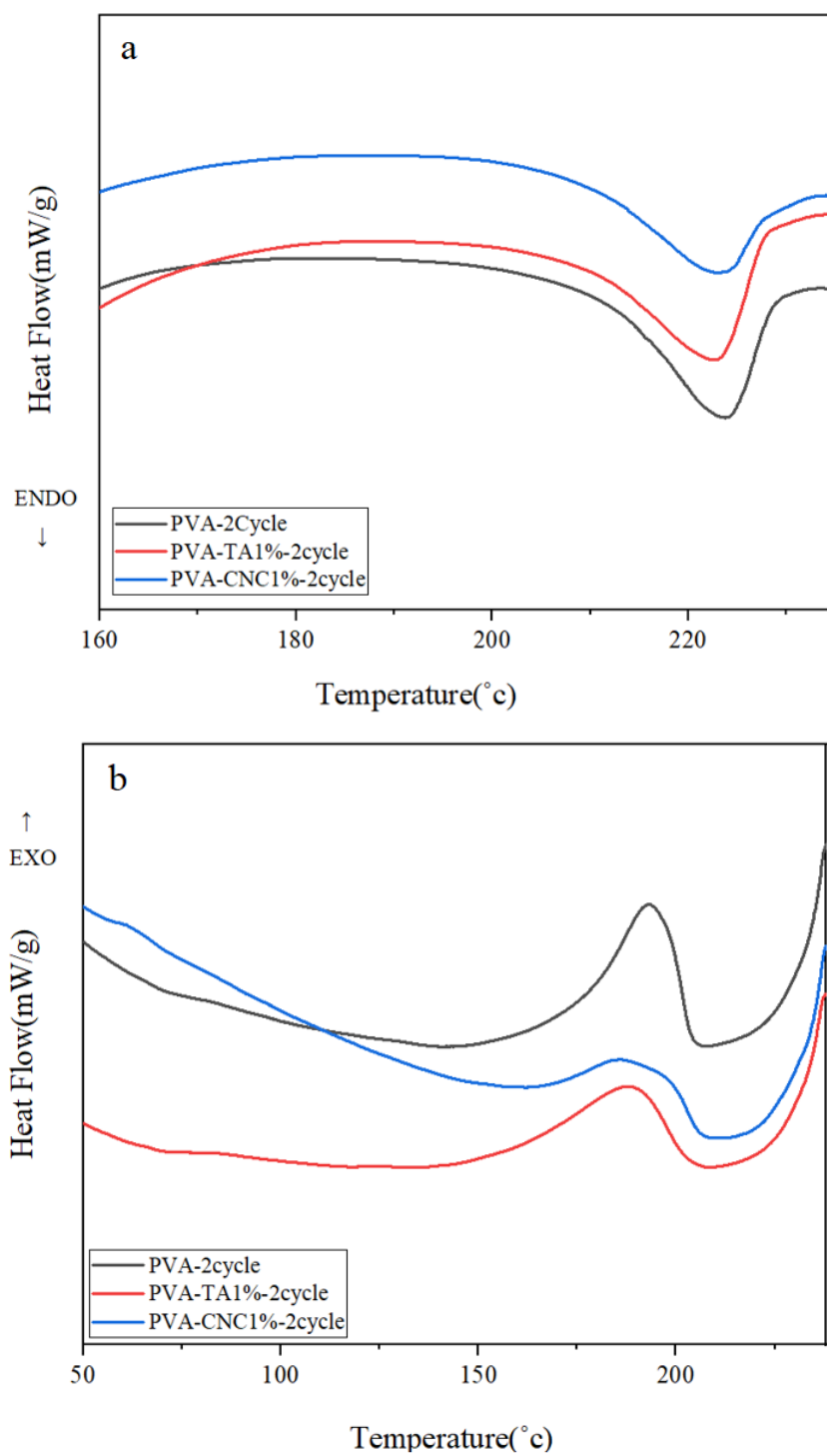
Figure S2. DSC measurements of PVA, PVA-CNC 1%, and PVA-TA 1% for second cycle of F-T process for first cycle of a) heating and b) cooling.
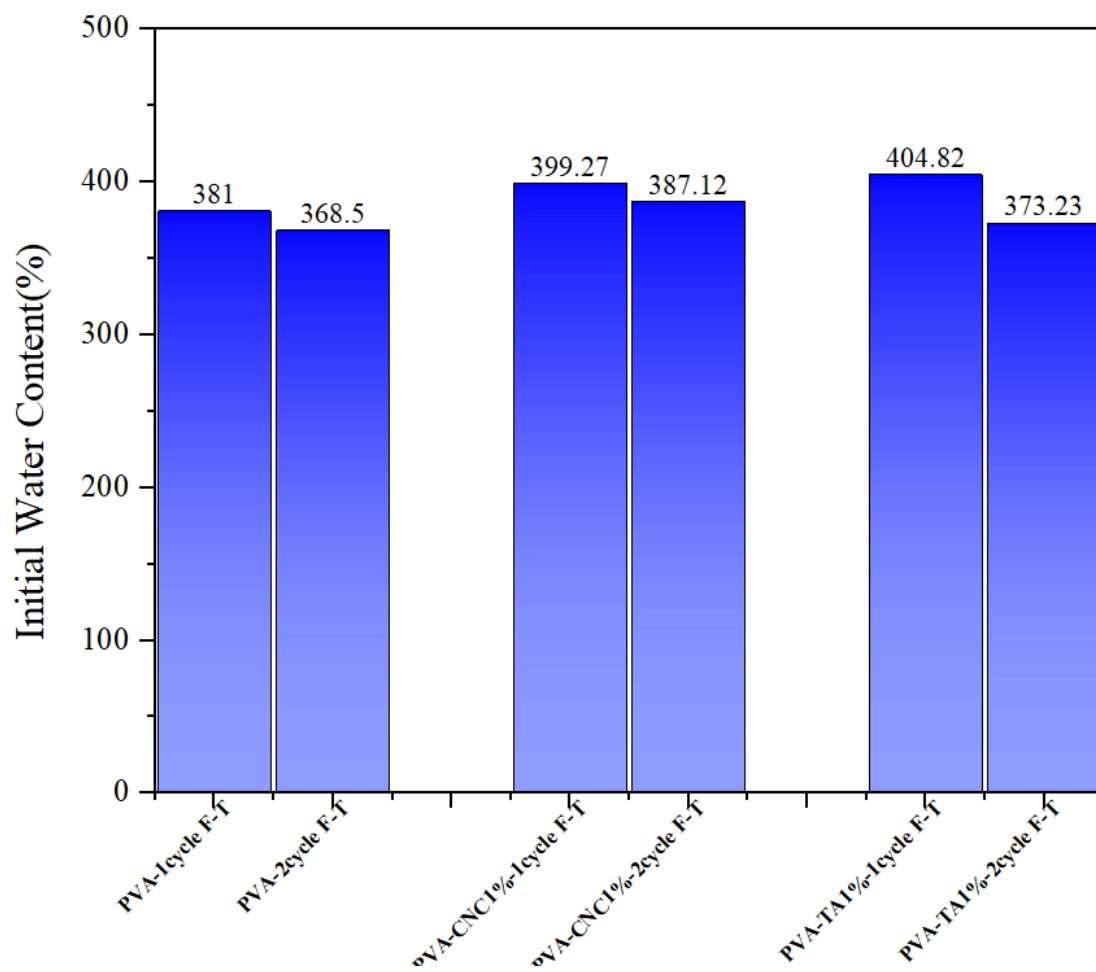
Figure S3. The water content of PVA, PVA-CNC 1%, and PVA-TA 1% for one and two cycle of F-T preparation method.
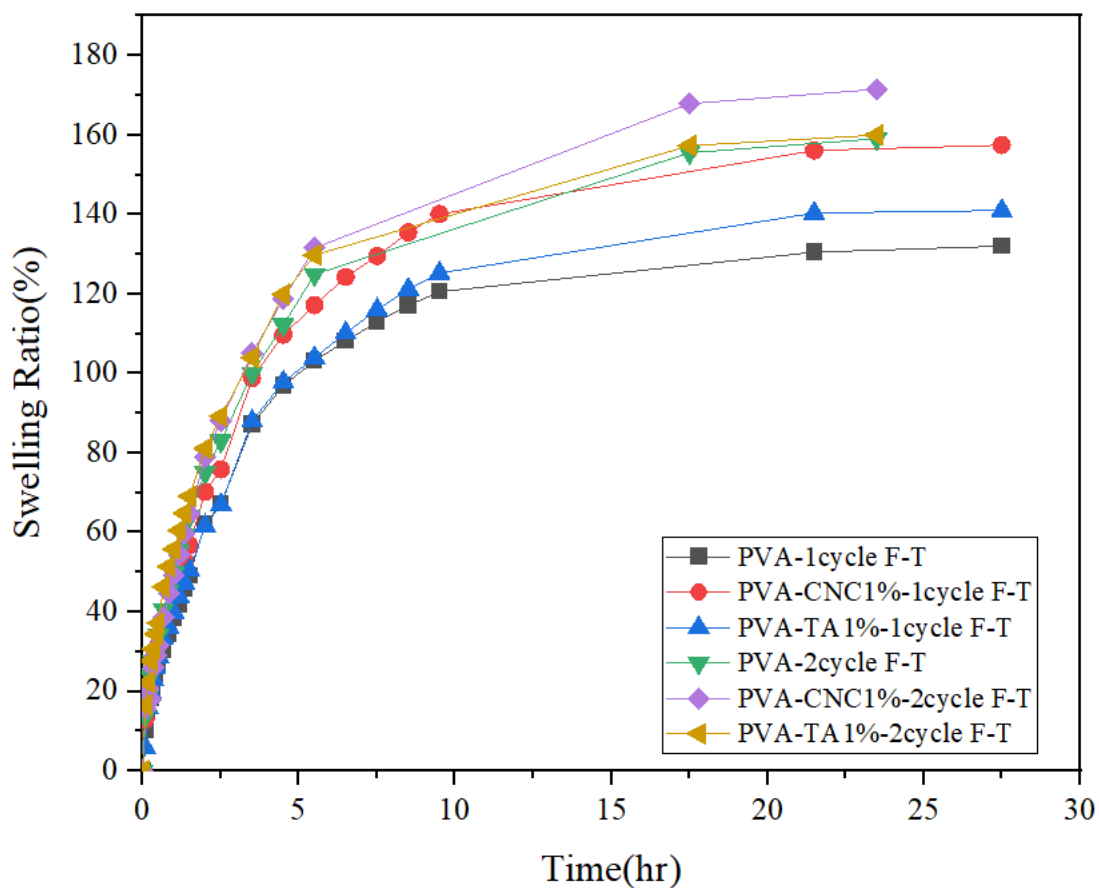
Figure S4. Swelling ratio for PVA, PVA-CNC 1%, and PVA-TA 1% for one and second cycle of F-T method.

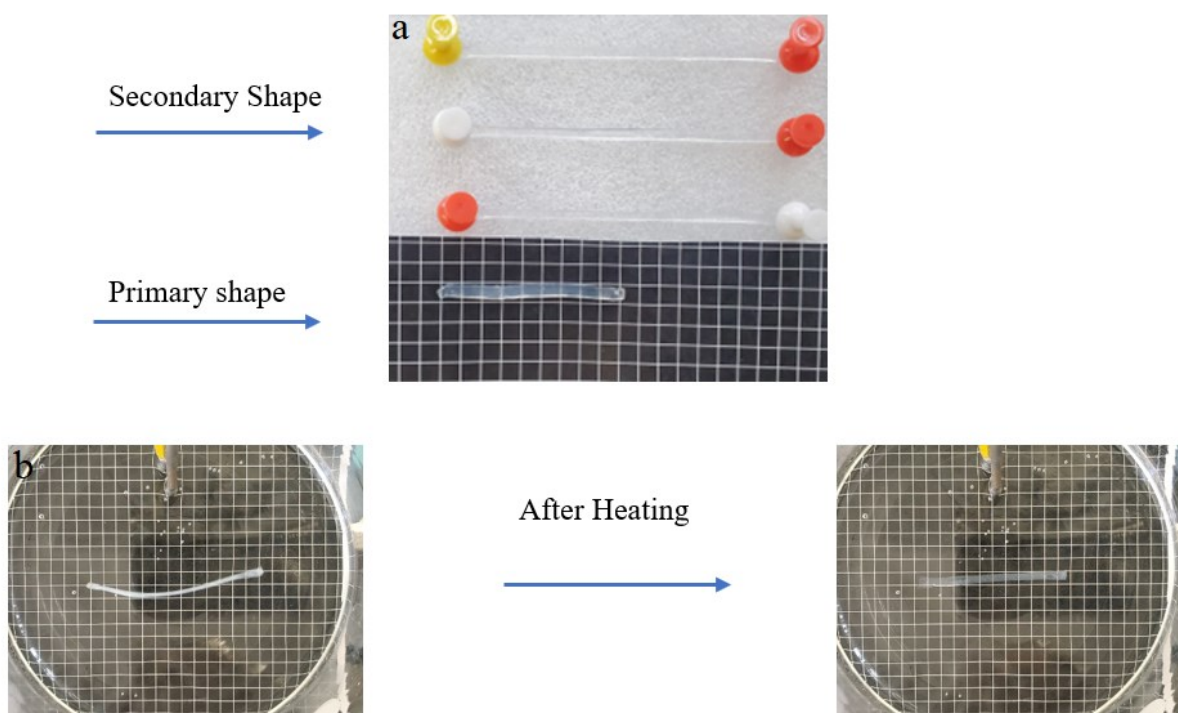Secondary Shape →

Primary shape →

After Heating →

Figure S5. Photos showing a) the shape-change process by using Freeze/Thaw method b) the fast thermally activated shape recovery of the PVA-CNC 1% and PVA-TA 1% hydrogel.